Investigating the impact of cattle path erosion on soil organic carbon and nitrogen, Okhombe Valley, KwaZulu-Natal Drakensberg, South Africa.

by

Ashleigh Blicq

Submitted in fulfilment of the academic requirements for the degree of Master of Science, in the School of Agricultural, Earth and Environmental Sciences, University of KwaZulu-Natal, Pietermaritzburg Campus.

October 2018

Abstract

While soil erosion is a natural geologic phenomenon, its exacerbation as a consequence of socio-economic and political factors, threatens rural sustainability and livelihoods. Smallholder rural farmers within the KwaZulu-Natal Drakensberg region of South Africa are reliant on the surrounding grasslands for livestock grazing. Mismanagement of land through overgrazing, overstocking and livestock trampling have led to excessive cattle path formation and resultant soil erosion, which negatively affects these montane grasslands. Community members have identified cattle path formation, as a grave concern, as the loss of land through increase erosion leads to gully formation and presents a safety hazard to residents and livestock. This study investigated the impact of cattle path erosion on soil properties, in particular soil organic carbon (SOC) and nitrogen (N) along a degraded slope profile. For this purpose four positions (reference site, top-slope, mid-slope and lower-slope) were identified and sampled at three soil depths (0-5 cm, 5-15 cm and 15-30 cm) along a degraded slope at Okhombe, Drakensberg region South Africa. Soil properties, soil nutrients, SOC and N were measured (over a two day period) and physical soil fractionation were completed to determine carbon (C) and N protection within soil aggregates. To understand SOC and N distribution, areas of erosion and deposition were determined by measuring fallout radionuclides caesium-137 (^{137}Cs) and excess lead-210 (^{210}Pb$_{ex}$). Soil property measurements revealed that the undisturbed reference site contained higher nutrient content and greater C and N protection within soil aggregates compared to the degraded slope profile. This suggests that nutrient loss has occurred on the degraded slope, possibly as a result of cattle path erosion. Due to the low radioactive activity of the samples, count times for ^{210}Pb$_{ex}$ and ^{137}Cs ranged from 24- 48 hours, using detection limits of 0.3 dpm g^{-1} for ^{210}Pb$_{ex}$ and 0.05 dpm g^{-1} for ^{137}Cs. The analysis of ^{137}Cs showed low activity, with 75% of the samples (n=36) having activities below the detection limit. Thus, the use of ^{137}Cs as an indicator for soil erosion could not be determined. Excess lead-210 indicated significant post-depositional movement and that this movement is spatially heterogeneous and temporally variable. As such, determining sedimentation rates within the study area was not possible, as ^{210}Pb$_{ex}$ did not decline with depth at a consistent rate. Excess lead-210 did however show that at areas of soil erosion, SOC and N concentrations were low, highlighting the physical removal of these soil constituents with the detachment and transportation of soil particles through sheet erosion. Knowledge of soil erosion processes will aid in the design and implementation of effective soil erosion and sediment control strategies. Improved understanding of the effect of cattle paths on soil properties and soil organic matter distribution will contribute to the ongoing efforts to rehabilitate rural landscapes to ensure sustainable land use management.

Declaration

I ASHLEIGH JUSTINE BLICQ declare that:

i. The research reported in this dissertation, except where otherwise indicated, is my original work.

ii. This dissertation has not been submitted for any degree or examination at any other university.

iii. This dissertation does not contain other persons' data, pictures, graphs or other information, unless specifically acknowledged as being sourced from other publishers.

iv. All authors and organisations have been fully acknowledged and can be found within the text and in the reference list.

v. This dissertation does not contain text, graphics or tables copied and pasted from the internet, unless specifically acknowledged, and the source being detailed in the dissertation and in the reference list.

____

Ashleigh Blicq

____

Professor Trevor Hill

Acknowledgments

Father, thank you for teaching me the wisdom of discipline and diligence. I have learnt that there is freedom and joy in hard work.

Prof Trevor Hill, thank you for the opportunity of allowing me to make use of radionuclides as a method in my research. It has been an extremely interesting topic. Thank you for being patient with me during this journey. Your time and effort are much appreciated.

Dr. Khatab Mohamed Abdalla, thank you for your expertise, guidance and support throughout this journey. Your leadership, insight and willingness to extend yourself to assist me is truly appreciated. Thank you for your constant support and encouragement.

Dr. Claudia Benitez-Nelson at the University of South Carolina, thank you for your expertise and incredible contribution to my research. Your willingness and enthusiasm to help has been greatly appreciated and has provided valuable insight.

This research originated from a project initiated, managed and funded by the Water Research Commission. Thank you to the WRC, National Research Foundation (NRF) and University of KwaZulu-Natal for sponsoring this research.

Nantale Edith, you have been my biggest cheerleader! Thank you for constantly praying for me, encouraging me and laughing with me! I appreciate you! - Avalanche Ash

Thank you to all the students who assisted me with field work, and many thanks to my amazing friends for all the support and encouragement!

To my family, thank you for carrying me through this season! I love and appreciate you guys so much!

Marcel, your selflessness and sacrifices have time and time again demonstrated your great love for me! I am tremendously grateful for your constant patience, support, and tough love. I am thankful for you and truly blessed and excited to experience life with you!

List of Abbreviations

^{7}Be	-	Beryllium-7
ρb and BD	-	Bulk density
C	-	Carbon
Ca	-	Calcium
CO_2	-	Carbon dioxide
^{137}Cs	-	Caesium-137
Cu	-	Copper
C:N	-	Carbon-nitrogen ratio
CSIR	-	Council for Scientific and Industrial Research
$^{210}Pb_{ex}$	-	Excess Lead-210
K	-	Potassium
KZN	-	KwaZulu-Natal
MWD	-	Mean weight diameter
Mn	-	Manganese
Mg	-	Magnesium
N	-	Nitrogen
Na	-	Sodium
Nc	-	Nitrogen content
Ns	-	Nitrogen stocks
OC	-	Organic carbon
OMG	-	Okhombe Inthathakhusa Monitoring Group
P	-	Phosphorus
^{226}Ra	-	Radium-226
^{222}Rn	-	Radon-222
SOC	-	Soil organic carbon
SOCc	-	Soil organic carbon content
SOCs	-	Soil organic carbon stocks
SOM	-	Soil organic matter
^{238}U	-	Uranium-238
WRC	-	Water Research Commission
Zn	-	Zinc

Table of Contents

List of Tables

List of Figures

List of Plates

Chapter One
Introduction

1.1 Introduction

Soil erosion is recognised as one of the most pressing environmental issues as it reduces ecosystem function, threatens food security, increases poverty and intensifies hydrogeological risk (Lal, 2003; Borrelli *et al.*, 2016; Correa *et al.*, 2016; Wang *et al*., 2016). For this reason, many international conventions, such as the Rio Summit (1992) and its Agenda 21, UN Framework Convention on Climate Change, Articles 3.3 and 3.4 of the Kyoto Protocol, the Millennium Development Goals and the Sustainable Development Goals, have recognised the significance of protecting and restoring soil resources and have strongly supported soil sustainable management (Lal, 2003). However, for soil sustainable management to be successful, an understanding of how land cover, climate and topography affect soil erosion processes and how soil erosion affects soil organic matter (SOM) is required for the improvement of land use practices (Ochoa *et al.*, 2016). This is particularly important when discussing water erosion, as it affects 56 % of the global agricultural areas (Correa *et al*., 2016).

According to the German Council on Global Change, soil erosion by water is one of the most significant forms of land degradation, where each year approximately 1094 million hectares of land area is affected (Lal, 2003; Parwada and Van Tol, 2017). Annually, soil erosion by water is responsible for a loss of approximately 100 000 km^2 (10 million hectares) of agricultural land globally. This occurs at a rate 40 times greater than that at which soil forms (Luffman *et al*., 2015). Globally, as millions of tonnes of soil are deposited into the ocean, extreme pressure is exerted on catchments at both points of removal and points of deposition. At points of removal, soil erosion affects agricultural productivity whilst at points of deposition, limits river capacity through sedimentation (Hagos, 2004). As a result, the economy of many countries are affected as losses through agriculture and fishery production, decreased tourism opportunities, increased cost in water purification, and degraded public health care occur (Chicas *et al*., 2016). This is particularly true for developing countries as communal areas are subject to incorrect agricultural practices, land abandonment, road construction and wild fires, which increases the vulnerability of the land to soil erosion (Ochoa *et al.,* 2016).

In South Africa (SA), soil erosion affects more than 85% of the country's land surface, where approximately 400 million tons of soil is lost per annum (Dlamini *et al*., 2011; Parwada and Van Tol, 2017). With rainfall as a key driver, water erosion is responsible for an average loss of 3 Mg ha^{-1} $year^{-1}$ of topsoil (Schmiedel *et al*., 2017) and is particularly prominent in the grassland region of the Drakensberg, KwaZulu-Natal which receives the majority of its rainfall in the summer months (Dlamini *et al*., 2011; Dlamini *et al*., 2014; SWSR, 2015). This region is crucial to water supply as the uThukela Catchment forms part of the main escarpment of South Africa and is significant in providing water to the provinces of KwaZulu-Natal and Gauteng (Temme *et al*., 2009; Mansour *et al*., 2012).

Water erosion occurs through rainsplash as sheet erosion when flow is unconcentrated or as rill and/or gully erosion when flow is concentrated. The outcome of the erosional processes depends on a combination of interactive effects namely; rainfall erosivity, soil erodibility, slope steepness and slope length, crop management and support practice (Le Roux *et al.*, 2008). Rill erosion is considered to be the most significant process that causes sediment production for transportation, where the persistent development of rills may lead to gully formation. Gully erosion is an indication of extreme land degradation, as they are unable to be filled by tillage operations and control techniques are costly and challenging to implement (Valentin *et al*., 2005; Luffman *et al*., 2015; Ollobarren *et al.,* 2016; Li *et al.,* 2017). Gully erosion is a major source of sediment pollution (Shellberg *et al*., 2016) particularly in SA where dongas (South African term for gullies) are a noticeable feature within the landscape (Laker, 2004; Dlamini *et al*., 2011).

The contribution of soil erosion to land degradation include; the loss of fertile topsoil and decline in soil productivity, and off-site impacts as the movement of sediment and delivery to water sources increases. The accumulation of eroded material leads to sedimentation, siltation and the reduction in capacity and/or lifespan of impoundments and rivers. It causes suspended sediment concentrations within streams to increase, producing adverse effects on aquatic ecosystem health, creating water management issues, particularly in a water scarce country such as SA (Le Roux *et al*., 2007; Le Roux *et al*., 2008; Maalim *et al*., 2013). According to the SA State of Environment Report, soil erosion costs the country approximately R2 billion per annum including costs of off-site purification of silted dam water (Le Roux *et al*., 2008; DEA, 2012).

Although the process of soil erosion is a naturally occurring process, human activities, such as overgrazing and overstocking, have accelerated this process where Smith *et al.,* (2000:355) state that "overgrazing is the main human induced factor causing accelerated water erosion in South Africa". Overgrazing is prominent in the Drakensberg region of KwaZulu-Natal (Dlamini *et al*., 2011; Dlamini *et al*., 2014), as these sloping rangelands are communally grazed by cattle which are an important component of rural smallholder livelihoods as cattle ownership symbolizes wealth. This economic value and cultural aspect of owning cattle within these communities leads to overstocking and overgrazing of the rangelands, where constant hoof action and trampling along paths (collective term used for: footpaths/trails, farming/wildlife trails, trekking routes, horse trails etc.) results in vegetation loss, decrease in soil surface coverage and soil compaction. This, combined with highly acidic soils of low productivity, leaves the rangelands vulnerable to soil degradation and threatens the natural functionality of the ecosystem as soil erosion results in the loss of soil, soil organic matter (SOM) and organic carbon (OC) (Oakes *et al*., 2012).

SOM is an important determinant of soil quality and is affected by loss of surface soil through erosion (Guoxiao *et al*., 2008; Saiz *et al*., 2016). The abundance of SOM promotes the regulation of carbon, therefore aiding in the resilience of soils to erosion (Saiz *et al*., 2016). According to Lal (2008), the amount of soil organic carbon (SOC) lost from global terrestrial ecosystems, since 1850 due to erosion, is 26 petagrams (Pg) (1 Pg = 1 billion tonnes). This is due to the concentration and turnover of SOC and total nitrogen (N) being the highest in the surface soil (Guoxiao *et al*., 2008; Lal, 2008; Abdalla *et al*., 2016; Han *et al*., 2018). Furthermore, as soils are the most important long-term OC reservoir in terrestrial environments, any manipulation to this reservoir may affect the concentration of atmospheric carbon dioxide (CO_2) (Guo and Gifford, 2002; Forrester *et al*., 2013; Chaplot and Cooper, 2015; Nosrati *et al*., 2015; Han *et al*., 2018). This is evident within global agricultural landscapes, where erosion causes a global carbon sink of 0.12 (range 0.06 to 0.27) petagrams of carbon per year (pg yr^{-1}) (Nosrati *et al*., 2015).

The abundance of SOC and N is intricately linked to the cycling of soil nutrients and is a critical determinant of soil quality, ecosystem and agricultural productivity, water quality and global climate (Jobbágy and Jackson, 2000; Resh *et al*., 2002; Guoxiao *et al*., 2008; Lal, 2008). Improved understanding of the effect of cattle paths on SOC and N stock distribution will therefore contribute to the ongoing efforts to reduce land degradation and to assistant in the recovery and rehabilitation of grasslands within rural landscapes. This will contribute to more sustainable land use management practices are implemented which could protect ecosystem services and thus, the livelihoods of the community.

1.2 Research Rationale

In South Africa, the majority of the areas affected by soil erosion are communally owned and are heavily utilized for cattle grazing (Birkett *et al*., 2016). This mismanagement of land leads to cattle path erosion, resulting in losses of fertile soil and therefore the loss of SOC and N (Wang *et al*., 2016). This critically threatens rural sustainability and food security (Chicas *et al*., 2016; Schmiedel *et al*., 2017) and it is therefore necessary to address the impact of cattle path erosion in communal areas and its associated impacts on soil properties.

This study was part of a larger Water Research Commission (WRC K5/2402) project that aimed to improve the understanding of the processes of erosion and sediment yield for different combinations of land uses (i.e. grassland, woodlands, agricultural crops/pastures, orchards and forest plantations) and scales, for traditional and commercial agricultural production systems. It is intended that these findings will aid in the understanding of the impacts of cattle path erosion on soil properties within a grazing community.

The study area, Okhombe, is part of the uThukela catchment region, which plays a pivotal role in water provision for the provinces of KwaZulu-Natal and the indirect provision for Gauteng via inter-basin transfer. However, lack of effective land use management plans within this communal area, has had negative impacts on the soil and water resources. Community-based soil conservation measures such as stone packs, stone lines, cattle steps and planting of indigenous and exotic vegetation have been implemented in certain areas in Okhombe through the Okhombe LandCare Project (Everson *et al*., 2007). Through this project, local groups were established and trained to sustain the management of natural resources within the community, with the focal point being the land degradation caused by cattle paths, as cattle are herded on a daily basis up and down the slopes to access pastures on surrounding hilltops (Sonneveld *et al*., 2005; Birkett *et al*., 2016). Approximately 4000 cattle and 2000 small stock (principally goats) graze in the area, where grazing on the hillslopes takes place during the summer months (September to May). The uncontrolled movement and grazing of cattle along the slopes dramatically increases the vulnerability of these rangelands to erosion (Parsons and Dumont, 2003; Gamoun *et al*., 2010).

1.3 Research Aim and Objectives

Land degradation and soil erosion are prominent within Okhombe as cattle path formation promotes soil loss through the reduction in vegetation cover and increased soil compaction. This results in poor water infiltration and increased runoff (Borrelli *et al*., 2016; Keesstra *et al*., 2016). This research therefore aims to investigate the impact of cattle path erosion on soil properties, specifically SOC and N, along a degraded slope profile in Okhombe Valley, Drakensberg. The objectives were set to highlight the SOC and N dynamics as a result of this erosion; as community members are concerned with the impact of erosion on their safety and livelihoods. The four objectives were:

1. Identify an applicable reference site to be used as a control and applicable sampling sites along the degraded slope (top-, mid- and lower-slope) that are intercepted by cattle paths.
2. Determine the soil properties and trace elements of the degraded slope.
3. Evaluate SOC and N within the soil profile and soil aggregates.
4. Evaluate fallout radionuclides caesium-137 (^{137}Cs) and excess lead-210 ($^{210}Pb_{ex}$) to estimate soil deposition rates, and to link the findings to SOC and N distribution.

Chapter Two
Literature Review

2.1 Introduction

The accelerated movement of water within landscapes, in response to anthropogenic modification of the land, has been recognised as primary driving force for soil erosion processes and soil evolution (Oakes *et al*., 2012; Jha *et al*., 2015; Nosrati *et al*., 2015; Ochoa *et al*., 2016). Soil erosion is a major issue threatening land resources throughout SA (Sonneveld *et al*., 2005; Wessels *et al*., 2007) where approximately 43% of the 57 million residents live in rural areas and rely on the natural environment for their livelihoods (DEA, 2012). Soil erosion is, however, not a new occurrence, as reports on the degree and intensity of erosion date back to the first decades of the twentieth century, indicating the severity of the problem and how widely it contributes to land degradation in South Africa (Pile, 1996; Sonneveld *et al*., 2005).

In SA, water erosion is particularly prominent in the grassland region of the Drakensberg, KwaZulu-Natal (Dlamini *et al*., 2011; Dlamini *et al*., 2014; SWSR, 2015). This area is characterized by "high (often intense) rainfall, duplex soils derived from sodium-rich parent materials, and steep slopes" (SWSR, 2015:270). These conditions, combined with overpopulation, impoverishment and poor farming and land husbandry practices, accelerate the process of soil erosion, thus exacerbating land degradation (Harrison and Shackleton, 1999; Peden, 2005; Wessels *et al*., 2007; Le Roux *et al*., 2008; DEA, 2012). This negatively impacts on ecosystem productivity due to loss of fertile soil, essential nutrients and OC (Pimental, 2006; Oakes *et al*., 2012; Chaplot, 2013; Wang *et al*., 2016). During the soil erosion process, SOC is lost by transport of surface runoff and sediments, which carry varying concentrations of soil C. This affects the lateral and vertical distribution of SOC within landscapes and influences the balance of SOC stock (Ma *et al*., 2014; Ellerbrock *et al*., 2016).

Investigating the impact of cattle path erosion on soil stores within the degraded slopes of the Drakensberg, will enhance our understanding of land degradation within degraded rural communities. Literature pertaining to soil erosion processes and mechanisms, SOC and N dynamics, the use of ^{137}Cs and $^{210}Pb_{ex}$ as a proxy for SOC and soil redistribution rates, and cattle path erosion in South Africa, will be discussed. Evaluating the spatial redistribution of SOC will help in the development of models used to predict SOC distribution within landscapes and aid in the development of sustainable land and water use management strategies for soil erosion control.

2.2 Soil Erosion Processes

Soil erosion and sedimentation are complex processes consisting of detachment, transportation and deposition of soil particles. These processes are brought upon by the impact of raindrops and overland flow of water (Le Roux 2011; Li *et al*., 2015; Maïga-Yaleu *et al*., 2015; Lu *et al.*, 2016). The process of detachment occurs when soil particles are dislodged from the soil mass by raindrops and overland flow and are made available for transport by surface runoff. This process describes the breaking-up of soil aggregates into individual components due to the kinetic energy of raindrops (Ma *et al*., 2014; Lu *et al*., 2016). Transportation of soil particles is defined by the transport capacity of the surface runoff, which is the maximum amount of sediment that can be carried by the runoff, without deposition occurring. Whilst, soil deposition occurs when the sediment load is greater than the total transport capacity of the flow and will therefore be deposited (Hagos, 2004; Oakes *et al*., 2012). There are three principal types of water erosion: splash erosion, sheet erosion and linear erosion (Chaplot, 2013).

Splash erosion occurs when the impact of raindrops on the soil surface causes soil particles to become detached and transported (Oakes *et al*., 2012; Chaplot, 2013; Cuomo *et al*., 2015). Detachment can be divided into two sub-processes comprising of 'aggregate break-down' and 'movement initiation of the break-down products' (Saedi *et al.*, 2016) where raindrop size and mass, drop velocity, rainfall intensity, kinetic energy, runoff depth, crop cover and wind speed affects soil detachment. Soil properties including; soil particle size distribution, soil shear strength, soil cohesion, SOM content and aggregate size, soil aggregate stability and surface crust, influence splash erosion (Lu *et al*., 2016; Saedi *et al.*, 2016). Splash erosion is localized as soil particles are not carried far from source (Oakes *et al*., 2012). Alternately, sheet erosion occurs when discharge is un-concentrated and soil particles are detached through raindrop impact under intense rainfall, where soil particles are removed down-slope by sheet flow (Oakes *et al*., 2012; Chaplot, 2013). Linear erosion results from the transport of detached soil particles by overland flow. This type of erosion typically results in the formation of rills, while overland flow is primarily responsible for gully erosion (Ollobarren *et al*., 2016).

The increased rate at which soil erosion occurs is a result of increased runoff on soil surfaces that are vulnerable to soil detachment (Van Oost *et al*., 2009). If soils have properties such as crusting, slacking and lack of macro-pores, which prevent water infiltration, the runoff coefficient will be greater (Liu *et al*., 2012). However, if the soil has a rough surface, runoff will be hindered by ponding water allowing water to infiltrate, thereby reducing soil erosion (Gao *et al*., 2016). Soils covered by vegetation generally experience increased infiltration due to better soil structure and protection against sediment detachment, reducing the vulnerability of the soil to erosion (Keesstra *et al*., 2016).

2.2.1 Controlling factors in sediment dynamics

The combined and interactive effects of the principle erosion factors that influence soil erosion by water, and control sediment dynamics, include: rainfall erosivity, soil erodibility, slope characteristics, vegetation cover and land use management (Parsakhoo *et al.,* 2014; Li *et al*., 2015; Maïga-Yaleu *et al*., 2015; Lu *et al.,* 2016).

2.2.1.1 Rainfall erosivity

The capability of rainfall and runoff to cause soil detachment and transportation is referred to as rainfall erosivity. This is a result of raindrop impact and the resultant runoff (Le Roux, 2011). The erosive power of rainfall depends upon the kinetic energy (E_K) of the rain, which is controlled by the interactions between raindrop size and mass, drop velocity, rainfall intensity and duration, and wind speed (Le Roux, 2011; Lu *et al*., 2016; Saedi *et al.,* 2016). Kinetic energy plays a significant role in rainfall erosivity as it represents the total rainfall energy available for detachment and sediment transport and is generally used in soil erosion modelling (Nel and Sumner, 2007).

2.2.1.2 Soil erodibility

Soil erodibility refers to the ability of a soil to resist the force of impact from rainfall and runoff. It measures how susceptible soil particles are to detachment and sediment transportation (Gyssels *et al.,* 2005; Le Roux, 2011). Soil chemical and physical properties, and their interactions, are the most significant determinants of erodibility. Aggregate stability and infiltration capacity are the primary factors affecting erodibility, where these properties vary according to parent material, soil structure, shear strength, and organic and chemical content (Gyssels *et al.,* 2005; Le Roux, 2011; Lu *et al*., 2016; Saedi *et al.,* 2016). The soil parent material for many areas of South Africa are characterised by low resilience, making them vulnerable to soil degradation (Laker, 2004). Soil organic matter and chemical content provide an indication of the susceptibility of a soil to erosion. These properties play a vital role in aggregate stability and soil structure (Bronick and Lal, 2005) as high concentrations of SOC are linked to an increase in soil aggregation where "calcium (Ca^{2+}) and magnesium (Mg^{2+})

cations improve soil structure through cationic bridging with clay particles and SOC" (Bronick and Lal, 2005:12). On the contrary, sodium (Na^+) acts as a dispersive agent, causing clay particles to separate and soil aggregates to break-up which exacerbates soil erosion (Laker, 2004; Bronick and Lal, 2005). Soil organic carbon therefore plays a vital role in combating soil erosion as it promotes stable soil aggregation and soil structure which allows for larger pore spaces to be available for root growth, thus increasing the concentration of SOM present in the soil (Périé and Ouimet, 2008; Chaplot and Cooper, 2015; Rawlins *et al*., 2015).

2.2.1.3 Slope characteristics

Slope length, aspect and gradient affect the extent and degree to which soil erosion occurs. According to Laker (2004:350), "although slope length and slope form are important, slope gradient is by far the most important slope parameter related to erosion". The kinetic energy of the runoff water, which is responsible for the transportation of sediment, increases exponentially as the gradient of the slope increases. Erosion on gentle slopes usually occurs less often, as overland flow tends to be slow, allowing for water to pond which protects the soil from the impact of raindrops (Le Roux, 2011). Slope length behaves in a similar manner to slope gradient, where as the length of the slope increase, so too does the runoff and potential to erode. Long steep slopes, which are common in the Drakensberg, cause the land to be vulnerable to erosion in particular when vegetation cover is sparse or removed (Le Roux, 2011).

2.2.1.4 Vegetation cover and land use management

Changes in land cover or land use cause the physical and hydrological properties of soil to vary (Fu *et al*., 2003). This is crucial, as these properties play a significant role in the structure, function and processes of the environment. Vegetation cover protects the soil from erosion, as above-ground biomass retards water movement, preventing detachment and transportation of soil particles and promotes infiltration (Gyssels *et al*., 2005; Pimentel, 2006). In addition, the role of below-ground biomass improves soil aggregate stability, protecting the soil from erosion. Roots aid in joining soil particles to form stable macro-aggregates, increase soil porosity and supply decomposable organic deposits to the soil (Laker, 2004; Gyssels *et al*., 2005). According to Laker (2004), the type of vegetation within an area is important in determining the effectiveness of vegetation cover in preventing erosion. Grasses usually provide more soil protection than other vegetation types, as they have greater basal coverage and a denser - fine root system that binds soil particles (Laker, 2004). Changes in soil vegetation are often a result of change in land use, associated with population growth, climate change or technological innovations (Laker, 2004; Pimentel, 2006).

In Africa, mismanagement of agricultural land due to overstocking and overgrazing is a major causative factor of erosion (Rowntree *et al*., 2004). Overstocking of livestock within rural communities leads to overgrazing, which results in changes to grass species composition, removal of vegetative cover, decreased in biomass, and increased exposure of soil, making rangelands susceptible to erosion (SWSR, 2015). In Okhombe, the overstocking and overgrazing of cattle has led to the formation of numerous cattle paths, as the cattle are herded on a daily basis up and down the slopes to access pastures on top of the hills (Birkett *et al*., 2016). Cattle paths are highly susceptible to soil erosion as they follow steep inclines and are often situated on shallow soils and exposed to harsh climates (Grab and Kalibbala, 2008). In addition, trampling by cattle removes vegetation, reduces infiltration and increases runoff as soil compaction and surface crusting occurs (Wilson and Seney, 1994; Evans, 1998; Laker, 2004; Gamoun *et al*., 2010).

Trampling causes reduction in interstitial spaces for water capture and seed germination and restricts the capacity of the surface to capture and store soil water (Gamoun *et al*., 2010). Furthermore, hoof action breaks-up naturally occurring soil aggregates and increases the compaction of the soil surface layer, thus increasing the bulk density (ρb) (Castel and Cantero-Martinez, 2003). Highly compacted soils have bulk densities ranging between 1.4 to 1.6 g cm^{-3} (Hossain *et al*., 2015) and cause pore volume to decrease (Logsdon and Karlen, 2004) as ρb is inversely proportional to total porosity which provides a measure of the pore spaces available in the soil for air and water movement (Castel and Cantero-Martinez, 2003). Alternatively, soils that have a high OM content will have a ρb of <1.0 g cm^{-3}, with increased pore volume for root growth and the movement of air and water (Hossain *et al*., 2015).

The contribution of soil erosion to land degradation not only includes the loss of fertile topsoil and the decline in soil productivity, but also results in off-site impacts as the movement of soil particles increases the delivery of sediment to water sources (Le Roux *et al*., 2007; Le Roux *et al*., 2008; Maalim *et al*., 2013). The accumulation of eroded material leads to sedimentation and siltation of rivers and causes increased suspended sediment concentrations within streams. This results in adverse effects on ecosystem health, where the biodiversity of the fauna, flora and microbes in the soil are negatively affected (Le Roux *et al*., 2007; Le Roux *et al*., 2008; Maalim *et al*., 2013; Parsakhoo *et al*., 2014). These cumulative effects have significant implications for the provision of ecosystem services, in particular, impacting water quality in marginalised rural communities (Lal, 2003; Sonneveld *et al*., 2005; Pimental, 2006; Wang *et al*., 2016).

2.3 Rill and gully erosion

Rill erosion occurs when concentrated flow exceeds a specific point of soil resistance and forms small yet well-defined channels, which are easily filled by tillage methods (Wirtz *et al.,* 2012; Di Stefano *et al*., 2013; Li *et al*., 2015; Shen *et al*., 2016). Over time and after excessive erosion, these rills enlarge into deep trenches, known as gullies (Poesen *et al*., 2003; Luffman *et al*., 2015; Ollobarren *et al*., 2016). Gullies are watercourses characterised by "steep channel walls, a stepped longitudinal profile, and commonly an abrupt channel head" (Mousazadeh and Salleh, 2014:507). Unlike rills, gullies are unable to be filled by tillage operations, and control techniques are costly and challenging to implement (Valentin *et al*., 2005; Luffman *et al*., 2015; Ollobarren *et al.,* 2016; Li *et al.,* 2017). Gullies are therefore an indication of extreme land degradation and significantly affect rural livelihoods as they impinge on farming and agriculture, and produce much sediment which leads to siltation of water sources downstream and may cause flooding (Li *et al.*, 2017).

2.4 Soil aggregates and soil property dynamics

Soil aggregates are "secondary particles formed through the combination of mineral particles with organic and inorganic substances" (Gelaw *et al*., 2015:690; Torres-Sallan *et al*., 2018). Their dynamics and stabilization are complex process driven by multiple factors related to soil and vegetation characteristics, land management and climate (Erktan *et al*., 2015). Aggregates are usually classified as large macro-aggregates (>2000 µm), small macro-aggregates (250-2000 µm), micro-aggregates (53-250 µm) and silt plus clay sized aggregates and particles (<53 µm) (Six *et al*., 2000; De Gryze *et al.,* 2004; Chaplot and Cooper, 2015; Totsche *et al*., 2017; Torres-Sallan *et al*., 2018).

Each aggregate size group differs in properties, such as binding agents and C and N distribution, where "SOC and N retention in soils is characterised by short-term storage in macro-aggregates (result of weakly associated micro-aggregates) and long-term sequestration in micro-aggregates" (Gelaw *et al*., 2015:690; Totsche *et al*., 2017). The short-term storage of SOC and N, within macro-aggregates, can be attributed to the mineralization of SOM binding micro-aggregates to macro-aggregates. Alternatively, SOM can be physically protected from microbial attack by adsorption to clay minerals and the formation of micro-aggregates, resulting in long-term C sequestration (Beare *et al.*, 1994). Macro-aggregates are less stable than micro-aggregates because of the nature of the binding agents involved in their formation. This causes SOC, associated with macro-aggregates, to be lost more rapidly than SOC associated with micro-aggregates, as macro-aggregates are more sensitive to disruptive forces brought about through land use changes, and to dispersion that results from raindrop impact (Beare *et al.,* 1994; Gelaw *et al*., 2015). Thus, SOC and N are more protected in micro-aggregates and less protected in macro-aggregates, as micro-aggregates are more stable and less sensitive to dispersion than macro-aggregates.

Soil aggregation is beneficial to the environment as it "enhances aeration, structure, water holding capacity and infiltration which improves root establishment and plant growth" (Torres-Sallan *et al*., 2018:52). It acts as an indicator of soil quality due to the impact it has on soil functions and degradation, such as water availability to plant roots and run-off. This occurs as a result of the influence it has on pore size distribution, erodibility and decreases in oxygen diffusion, which are related to the formation of surface crusting by slaking (forces related with trapped air) (Rawlins *et al.,* 2015). Furthermore, aggregation physically protects SOM from microorganisms and their enzymes, preventing mineralisation of SOM and CO_2 emissions into the atmosphere. Therefore, soil aggregates have the potential to improve SOM stabilization resulting in increased turnover times of OC in soils and therefore play a significant role in C sequestration (Six *et al*., 2000; Chaplot and Cooper, 2015; Erktan *et al*., 2015; Torres-Sallan *et al*., 2018). This is of particular importance as soils are the largest terrestrial OC pool storing 2344 Pg C (1 Pg = 1 billion tonnes) of SOC in the top three metres, to play a role in the global carbon cycle (Jobbágy and Jackson, 2000; Paul *et al*., 2008; Yigini and Panagos, 2016).

Land use and land use management, lithology and local climate changes (Márquez *et al*., 2004; Gelaw *et al*., 2015) affect soil aggregate size distribution and aggregate stability. Soil organic carbon dynamics are thus impacted, as the balance of SOC is determined by gains in organic inputs, and losses due to OM turnover which is influenced by soil aggregation (Chaplot and Cooper, 2015; Yigini and Panagos, 2016). Soil organic carbon and clay content are significant determining factors of water stable aggregation where SOM influences soil physical processes including bulk density (ρb) and water stable aggregation (Gelaw *et al*., 2015). Unsuitable land use management practices, through overstocking and overgrazing, significantly affects soil aggregate stability. These practices lead to vegetation removal and promotes soil compaction through trampling (Maïga-Yaleu *et al*., 2015; Doetterl *et al*., 2016). Furthermore, water erosion has the most significant impact on SOC and N storage as the susceptibility to erosion increases due to soil compaction where raindrop impact and overland flow cause aggregates to break-down (Guoxiao *et al*., 2008; Ma *et al*., 2014; Maïga-Yaleu *et al*., 2015; Doetterl *et al*., 2016). This results in the detachment and transport of SOM and the physical removal of SOC and N (Wilson and Seney, 1994; Laker, 2004; Gyssels *et al*., 2005; Borrelli *et al*., 2016). Moreover, the break-down of soil aggregates increases the exposure of OM to oxidizing conditions, resulting in increased CO_2 emissions (Chaplot and Cooper, 2015).

Sarno *et al*., (2004) suggest that a decrease in SOC increases the susceptibility of soil to erosion, which in turn increases the rate of SOC loss (Guoxiao *et al.,* 2008). Subsequent to the loss of SOC and N, "a deficiency of plant nutrients, the deterioration of soil structure, a diminished soil workability, and a lower water-holding capacity" (Guoxiao *et al*., 2008:2007) can occur, impacting on ecosystem functionality (Dabney *et al*., 1999; Guoxiao *et al*., 2008; Borrelli *et al*., 2016; Schmiedel *et al*., 2017). The sequestration capacities of the soil is reduced, as a loss of SOC decreases the uptake of C in terrestrial environments (Janueau *et al*., 2014). Soil erosion not only negatively impacts soil dynamics (Parsakhoo *et al.*, 2014), but the unimpeded runoff modifies stream flow regime and produces substantial amounts of sediment leading to water quality and aquatic ecosystems being adversely affected (Yüksel *et al*., 2008; Nosrati *et al*., 2015). The effects of soil degradation are therefore experienced throughout the ecosystem, as the erodibility of soils increases as aggregate stability decreases, creating a significant land use management issue.

2.5 ^{137}Cs and ^{210}Pb$_{ex}$ as a proxy for soil erosion

In soil erosion studies, the use of traditional measurement techniques (for example erosion plots) to document soil redistribution have presented many limitations (for example erosion plots are costly to install and need to be monitored for extensive periods etc.). Attention has therefore been directed to the use of environmental radionuclides to link soil redistribution patterns to SOC and total N patterns (Guoxiao *et al*., 2008; Humphries *et al*., 2010; Nosrati *et al*., 2015). The use of fallout radionuclides presents a unique opportunity to document sediment transportation and deposition rates and to trace the movement of sediment through landscapes (Walling, 2012; Parsons and Foster, 2011).

The fallout radionuclides caesium-137 (^{137}Cs), lead-210 (^{210}Pb) and beryllium-7 (^{7}Be), have proved to be an effective way of studying soil redistribution patterns, as they are rapidly fixed on reaching the soil surface and their post-fallout redistribution offers a means of providing information on soil redistribution within the landscape (Walling, 2012). In essence, soil cores are collected at numerous points across a field, where the measurements of radionuclide areal activity density or inventory are taken. Points of erosion and deposition can be identified by comparing the measured inventory with those of a reference inventory, inventory collected from an adjacent stable undisturbed site. Areas of erosion will have inventories less than that of the reference site, whereas areas of deposition will have inventories greater than that of the reference site (Walling, 2012; Poręba, 2006; Wakiyama *et al*., 2010; Mabit *et al*., 2014).

It is assumed that inventories collected in the disturbed site were once equal to the inventory collected from the undisturbed reference site. The rate and pattern of soil erosion and deposition within a study area is then calculated by using ^{137}Cs and ^{210}Pb measurements and models that convert these measurements to estimates of soil redistribution rates (Ritchie *et al*., 2007). Conversion models used with ^{137}Cs measurements are either empirical models or theoretical models. Empirical models determine the extent of the loss or gain in ^{137}Cs inventory, relative to the reference inventory, by using empirical measurements collected from long-term erosion-plot data (Walling *et al*., 2002; Walling, 2012). Alternatively, theoretical models consider the main factors (including the erosion and deposition rates) that will influence the magnitude of the ^{137}Cs inventory. These factors are then incorporated into an algorithm which estimates the expected inventory for a given erosion or deposition rate (Walling, 2012). Some examples of these models include the Mass-Balance Models, Profile Distribution Models and Diffusion and Migration Models (Walling *et al*., 2002).

Fallout radionuclide, ^{137}Cs, is man-made and was released into the atmosphere by the testing of above-ground thermonuclear weapons (bomb tests) in the late 1950s to early 1960s (Walling, 2012; Zapata *et al*., 2002; Poręba, 2006; de Neergaard *et al*., 2008; Wakiyama *et al*., 2010; Mabit *et al*., 2013; Nosrati *et al*., 2015). Bomb testing caused ^{137}Cs to be injected into the stratosphere, where it was dispersed globally before settling as fallout (Walling, 2012). Further fallout occurred due to the Chernobyl accident in 1986, affecting parts of Europe and surrounding areas. Maximum fallout is found within the northern hemisphere as most of the bomb testing occurred there, this presents some limitations on the use of ^{137}Cs in the southern hemisphere, as fallout received in the south is approximately 30% of that received in the north (Walling, 2012; Humphries *et al*., 2010; Courtier *et al*., 2017). Southern hemisphere investigations have been conducted in Brazil and Australia, and one study has been carried out in southern Africa (Humphries *et al*., 2010). Caesium-137 ($t_{1/2}$ 30.1 years) has a high affinity for fine soil particles, and its world-wide distribution has made it almost a universal environmental tracer for studying up-slope soil erosion and downstream sedimentation (Wakiyama *et al*., 2010).

Compared to ^{137}Cs, ^{210}Pb ($t_{1/2}$ 22.3 years) is produced in the decay chain of Uranium-238 (^{238}U) and is a naturally occurring radionuclide. A product of the ^{238}U decay chain is radium-226 (^{226}Ra, $t_{1/2}$ 1,600 years), which decays to gaseous radon-222 (^{222}Rn, $t_{1/2}$ 3.8 days). This undergoes numerous short-lived decays resulting in ^{210}Pb (Walling, 2012; Wakiyama *et al*., 2010; Mabit *et al*., 2014; Courtier *et al*, 2017; Meusburger *et al*., 2018). As this decay process occurs, a portion of the ^{222}Rn is released from the soil into the atmosphere, where it decays to ^{210}Pb, and is deposited on the earth's surface as fallout (Fang *et al*., 2013; Gaspar *et al*., 2013; Szmytkiewicz and Zalewska, 2014; Meusburger *et al*., 2018). This is referred to as unsupported or excess ^{210}Pb ($^{210}Pb_{ex}$) and is the component of interest for erosion and depositional studies. The remaining ^{222}Rn within the soil decays to ^{210}Pb, and is called supported ^{210}Pb as this is an *in situ* product of ^{226}Ra (Fang *et al*., 2013; Gaspar *et al*., 2013; Mabit *et al*., 2014). The activity of $^{210}Pb_{ex}$ decreases with sediment depth and is used to determine the rate of sediment accumulation, linear accumulation rates, and for dating consecutive sediment layer (Szmytkiewicz and Zalewska, 2014). It is absorbed onto soil and sediment particles where its redistribution in the soil and across the landscape is associated with the movement of soil particles due to land use practices, erosion and sediment transport processes (Fang *et al*., 2013; Gaspar *et al*., 2013; Mabit *et al*., 2014). Currently, less information regarding the global variation of $^{210}Pb_{ex}$ fallout is known compared to ^{137}Cs (Walling, 2012).

Takenaka *et al*., (1998) suggests that the distribution of ^{137}Cs be related to the existence of SOC, as ^{137}Cs and SOC move along slopes at the same rate and along similar physical paths through soil erosion. Likewise, according to Teramage *et al*., (2013), both ^{137}Cs and $^{210}Pb_{ex}$ are strongly adsorbed by OM and fine soil particles after deposition. This leads to the movement of these fallout radionuclides depending on the movement of the soil components (Gaspar *et al*., 2013; Mabit *et al*., 2014; Meusburger *et al*., 2018). This demonstrates that fallout ^{137}Cs and $^{210}Pb_{ex}$ can be used to directly quantify dynamic SOC and soil redistribution by erosion within a landscape (Nosrati *et al*., 2015). The benefit of using the ^{137}Cs technique is that it can provide retrospective information on medium-term redistribution patterns of soils within the landscapes, without long-term monitoring programs. Whereas $^{210}Pb_{ex}$ provides retrospective assessment of long-term soil redistribution rates over a period of 100 years. The use of fallout radionuclides as a proxy for soil erosion and SOC distribution could therefore contribute to an understanding of soil processes within a landscape (Richie *et al*., 2007; Nosrati *et al*., 2015).

Caesium-137 and $^{210}Pb_{ex}$ have been applied to erosion-based studies. For example, a study conducted by Fang *et al*., (2013) used $^{210}Pb_{ex}$ measurements to assess the long-term rates and spatial patterns of soil redistribution in an agricultural catchment in the black soil region of north-eastern China. In another study, Collins *et al*., (2001) reported on the use of ^{137}Cs measurements to quantify medium term (± 40 years) soil erosion and redistribution rates in cultivated and uncultivated areas within the Upper Kaleya River Basin in southern Zambia. Locally, a study conducted by Humphries *et al*., (2010) on the Mkuze River floodplain used ^{137}Cs and ^{210}Pb to determine sedimentation rates. This study will be discussed below in more detail, to provide an example of applicability within a local context.

2.5.1 The Mkuze River floodplain, South Africa – A Case Study

Floodplain wetlands such as the Mkuze Wetland System is an important sink for solutes. Humphries *et al*., (2010) conducted a study which represented "the first attempt known to the authors to derive sediment accumulation rates using ^{137}Cs and ^{210}Pb in a southern African wetland. The study describes and examines processes of clastic and chemical sedimentation on the Mkuze River floodplain and considers their implications for the long-term evolution of the wetland system" (Humphries *et al*., 2010:89). With short-term sedimentation rates of 0.25 to 0.50 cm/y, ^{137}Cs and ^{210}Pb measurements indicated that the Mkuze River floodplain system is:

1. Rapidly aggrading ("the accumulation of sediment in river channel raising the stream-bed height" (Mugade and Sapkale, 2015:209) and,
2. Should experience avulsion often ("diversion of a majority of flow from one channel into another, leading to a total or partial abandonment of the previous path" (Field, 2001: 95).

These results highlight the importance of the floodplain, as it acts as a sink for solutes which concentrate in the groundwater and precipitate out (solidify) through evapotranspiration. The study concluded that the Mkuze River floodplain system "is an actively evolving system, which continues to aggrade as a result of the combination of clastic and chemical sedimentation" (Humphries *et al.*, 2010:89). The study showed that the use of radionuclides can be applied toward understanding wetland formation, evolution and functionality in a region.

2.6 Cattle path erosion

The overcrowding and overstocking of livestock within rural communities of SA can be partly attributed to the formation of the 'homelands' (now communal areas) or self-governing territories, which were established under the Natives Land Acts of 1913 and 1936 during the

Apartheid era (Pile, 1996; Wessels *et al*., 2007; Wessels *et al*., 2008). This resulted in the involuntarily resettled of black people to designated areas, were approximately 94% of the displaced people were forced to move to the reserves (Pile, 1996). This adversely affected their livelihoods as these people, who were once a part of a stable community, were uprooted and forced to live in areas where the unsustainable land was unable to support them (Wessels *et al*., 2008). The establishment of the existing rural landscape and subsistence farming was thus partly a result of policy, which has dictated the arrangement of many rural communities present distribution.

In the 1940s the Betterment Scheme policy was implemented, with the objective to improve land management in rural communities. This resulted in the transformation of the formally scattered homesteads into planned villages, and the reduction of livestock numbers was enforced (Pile, 1996; Peden, 2005; Sonneveld *et al*., 2005). The government invested in job creation and soil conservation works (contour banks, small dams and tree planning) within specific areas, including the KwaZulu-Natal Drakensberg region. However, this policy "adopted an authoritarian and punitive approach with little educational input" (Peden, 2005:168) which resulted in resistance from community members, where soil conservation works were often neglected and destroyed (Pile, 1996; Peden, 2005). Post-apartheid, state agriculture policy began to support smallholder black farmers, where it committed to land reform, increasing access to finance, empowering women, and supporting young people in agriculture. Rangeland scientists then noted, at a policy-making symposium for communal rangelands, that increased educational support, which adopted a community based approach, and institutional capacity building in communal areas, was required (Peden, 2005).

Today, communal areas continue to reflect the consequences of Apartheid where increases in human population and land degradation remains a prominent feature. Soil erosion continues to severely affect the livelihoods of these communities as the impacts of land degradation on the grasslands is evident (Sandhage-Hofmann *et al*., 2015). Furthermore, cattle are communally owned and have significant cultural value which leads to extensive grazing and overstocking, increasing the vulnerability of the rangelands to erosion, making management an ongoing issue (Dlamini *et al*., 2011; Dlamini *et al*., 2014). It is however the mismanagement of the movement of cattle for foraging that threatens the sustainability of the landscape, particularly in sloping rangelands, as grazing consists of various complex processes, namely: item selection for foraging, herbivory and trampling (Parsons and Dumont, 2003; Gamoun *et al*., 2010). The movement of cattle up-and-down the sloping rangelands leads to loss in vegetation, decrease in soil surface coverage and increase in soil compaction, as constant hoof action and trampling by cattle along paths, increases the susceptibility of the rangelands to erosion (Oakes *et al*., 2012).

Livestock trampling and the removal of vegetation are usually the first consequences of cattle path formation (Wilson and Seney, 1994; Grab and Kalibbala, 2008). Furthermore, the natural movement of water down-slope is impeded by cattle path, which is crucial in a region characterized by event-driven summer storms (Birkett *et al*., 2016). On slopes with no cattle paths, water flows in sheets over the surface, creating a larger surface area for infiltration to occur. On slopes with cattle paths, water flows over the surface in sheets until it is intercepted by the cattle path and then follows the path to the foot of the slope. This results in reduced surface area for infiltration, increased velocity of the water and increased runoff (Birkett *et al*., 2016). Cattle paths which are often considered as 'small-scale landscape influences' have the ability to transform slopes through erosion, as they severely affect agricultural productivity, downstream water sources and cause gully formation (Grab and Kalibbala, 2008).

2.7 Conclusion

The abundance of SOM within soils act as an indicator of soil health and contributes to the provision of quality ecosystem services within rural communities (Egoh *et al*., 2011). The Okhombe region in Drakensberg KwaZulu-Natal, is highly susceptible to soil erosion due to: sloping topography; overstocking (approximately 4000 cattle and 2000 small stock) (Sonneveld *et al.*, 2005; Birkett *et al*., 2016); overgrazing (where the complete loss of highly palatable grass species has occurred) (Sonneveld *et al.*, 2005); and trampling by cattle, resulting in cattle path formation. Continuous trampling and hoof action, by cattle, cause soil aggregates to break-up and SOC and N to be lost as cattle paths expose the soil, making it vulnerable to erosion. As a result, community livelihoods are threatened as gully formation transforms the landscape and loss of SOC and N occur, which leads to further degradation as soil structures become less stable and more prone to erosion.

Determining the impact of erosion on soil properties by applying fallout radionuclide activity as a proxy for soil erosion and SOC distribution within landscapes, could provide an indication on how SOC and N are affected by cattle path erosion. Fallout radionuclides ^{137}Cs and $^{210}Pb_{ex}$ are rapidly fixed to soil particles and follow the movement of these soil components where points of erosion and deposition can be identified by comparing reference inventory with inventory collected from a disturbed site. This research will contribute to the ongoing efforts to minimize land degradation within Okhombe as the loss of land through excessive erosion, and the depth and extent of ever expanding gullies, are of utmost concern to the residence. This is significant as deep expanding gullies increase the risk of flooding and present a safety hazard to livestock and community members.

Chapter Three
Methods

3.1 Introduction

This chapter is subdivided into two sections, site description and experimental design. The site description provides detail of the biophysical climate, vegetation and geology aspect, whilst the experimental design outlines the soil sampling procedures and soil analysis completed through physical fractionation and the use of fallout radionuclides.

3.2 Study Area

Okhombe (within $28^{0}71'$ S; $29^{0}08'$ E and $28^{0}42'$ S; $29^{0}05'$ E) is a communal grazing area situated 50 km northwest of Bergville located within the Upper Thukela Catchment of the KwaZulu-Natal Province of South Africa (Figure 3.1). This catchment plays a vital role in water provision for the provinces of KwaZulu-Natal and Gauteng as it forms part of the main escarpment (watershed) of South Africa. Okhombe forms part of the Drakensberg foothills and lies within 10-20 km of the north-eastern border of Lesotho and the Free State Province and falls within the administrative boundaries of the uThukela District Municipality (Sonneveld *et al*., 2005; Temme *et al*., 2008; Temme *et al*., 2009; Mansour *et al*., 2012). The uThukela District Municipality is primarily rural with high levels of poverty, unemployment rates at 49% and a low revenue base, as 36% of the population earn between R6 000 and R18 000 per annum. Services are limited with poor infrastructure (South Africa, 2010).

The climate of the area is sub-humid with a mean annual rainfall ranging from 800 mm to 1265 mm (Marx, 2011), with seventy percent of the annual rainfall received during the summer months (November - March) (Everson *et al*., 2007; Temme *et al*., 2008; Temme *et al*., 2009). Temperatures vary with a change in season from moderate summers to cool winters. From November to February high temperatures are experienced with very low temperatures occurring in May to July. The mean air temperatures range between 11.5^{0}C and 16^{0}C, where frost occurs from late April to early September. Although snow falls at higher elevations, the Okhombe ward seldom receives snow (Tau, 2005; Mansour *et al*., 2012). The vegetation is predominately grassland, with a mosaic of indigenous forest and shrubs (Temme *et al*., 2008; Mansour *et al*., 2012).

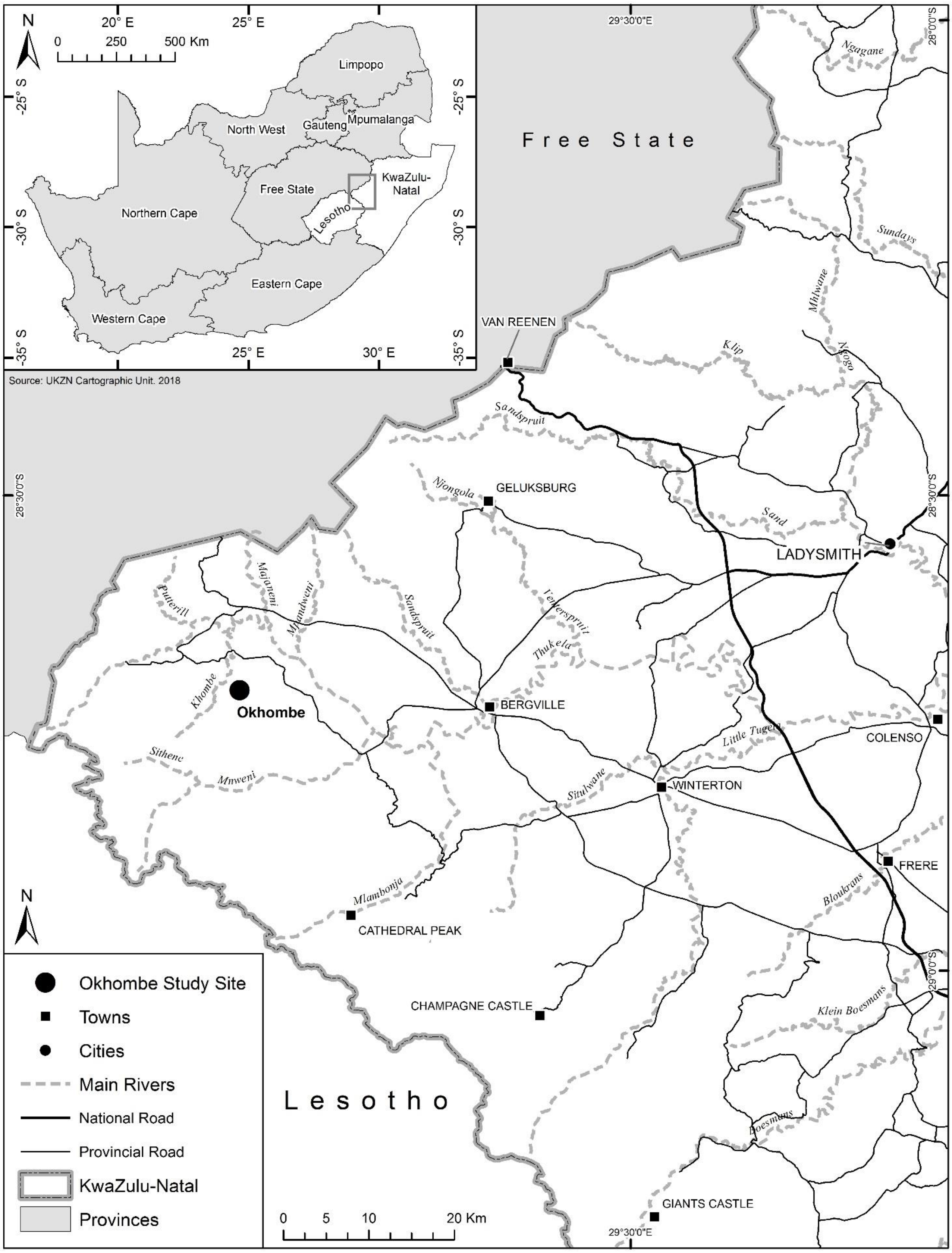

Figure 3.1. Location of Okhombe catchment in South Africa.

According to the Acocks classification of vegetation types, the area is under Southern Tall Grassveld and Highland Sourveld (Veld type 44a) (Everson *et al*., 2007; Temme *et al*., 2008) or Northern Drakensberg Highland Grassland (GD5) (Mucina and Rutherford, 2006; Marx, 2011). Sourveld is characterised by high rainfall (approximately 625mm or more per annum) and acidic soils, making grazing capacity low compared to sweetveld (van Oudtshoorn, 2012). Grasses provide palatable grazing during the growing season as nutrients are stored within the roots. However, during autumn and the dry season grasses are unpalatable and very low in nutritional value (van Oudtshoorn, 2012). Sourveld grasses can tolerate mild overgrazing however, the recovery of composition back to palatable grasses, after overgrazing, is slow. Generally sourveld grasses produce high volume forage, but of low quality (van Oudtshoorn, 2012).

Okhombe is located 1200 to 1800 m above sea level, with the topography of the region forming part of the Eastern escarpment of South Africa, reaching heights of 3500 m. The geology of the study area consists predominately of rock types belonging to the Triassic and Permian age, the Beaufort Group, which was comprehensively intruded by dolerite sills and dykes in the Jurassic. On slopes and plateau, a mixture of mudstone, sandstone, tillite, ampholite, and basalt are commonly found (Sonneveld *et al*., 2005; Temme *et al*., 2008; Mansour *et al*., 2012). The high relief and associated steep gradients have been designated as communal grazing land, resulting in accelerated erosion through the use of cattle paths. The excessive erosion has led to the formation of rills and dongas which are prominent features of the landscape (Sonneveld *et al*., 2005; Dlamini *et al*., 2011).

3.2.1 Soil Erosion in Okhombe

In the early 1960s the Okhombe catchment was re-planned for agricultural production, where communal grazing was designated to the mountain slopes and plateau and cropland to the lower areas alongside the rivers. This forced community members to re-locate to one of the six nearby sub-wards (villages) namely: Enhlanokhombe, Oqolweni, Sgodiphola, Ngubhela, Mpameni and Mahlahathini (Sonneveld *et al*., 2005; Tau, 2005). Communal grazing areas were specifically designed to incorporate fenced grazing camps for the accommodation of livestock. Currently, these camps are not in use and the movement of cattle is mismanaged. There are approximately 4000 cattle and 2000 small stock (principally goats) in the area, where grazing on the hillslopes takes place during the summer months (September to May) (Plate 3.1a). In winter, the cattle are allowed to graze the remains of crops, mostly maize stalks, in the valley bottoms, since grass becomes unpalatable (Sonneveld *et al.*, 2005; Birkett *et al*., 2016). The lack of security and theft has resulted in the cattle being kept close to the homestead, where they are moved up and down the slopes on a daily basis (Plate 3.1b) (Sonneveld *et al*., 2005). This intensified movement of cattle leads to cattle path formation, as no formal management plan for grazing exists within this area.

Cattle path formation occurs as constant hoof action and trampling creates a channel for rain water to flow, as it follows the cattle paths to the foot of the slope (Birkett *et al*., 2016). The increased runoff and soil erosion affects downstream water sources and cause 'donga' formation – "distinct gullies carved out of the slope by surface runoff and contraction and expansion cycles" (Marx, 2011:22) (Plate 3.2).

Plate 3.1. (a) Plateau at Okhombe with homestead in the background against the backdrop of the Drakensberg(b) Livestock grazing on the hillslopes, with cattle paths evident in the background.

Plate 3.2. Cattle hoof prints in a donga below the study site.

Dongas are a common feature within the Okhombe region where community members struggle to access schools, halls and shops, as dongas migrate closer to homesteads, telephone poles and communal gardens (Everson *et al*., 2007). Dongas result in large quantities of silt being washed away into river systems where they are transported into dams that form part of the Tugela-Vaal water transfer scheme i.e. Woodstock Dam and Sterkfontein Dam (Peden, 2005; Everson *et al*., 2007; Dlamini *et al*., 2011). This silt not only reduces the capacity of the storage reservoirs, but is expensive to remove. According to the SA State of Environment Report, soil erosion costs the country approximately R2 billion per annum including costs for off-site purification and silted dam water (Le Roux *et al*., 2008; DEA, 2012).

Everson *et al*., (2007: v) state that the community members attribute donga formation to community practices such as “uncontrolled livestock movement, moulding bricks, use of sedges and incorrect tillage practices”, where they are aware that water and soil erosion are linked and have stated that dongas become seasonal streams. Land degradation and soil erosion is therefore prominent within the Okhombe community, and is recognised as a concern. Land rehabilitation is therefore vital in this community as land productivity and water resources are under threat.

3.2.2 Okhombe LandCare Project

De Beer *et al.,* (2005) stated that one of the limitations in managing land degradation involves educating people on the benefits of implementing soil erosion control measurements. In 1998, community involvement in land conservation within Okhombe became possible through the launch of a government initiative National LandCare Programme pilot project (Peden, 2005; Everson *et al*., 2007). This project aimed to create jobs through promoting community awareness and involvement in rehabilitating degraded areas within the catchment. It included objectives that addressed complex issues which affect the livelihoods and provision of ecosystem services within the community i.e. environmental education and awareness, rangeland management, community gardens, and craft and eco-tourism. These issues were addressed in various ways. Community education was imparted through informal workshops and training, whilst land rehabilitation was addressed through physical structures such as stone packs, stone lines, swales and cattle steps and by planting indigenous and exotic vegetation, such as vetiver grass, along contour lines and trees in micro-catchments.

The Okhombe LandCare Project was coordinated by the University of KwaZulu-Natal (formerly University of Natal), the Department of Environmental Affairs and Tourism, Council for Scientific and Industrial Research (CSIR), Bergwatch and Ezemvelo KZN Wildlife; where local groups were established and trained to sustain the management of natural resources within the community. These groups included: the Okhombe Inthathakhusa Monitoring Group (OMG) - responsible for monitoring the effect of soil erosion control measures; the Okhombe LandCare Trust - responsible for raising funds and managing community conservation efforts; the Okhombe Livestock Committee - responsible for managing communal grazing; and the Okhombe Tourism task team - responsible for encouraging community-based tourism.

The project was successful in educating the community and in rehabilitating many of the degraded areas. It was said that the rehabilitation activity “probably involved more people in the project than any other, and is certainly the most recognised and understood component of the project’s work” (Everson *et al*., 2007: 2); where the majority of the rehabilitation areas have clearly shown signs of stabilization. However, long-term sustainable management within Okhombe depends upon the capability of the community to identify and describe problems and to come up with solutions that can be implemented on an ongoing basis. This is possible through the payment for ecosystem services initiative, developed by the Maloti Drakensberg Transfrontier project. This initiative has the potential to encourage effective management of these natural resources within the community as it aims to secure the supply of ecosystem services, particularly water resources (Everson *et al*., 2007). Records kept by the Okhombe Monitoring Group on the decrease in soil erosion and the improvement of water quality, play a vital role in contributing to baseline data needed for this initiative, as research on water services will be required at community, local and national level. The LandCare Project has thus far been successful, where it has highlighted the need to integrate social and technological issues when generating solutions to environmental problems. This work remains an ongoing process.

3.3 Experimental Design

A 10 x 10 m grid sampling design was used to collect soil samples within the study area (de Neergaard *et al*., 2008), as the landscape surface forms are undulating (Pennock and Appleby, 2002). Soil samples were collected over a two-day period in four treatments, namely: the undisturbed reference site (1460 m above sea level (asl) which was used as a control; and the three degraded sampling sites i.e. top-slope (1439 m asl), mid-slope (1403 m asl), and lower-slope (1362m asl) (Plate 3.3). The slope positions were visibly determined according to the topography. Each degraded treatment represented a slope position; upper, mid and foot slope affected by cattle path erosion (excluding the control). Sampling was replicated three times at each slope position using a randomized 10 x 10 m grid.

Plate 3.3 Sampling positions along the slope at Okhombe.

3.4 Measurement of Slope and Vegetation

To determine the gradient of a slope, an Abney Level and measuring tape was used. The slope was measured downslope from the reference site to the lower-slope. This was conducted by the observer who stood at the sampling point with the Abney Level, while the assistant held the measuring rod at a distance of 50 m, 40 m, 21 m and 10 m away from the observer. Distances between sample points varied according to the form of the slope, and were measured using the measuring tape. The greatest distance between measurements was 50 m and the least was 10 m. The change in slope angle was read from the Abney Level and recorded in degrees. This process was replicated at each sample position (three sample positions) and averaged, where eleven angle readings were recorded along each profile. The recorded data was tabulated using Microsoft Excel, were the vertical distance was calculated to determine the difference in height between two points (Appendix A). From these values, slope length (m) and gradient (%) were determined. An average value for the slope length and gradient was taken and a slope profile was created.

The Braun-Blanquet classification method (Zietsman, 2003) was used to determine the vegetation cover and abundance at each 10 x 10 m sampling plot within each slope position (reference site, top-, mid- and lower-slope). The classification measured the aerial cover of shrubs and of grass at each plot. This process was replicated at each sample position where the average value was used.

3.5 Reference Site Selection

Radionuclides ^{137}Cs and $^{210}Pb_{ex}$ are rapidly fixed on reaching the soil surface where their post-fallout redistribution is associated with the movement of soil particles (Gaspar *et al*., 2013; Mabit *et al*., 2014). This movement of ^{137}Cs and $^{210}Pb_{ex}$ with soil particles provides information on soil redistribution within the landscapes, thus proving to be a potential technique in soil erosion studies. The successful execution of the ^{137}Cs and $^{210}Pb_{ex}$ technique is dependent on the selection of a reference site (Walling, 2012). The reference site is a stable undisturbed site, where no erosion or deposition occurs and is used to establish a ^{137}Cs and $^{210}Pb_{ex}$ inventory (Ritchie *et al*., 2007; Walling, 2012). Sample sites, where the measured ^{137}Cs and $^{210}Pb_{ex}$ is less than the ^{137}Cs and $^{210}Pb_{ex}$ found at the reference site, will be assumed to be eroding, while sites that have more ^{137}Cs and $^{210}Pb_{ex}$ than the ^{137}Cs and $^{210}Pb_{ex}$ found at the reference site will be assumed to be depositional sites (Porto *et al*., 2003; Ritchie *et al*., 2007; Walling, 2012). Walling (2012) provides a list of guidelines to help in the selection of an ideal reference site; the site should:

- not experience any soil erosion or deposition,
- have continuous vegetation cover,
- have perennial grass or low herb cover, and
- be located as close as possible to the disturbed sample sites.

The reference site within the study area was located on the plateau of a hill at 1460 m above sea level (Plate 3.4). The area had no evidence of soil erosion or deposition and vegetation cover was continuous. The vegetation is classified as Highland Sourveld (Veld type 44a) (Everson *et al*., 2007; Temme *et al*., 2008) or Northern Drakensberg Highland Grassland (GD5) (Mucina and Rutherford, 2006). The disturbed sites were located below the reference site along the slope.

Plate 3.4. Reference site located on the plateau at Okhombe.

3.6 Bulk Density

Soil samples for bulk density were collected within all sampling treatments (reference site, top- mid- and lower-slope). Samples were collected from the centre of each plot using a volume specific ring (5 cm internal diameter; 100 cm^3) (Plate 3.5a and b). Samples were taken at three depth intervals: 0-5 cm, 5-15 cm and 15-30 cm; thus nine samples per site were collected in total (three samples per plot). Samples were placed into zip-lock bags, labelled and transported to the University of KwaZulu-Natal for further analysis.

Plate 3.5. (a) Sampling for bulk density using a volume specific ring (5 cm internal diameter; 100 cm^3) (b) Soil sample for bulk density.

3.7 ^{137}Cs and ^{210}Pb$_{ex}$ and Soil Properties

Using a soil auger, samples for ^{137}Cs and ^{210}Pb$_{ex}$ analysis, and soil properties were collected from three points within each plot at depths of 0-5 cm, 5-15 cm and 15-30 cm and composited to form three independent samples representing each depth (nine samples per site) (Plate 3.6).. Soil samples were air-dried for 48 hours and passed through a 2 mm sieve. Soil sub-samples weighing 500g were taken from each position (reference site, top-, mid- and lower-slope) and depth interval (0-5 cm, 5-15 cm and 15-30 cm), and were sent to Cedara College of Agriculture Soil for soil property analysis. Soil sub-samples weighing 6g representing each position and depth were ground and sent to the School of Earth, Ocean and Environment at the University of South Carolina, Columbia, USA for ^{137}Cs and ^{210}Pb$_{ex}$ analysis. The cost for the analysis of radionuclides at the University of South Carolina, was within the available budget compared to that of other laboratories.

Plate 3.6. Sampling for ^{137}Cs, $^{210}Pb_{ex}$ and soil properties at reference site using a soil auger.

3.8 Laboratory analysis

Soil physical and chemical properties where measured and total C and N were analysed using LECO CNS-2000 Dumas dry matter combustion analyser GRAMMAR (LECO Corp., St. Joseph, MI) to evaluate SOC content and nitrogen content. Soil bulk density (ρb) was calculated using the core method, where representative sub-samples were weighed and placed into foil containers of known weight and were oven dried at 105^{0}C for 24 hours (Bilskie, 2001). It is important that an accurate measurement of bulk density of the soil is obtained, as it is required to convert the measured radionuclide concentration to the total inventory (Bq m^{-2}) and it is needed for C stock calculations. The weight of both the oven-dry sub-sample and the container was recorded and bulk density was calculated using Equation (1):

$$\rho b\ (g/cm^3) = \frac{\text{Dry soil weight (g)}}{\text{Soil volume (cm}^3\text{)}} \tag{1}$$

SOC stocks (SOCs) and nitrogen stocks (Ns) were calculated using the Equation (2) adapted from Abdalla *et al*., (2016):

$$\text{SOCs} = \text{SOCc} \times \rho b \times T\left(1 - \frac{PF}{100}\right) b \tag{2}$$

Where SOCs is SOC stock (kg C m^{-2}); SOCc is soil organic carbon content in the ≤ 2 mm soil material (g C kg^{-1} soil); ρb is the bulk density of the soil (kg m^{-3}); T is the thickness of the soil layer (m); PF is the proportion of fragments of >2 mm in percent; and b is a constant equal to 0.001.

3.9 Soil physical fractionation by wet sieving

Several methods have been put forward for determining soil aggregate-size distribution and stability, including physical fractionation (Márquez *et al.*, 2004; Arthur *et al*., 2014). Physical fractionation is achieved by applying various degrees (moderate or strong treatments) of dispersion to break bonds between soil aggregates (Christensen, 2001; Six *et al*., 2002; Moni *et al*., 2012). Density and/or size separation is then used to separate pools of SOM according to their size and extent of organo-mineral interaction. Various methods of dispersion can be used, moderate dispersion treatments include: shaking with or without glass beads, mild sonication, slaking, blade mixing and wet sieving (Moni *et al*., 2012). Strong dispersion treatments include: chemical dispersion and high-energy sonication treatments (Moni *et al*., 2012). Moderate dispersion through wet sieving according to Elliot (1986) (Six *et al*., 2002; Márquez *et al.*, 2004) is the most common method used for physical fractionation (Figure 3.2). Soils were submerged and sieved in water to imitate the natural stresses that occur when water enters into soil aggregates. The degree to which disruption occurs is determined by the moisture content of aggregates before wet sieving. Capillary-wetted pre-treatment by submerging air-dried soil in water prior to wet sieving allows for slaking to occur. During slaking unstable and/or weak soil aggregates are broken, as air that is trapped inside the soil pores causes pressure to build inside the aggregates resulting in disruption. Aggregates that are more stable will resist slaking (Six *et al*., 2002; Márquez *et al.*, 2004; Moni *et al*., 2012).

Physical fractionation isolates SOC pools that are sensitive to changes in climate, land use and land use management, thus increasing the detection limits for determining SOC storage (Six *et al*., 2002). This method highlights soil processes and mechanisms involved in SOC storage, where "aggregation increases in less disturbed systems and organic materials within soil aggregates (especially micro-aggregates) have lower decomposition rates than those located outside of aggregates" (Six *et al*., 2002:1982). Physical fractionation will indicate soil stability within the study area through the isolation of SOC within soil aggregates. This will determine the impact of cattle path erosion on soil properties as erosion causes soil aggregates to break-down and SOC and N to vary along slopes (Nosrati *et al*., 2015).

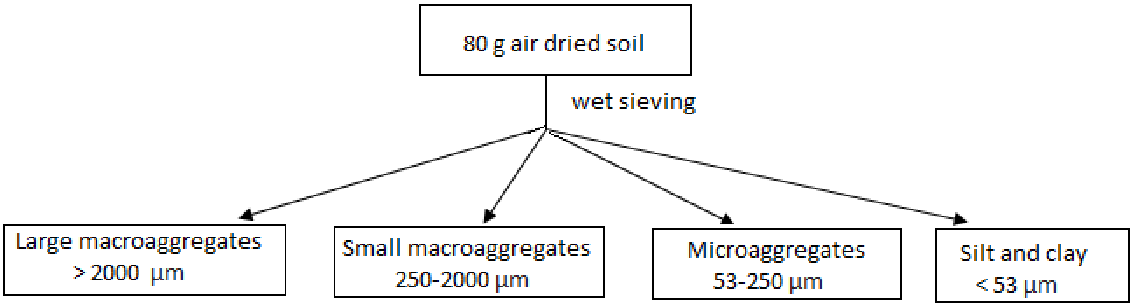

Figure 3.2. Fractionation by wet sieving to isolate aggregate and aggregate-associated organic matter fractions. Adapted from Six *et al*., (2002).

Physical fractionation was conducted to separate the water stable soil aggregates at each depth (0-5 cm, 5-15 cm and 15-30 cm) within each sampling treatment (reference site, top-, mid- and lower-slope). Wet sieving methods described by Elliott (1986) were used. Soil samples were air-dried for 48 hours and then passed through an 8 mm sieve to remove large stones. A sub-sample weighing 80 g was placed on a 2 mm sieve and submerged in water for 5 mins. Thereafter, the nested samples were wet sieved for 2 minutes, by moving the sieve up and down 50 times. The material that did not pass through the 2mm sieve was backwashed into a pre-weighed container. The wet sieving procedure was repeated using a 0.25 mm and a 0.053 mm sieve which resulted in four aggregate classes being collected form each treatment (2 mm, 0.25-2 mm, 0.053-0.25 mm, and > 0.053 mm). The mean weight diameter (MWD) for the water stable aggregates within each treatment was calculated using Equation (3):

$$MWD = \sum_{i=1}^{n} XiWi \tag{3}$$

where Xi is the mean diameter for each fraction size, Wi is the proportional weight of the fraction from the total dry weight of soil used, and n is the number of aggregate classes separated (Abdalla *et al*., 2016). To evaluate SOCc and Nc within the four aggregate classes, samples were air-dried for 48 hours and ground to a fine powder using pestle and mortar. Soil sub-samples weighing 2 g representing each treatment, depth, and fraction were sent to the Soil Science Laboratory of the School of Agriculture, Earth and Environmental Sciences of the University of KwaZulu-Natal where total C and N were analysed using LECO CNS-2000 Dumas dry matter combustion analyser (LECO Corp., St. Joseph, MI).

3.10 Laboratory processing and analysis of ^{137}Cs and $^{210}Pb_{ex}$

Measurements of ^{137}Cs and ^{210}Pb were undertaken by gamma ray spectrometry using a low-energy Germanium well type detector system calibrated using known standards in the same geometry as the samples (Humphries *et al*., 2010). All gamma data were processed using HYPERMET and all errors were determined from counting statistics and the error associated with the HYPERMET curve-fitting routine (Humphries *et al*., 2010). Total ^{210}Pb was determined by its emission at 46.5 keV and supported ^{210}Pb determined by measuring the 226Ra activity of the sample via its daughter ^{214}Pb at 295 and 352 keV. Unsupported or $^{210}Pb_{ex}$ was calculated from the difference between total ^{210}Pb and the supported ^{210}Pb activity (Lubis, 2006; Gaspar *et al*., 2013; Meusburger *et al*., 2018). Cesium-137 was determined using its gamma emission at 662 keV (Poręba, 2006). Due to the extremely low activity of the samples, count times ranged from 24- 48 hours, with detection limits of 0.3 dpm g^{-1} and 0.05 dpm g^{-1} (disintegrations per minute - per gram) for $^{210}Pb_{ex}$ and ^{137}Cs, respectively. The measured radionuclides (dpm g^{-1}) were converted to an inventory (dpm cm^{-2}) using the soil depth, and an assumed particle density of 2.5 g cm^{-3}.

3.11 Laboratory processing and analysis of soil properties

The following laboratory procedures and methods were used by the Soil Fertility and Analytical Services Section at Cedara College of Agriculture Soil (Manson and Roberts, 2000).

3.11.1 Particle size distribution of soils and soil texture

After dispersion and sedimentation, suspended clay and fine silt were determined; while sand fractions were determined by sieving (Day, 1965). Hydrogen peroxide was used to treat a 20g soil sample (<2 mm) to oxidise the organic matter. De-ionized water was added to the sample until it was 400 ml; and the sample was left overnight. The clear supernatant was siphoned off and more de-ionized water was added to the sample and it was left overnight. The clear supernatant was siphoned off again and dispersing agents (NaOH and sodium hexametaphosphate) were added to the sample. The sample was stirred on Hamilton Beach stirrers, where the suspension was made up to 1 litre in a measuring cylinder and the clay (<0.002 mm) and fine silt (0.002-0.02 mm) fractions measured with a pipette after sedimentation. Fine silt plus clay was measured after 4-5 min (exact time depends on temperature) at 100 mm, and clay after 5-6 h at a depth of 75 mm. Sand fractions include very fine sand (0.05 - 0.10 mm), fine sand (0.10 - 0.25 mm), medium sand (0.25 - 0.50 mm) and coarse sand (0.50 - 2.0 mm) which were determined by sieving. Coarse silt (0.02-0.05 mm) was estimated by difference. Once the particle size distributions of the two soils were known, their textural class was determined from a diagram (textural triangle) defining particle size limits of the various textural classes (Soil Classification Working Group, 1991).

3.11.2 pH (KCl)

To determine pH; 25 ml of 1*M* KCl solution was added to 10 ml of soil, where the suspension was stirred at 400 r.p.m. for 5 min using a multiple stirrer. The suspension stood for approximately 30 minutes, and the pH was measured using a gel-filled combination glass electrode while stirring.

3.11.3 Extractable (1 M KCl) calcium, magnesium and acidity

To determine Extractable (1 M KCl) calcium, magnesium and acidity, 25 ml of 1 *M* KCl solution is added to 2.5 ml of soil where the suspension is stirred at 400 r.p.m. for 10 min using a multiple stirrer. The extracts were filtered using Whatman No.1 paper. Five millilitres of the filtrate was diluted with 20 ml of 0.0356 *M* $SrCl_2$, and Ca and Mg determined by atomic absorption. Extractable acidity was determined by diluting 10 m of the filtrate with 10 ml of de-ionised water containing 2-4 drops of phenolphthalein, and titrated with 0.005 *M* NaOH.

3.11.4 Extractable (Ambic-2) phosphorus, potassium, zinc, copper and manganese

The Ambic-2 extracting solution consisted of 0.25 *M* NH_4CO_3 + 0.01 *M* Na_2EDTA + 0.01 *M* NH_4F + 0.05 g L^{-1} Superfloc (N100), adjusted to pH 8 with a concentrated ammonia solution. Twenty-five millilitres of this solution were added to 2.5 ml soil, and the suspension was stirred at 400 r.p.m. for 10 min using a multiple stirrer. The extracts were filtered using Whatman No.1 paper. Phosphorus was determined on a 2 ml aliquot of filtrate using a modification of the Murphy and Riley (1962) molybdenum blue procedure (Hunter, 1974). Potassium was determined by atomic absorption on a 5 ml aliquot of the filtrate after dilution with 20 ml de-ionised water. Zinc, Cu and Mn are determined by atomic absorption on the remaining undiluted filtrate.

3.12 Statistical Analysis

Genstat 18th Edition software was used for statistical analyses. A Two-way Analysis of Variance (2-way ANOVA) was performed to test for significant differences between SOC and N at depth intervals 0-5 cm, 5-15 cm and 15-30 cm within each slope position (reference site, top-slope, mid-slope and lower-slope) and within soil aggregate classes (2 mm, 0.25-2 mm, 0.053-0.25 mm, and > 0.053 mm). Tukey Multiple Comparisons was performed to compare the treatment means, at a 95% confidence level.

3.13 Conclusion

The study site of Okhombe is located 50 km from Bergville in KwaZulu-Natal, positioned between altitudes of 1200 to 1800 m above sea level and the topography of the area forms part of the Eastern escarpment of South Africa. A 10 x 10 m grid sampling design was used to collect soil samples at an undisturbed reference site and at specific positions along a degraded slope affected by cattle path erosion. Three replicates were collected using a 10 x 10 m grid in all treatments; thus having 3 plots at each site. Soil samples were collect at each plot at intervals of 0-5, 5-15 and 15-30 cm, thereafter soil samples were sent to various laboratories for analysis. Bulk density, soil properties and fallout radionuclides were measured per sample. Grass cover was measured at each slope position using the Braun-Blanquet classification method (Zietsman, 2003).

The use of physical fractionation determined soil aggregate-size distribution and indicates SOC and N protection within the soils. Using the inventories obtained through the measurements of fallout radionuclides ^{137}Cs and $^{210}Pb_{ex}$, provides insight into understanding soil erosion and redistribution processes. The objective of the methods were to determine an appropriate experimental design to facilitate determining the impact of cattle path erosion on SOC and N.

Chapter Four

Results

4.1 Introduction

The results obtained from the grassland sites at Okhombe, Drakensberg are presented in this chapter. These results cover slope gradient, soil properties from 0-30 cm soil depth, SOC and N redistribution, and SOC and N protection within soil aggregates which was undertaken by wet aggregate fractionation. In addition, ^{137}Cs and $^{210}Pb_{ex}$ isotopes were measured to consider their applicability to local soil erosion studies. Trends found within the data are graphically presented, tabulated and described.

4.2 Slope and Vegetation

Eleven slope profile readings were taken downslope from the reference site to the lower-slope (arrows indicate angle reading points in Figure 4.1). The slope length was 445 m and average slope gradient 25 % (Figure 4.1) (Appendix A). The gradient of the slope is flat at the reference site (13 %) (1460 m above sea level), increasing in steepness leading to the top-slope (28 %) (1439 m above sea level) (Table 4.1). The top-slope steeply leads to the mid-slope (30 %) (1403 m above sea level) and becomes gentle at the lower-slope (19%) (1362 m above sea level).

The Braun-Blanquet vegetation classification (Zietsman, 2003) was used to determine vegetation cover and abundance at each 10 x 10 m sampling plot within each slope position (reference site, top-, mid- and lower-slope) (Table 4.1). The classification measured the aerial cover of shrubs and grass cover. The average grass cover at the reference site was 100 %. Grasses became increasingly sparse downslope with an average of 40 % grass cover at the top-slope and 10 % at the mid-slope. At the lower-slope grass cover increased to 50 %.

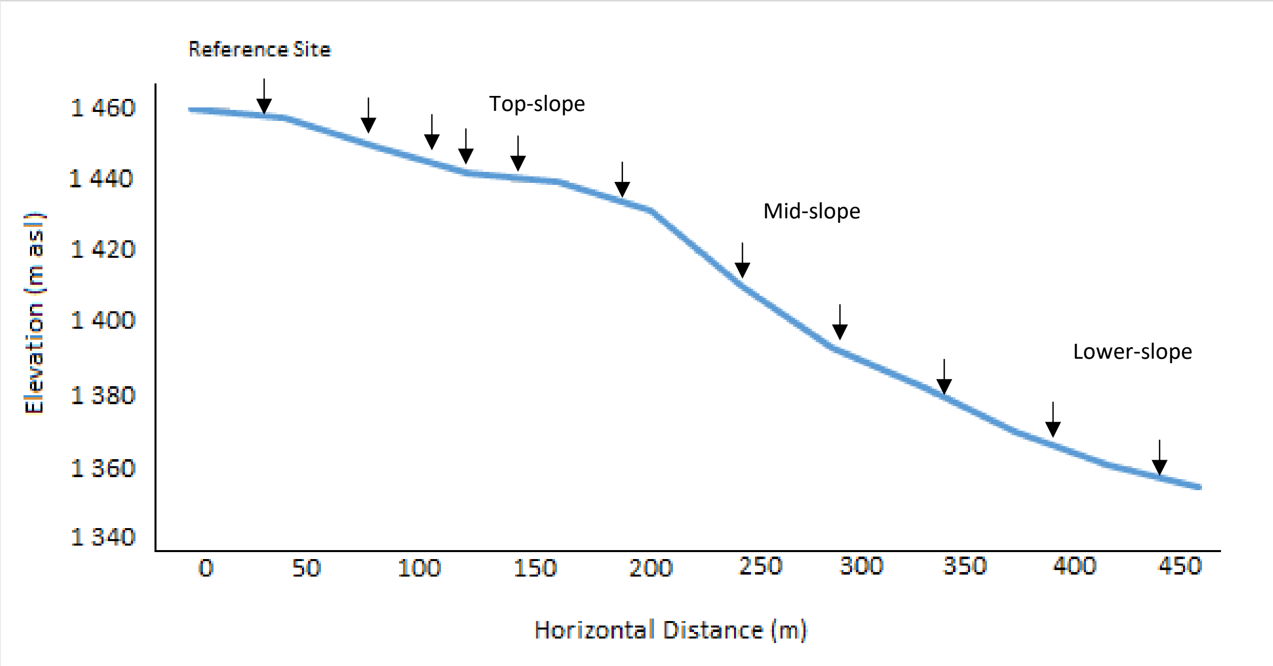

Figure 4.1. Slope profile, Ohkombe, Drakensberg region (Elevation m asl – metres above sea level). Arrows represent position of measurement. Mean (n = 3)

Table 4.1. Vegetation abundance at each sample position using the Braun-Blanquet classification method (Zietsman, 2003).

Sample Position	Slope angle (%)	Grass Cover	Shrub Cover
Reference Site	13	5	r
Top-slope	28	3	1
Mid-slope	30	2	3
Lower-slope	19	3	r

Note: The ratings for the Braun-Blanquet are: r = very small cover, rare occurrence, + = cover less than 1%, 1 = cover between 1-5%, 2 = cover between 5-25%, 3 = cover between 25-50%, 4 = cover between 50-75% and 5 = cover more than 75%.

4.3 Soil properties

4.3.1 Soil characteristics along the slope profile

The reference site, which is undisturbed (non-degraded) grassland had, to 30 cm depth, the highest SOCc and Nc, while the mid-slope had the lowest SOCc and the lower-slope had the lowest Nc values (Table 4.2). Soils at the reference site had 29.58 ± 3.56 g kg^{-1} of SOCc and 2.04 ± 0.31 g kg^{-1} of Nc, 80-90 % greater than the down-slope degraded positions (Appendix B).

Table 4.2. Weighted means of soil characteristics to 30 cm depth at different slope positions under degraded grassland in Okhombe, Drakensberg region. Data are weighted means ± SE; n = 3.

Soil Properties	Sample Position			
	Reference Site	**Top-slope**	**Mid-slope**	**Lower-slope**
SOCc, g kg^{-1}	29.58 ± 3.56 *	7.87 ± 1.31	5.05 ± 1.39	5.81 ± 1.1
Nc, g kg $^{-1}$	2.04 ± 0.31 *	0.57 ± 0.13	0.29 ± 0.02	0.28 ± 0.09
C:N, g kg $^{-1}$	14.56 ± 0.71	13.88 ± 0.72	18.89 ± 1.22 *	21.69 ± 4.1 *
SOCs, g C m^{-2}	3.97 ± 0.6 *	1.31 ± 0.19	0.77 ± 0.22	0.87 ± 0.14
Ns, g C m^{-2}	0.27 ± 0.05*	0.09 ± 0.02	0.04 ± 0.0	0.04 ± 0.01
BD, g cm^{-3}	1.19 ± 0.06*	1.46 ± 0.07	1.36 ± 0.04	1.34 ± 0.07
MWD, mm	2.72 ± 0.23*	1.77 ± 0.12*	1.07 ± 0.09*	1.02 ± 0.12*
Clay, %	39.8 ± 2.68 *	12.83 ± 2.2 *	27.33 ± 1.26*	30.16 ± 1.21*
Silt, %	18.83 ± 1.44	13.5 ± 2.25	15.83 ± 3.55	16.33 ± 0.64
Sand, %	40.83 ± 3.3*	73.66 ± 2.78*	56.83 ± 4.3*	53.5 ± 1.28*
P, mg l	3.94 ± 0.81*	2.39 ± 0.12	1.78 ± 0.37	1.78 ± 0.31
K, mg l	153.56 ± 44.64 *	88.66 ± 10.9	75.61 ± 6.23	133.72 ± 20.47*
Ca, mg l	351.17 ± 110.44*	386 ± 88.93*	216.28 ± 37.6*	240.34 ± 30.44*
Mg, mg l	135.78 ± 35.4*	101.5 ± 18.04*	71.00 ± 19.58*	100.77 ± 17.27*
pH (KCl)	3.94 ± 0.02*	3.88 ± 0.01*	3.94 ± 0.04*	3.81 ± 0.02*
Zn, mg l	0.38 ± 0.05*	0.25 ± 0.02	0.22 ± 0.02	0.21 ± 0.08
Mn, mg l	3.84 ± 0.5	10.11 ± 1.09*	5.06 ± 2.37	4.95 ± 0.89
Cu, mg l	1.08 ± 0.14*	0.35 ± 0.05*	0.18 ± 0.04*	0.83 ± 0.39*

Soil organic carbon content (SOCc), nitrogen content (Nc), carbon-nitrogen ratio (C/N), soil organic carbon stocks (SOCs), nitrogen stocks (Ns), bulk density (BD), mean weight diameter (MWD), clay (clay), fine silt (fine silt), sand (sand), phosphorus (P), potassium (K), calcium (Ca), magnesium (Mg), soil pH (KCl), zinc (Zn), manganese (Mn), and copper (Cu). Values followed by an asterisk (*) indicate significant differences between slope positions given by Tukey's Multiple Comparison test. Level of significance at $P < 0.05$.

The top-slope had the greatest ρb (1.46 g cm^{-3} ± 0.07 g cm^{-3}) while the reference site had the least (1.19 cm^{-3} ± 0.06 g cm^{-3}). The soils at the degraded slope positions were 15-22 % denser than the reference site soils. Soil aggregate stability, as measured by MWD, was highest in the reference site soils and lowest in the lower-slope soils. High clay and silt content were found within the reference site and lower-slope while the top-slope has the highest sand content followed by the mid-slope (Table 4.2).

Concentrations of the macronutrient P, were highest at the reference site (3.94 mg l^{-1} ± 0.81 mg l^{-1}) and equally low in the mid and lower-slope (1.78 mg l^{-1} ± 0.37 mg l^{-1}). Similarly, soil cations Mg and K, are highest at the reference site, while Ca is most abundant at the top-slope.

Trace elements Zn and Cu were highest at the reference site, and Mn were most abundant at the top-slope (Table 4.2). Soil pH is acidic ranging from 3.81 to 3.94.

4.3.2 SOC and N distribution

Soil organic carbon and N content decreased down the soil profile from depths 0-5 cm to 15-30 cm. At the reference site SOC and N content was most abundant and declines downslope. At soil depths 0-5 cm, 5-15 cm and 15-30 cm, a significant difference existed between the reference site, top-slope, mid-slope and lower-slope (95% confidence level) (Figure 4.2, 4.3, 4.6a and 4.6b) (Appendix B).

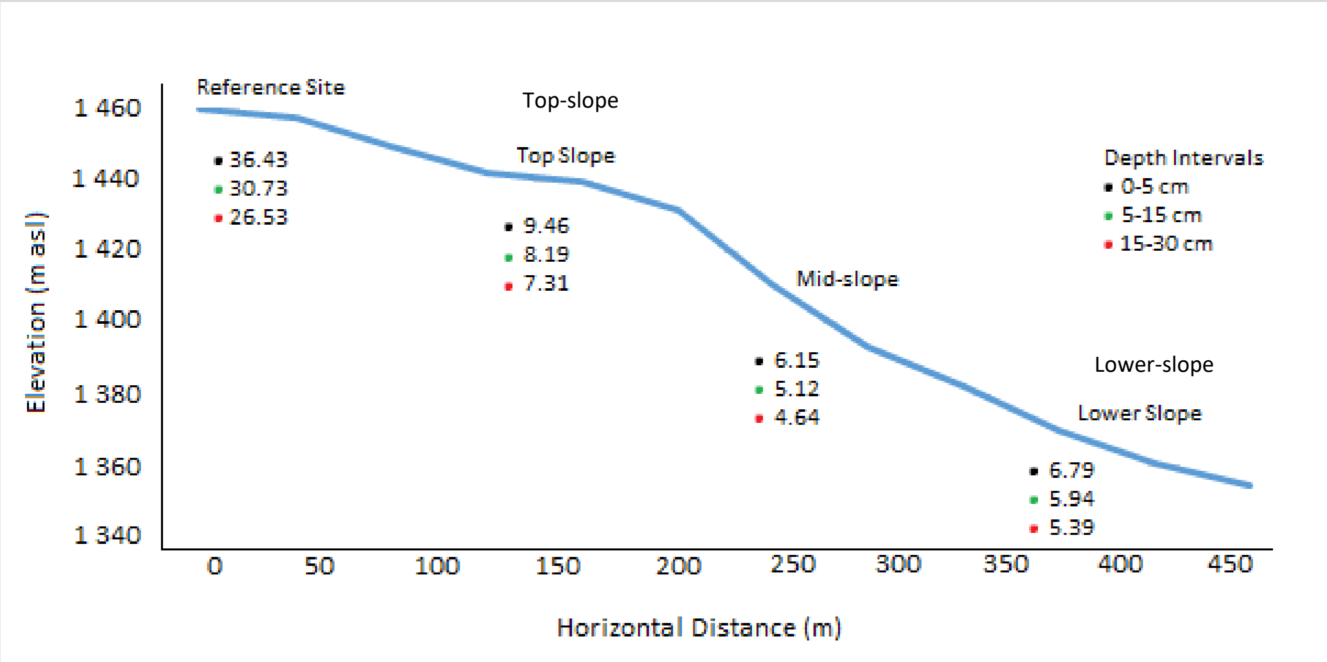

Figure 4.2. Soil organic carbon content (SOCc, g kg^{-1}) with soil depth and along the slope profile (Elevation m asl – metres above sea level). Mean (n = 3).

Conversely, soil organic carbon stocks (SOCs) increased down the soil profile from depths 0-5 cm to 15-30 cm, but decrease downslope from the reference site to the lower-slope (Figure 4.4 and 4.6c). A similar trend occurs in nitrogen stocks (Ns) distribution, as concentrations increase down the soil profile and decrease downslope, with the greatest Ns at the reference site and the lowest at the lower-slope (Figure 4.5 and 4.6d)

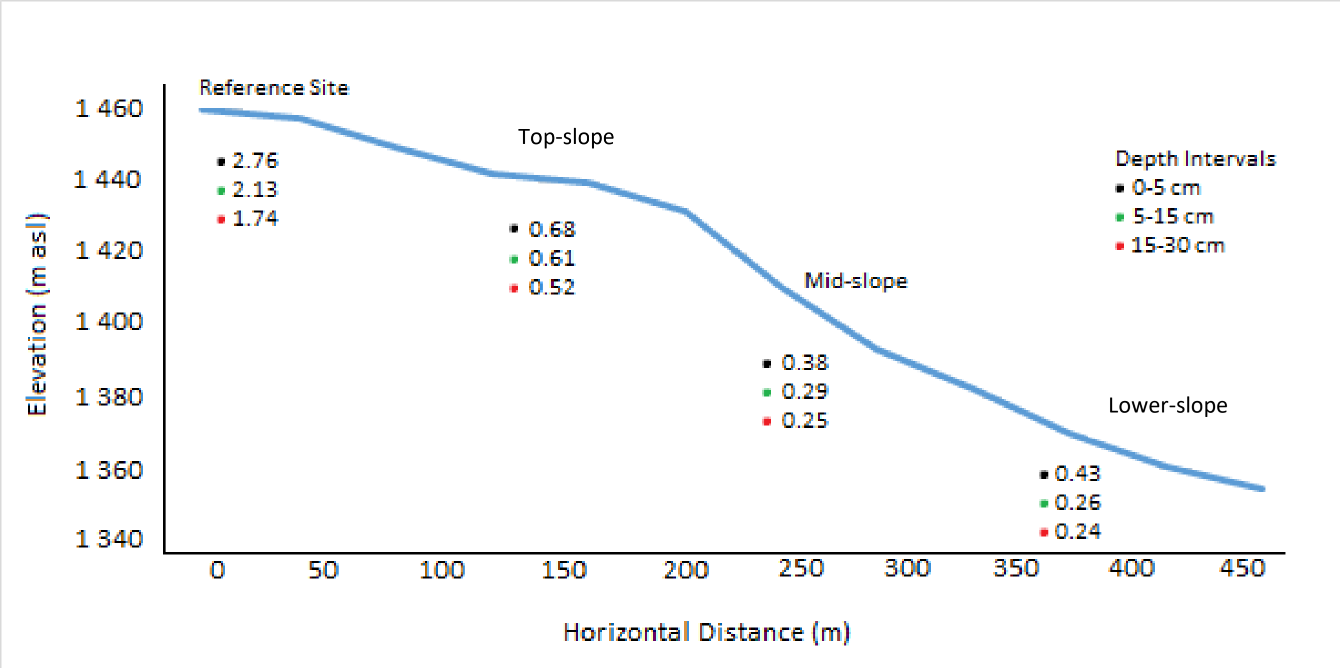

Figure 4.3. Soil nitrogen content (Nc, g kg^{-1}) with soil depth and along the slope profile (Elevation m asl – metres above sea level). Mean (n = 3)

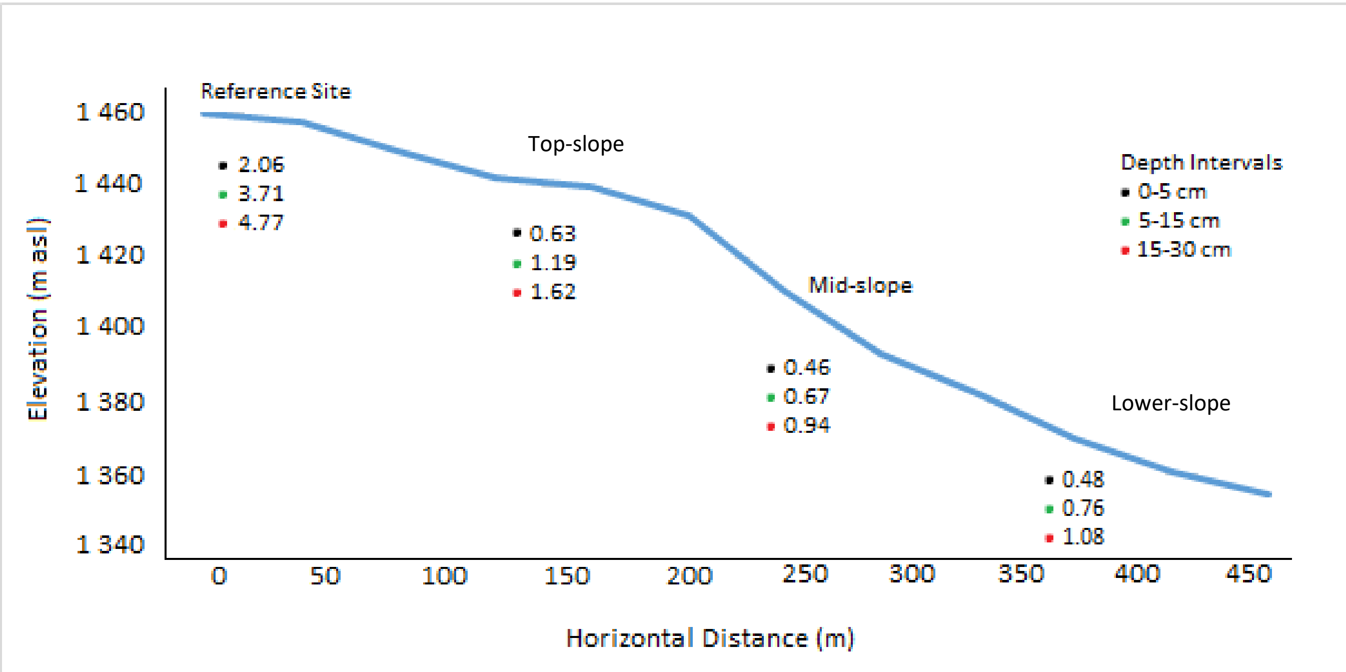

Figure 4.4. Soil organic carbon stocks (SOCs, g m^{2}) with soil depth and along the slope profile (Elevation m asl – metres above sea level). Mean (n =3)

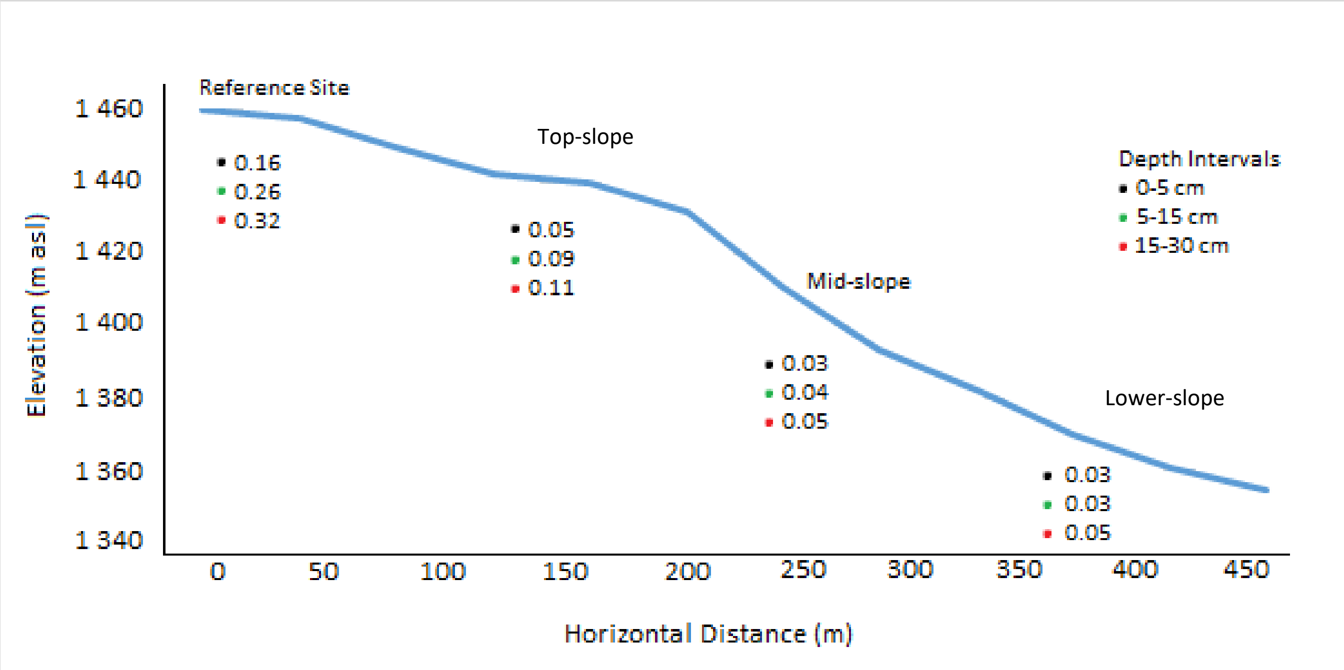

Figure 4.5. Soil nitrogen stocks (Ns, g m^{-2}) with soil depth and along the slope profile (Elevation m asl – metres above sea level). Mean (n = 3).

Throughout the soil depth profile, bulk density (ρb) within the reference site was the lowest and ranged between 1.15 ± 0.06 g cm^{-3} and 1.21 ± 0.01 g cm^{-3}. Bulk density at the top-slope, mid-slope and lower-slope varies with depth where no distinct trend is apparent (Figure 4.6e). At the reference site the MWD distinctly decreases with depth, while the decrease with depth is less apparent at the top-slope, mid-slope and lower-slope (Table 4.6f). At soil depths 0-5 cm, 5-15 cm and 15-30 cm, a significant difference exists between the reference site, top-slope, mid-slope and lower-slope (95% confidence level).

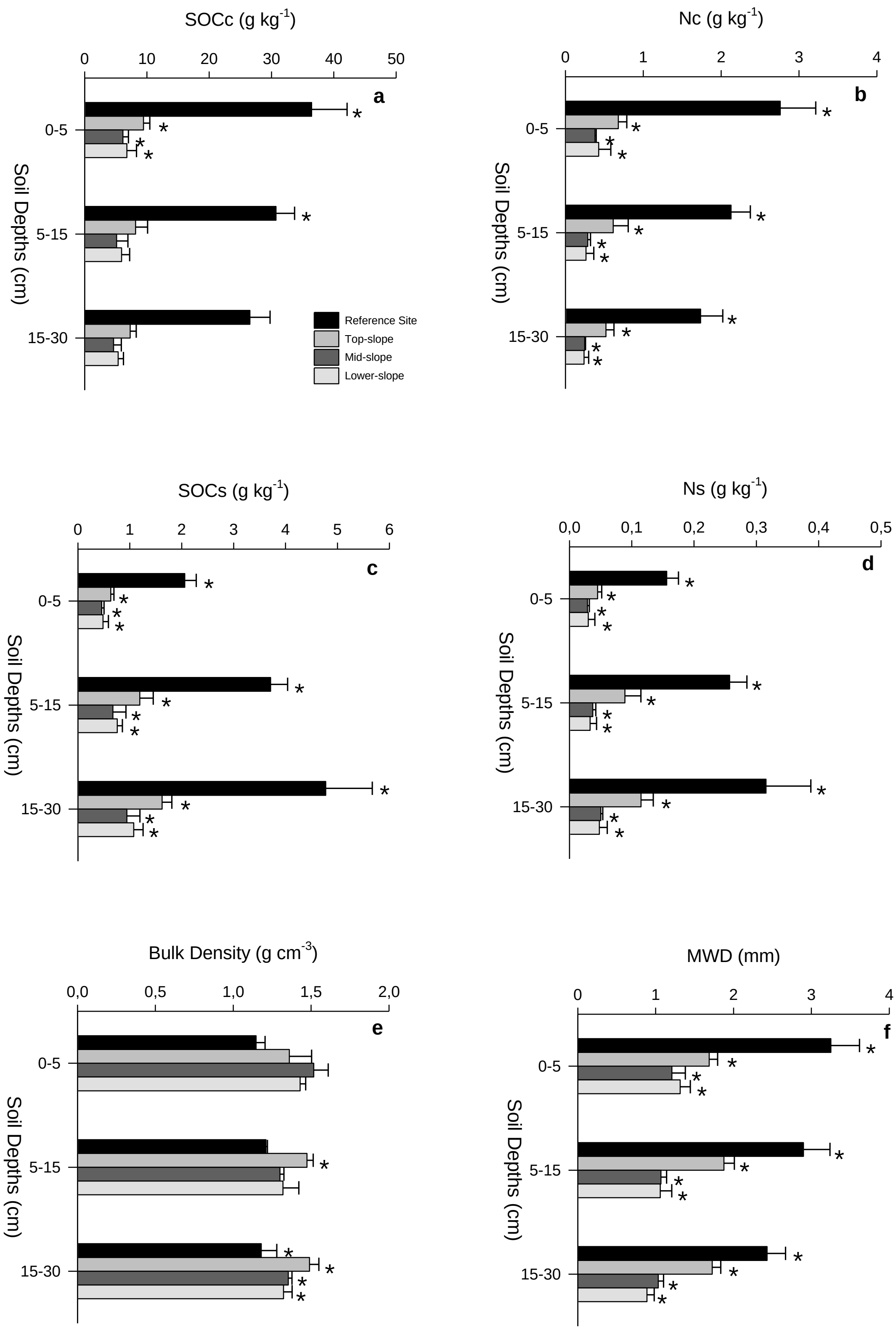

Figure 4.6. Relative distribution of (a) soil organic carbon content (SOCc); (b) nitrogen content (Nc); (c) soil organic carbon stocks (SOCs); (d) nitrogen stocks (Ns);(e) soil bulk density (ρb); (f) mean weight diameter (MWD); at soil depths 0-5, 5-15 and 15-30 cm. Values are the means ± standard error of soil samples. Bars with an asterisk (*) indicate significant differences between depth intervals at each slope position. Level of significance at $P < 0.05$. Mean (n=3).

4.4 Soil aggregate fractionations

For the soil aggregate classes (> 2000 µm, 250-53 µm, 53-250 µm and <53 µm) the weighted mean SOCc to 30 cm depth, was highest at the reference site (Table 4.3). The weighted mean SOCc in the <53 µm soil aggregate class showed significant difference between the reference site, top-slope, mid-slope and lower slope, where SOCc decreased from 40.01 g kg^{-1} in the reference site to 9.74 g kg^{-1} at the lower-slope. Soil organic nitrogen shows a similar pattern, where the weighted mean Nc to 30 cm depth is highest at the reference site (Table 4.4). In the 53-250 µm and <53 µm soil aggregate classes, Nc is significantly different at $P < 0.05$ between slope positions (Appendix C).

Table 4.3. Weighted means of soil organic carbon content to 30 cm depth (SOCc, g kg^{-1}) within soil aggregate classes in each sampling position. Data are weighted means ±SE; n = 3.

Aggregate size classes / **Sample Position**	**> 2000 µm**	**250-2000 µm**	**53-250 µm**	**<53 µm**
Reference Site	29.78 ± 0.37*	33.30 ± 0.46*	29.47 ± 4.48*	40.01 ± 3.51*
Top-slope	4.18 ± 0.11	9.27 ± 0.27	8.68 ± 1.15	22.61 ± 2.12*
Mid-slope	6.3 ± 0.09	6.35 ± 0.13	5.68 ± 1.55	11.20 ± 3.76*
Lower-slope	8.7 ± 0.08	8.43 ± 0.11	4.91 ± 0.91	9.74 ± 1.59*

Soil properties: Soil organic carbon content (SOCc). Values indicate mean ± standard error. Values followed by an asterisk (*) indicate significant difference in aggregate size at each slope position given by Tukey's Multiple Comparison test. Level of significance at $P < 0.05$.

Table 4.4. Weighted means of soil nitrogen content to 30 cm depth (Nc, g kg^{-1}) within soil aggregate classes in each sampling position. Data are weighted means ±SE; n = 3.

Aggregate size classes / **Sample Position**	**> 2000 µm**	**250-2000 µm**	**53-250 µm**	**<53 µm**
Reference Site	2.05 ± 0.37*	2.41 ± 0.46 *	2.04 ± 0.35*	3.07 ± 0.23*
Top-slope	0.64 ± 0.11	1.08 ± 0.27	0.80 ± 0.09*	2.33 ± 0.18*
Mid-slope	0.63 ± 0.09	0.63 ± 0.13	0.51 ± 0.1*	1.16 ± 0.26*
Lower-slope	0.72 ± 0.08	0.69 ± 0.11	0.29 ± 0.06*	0.79 ± 0.09*

Soil properties: Nitrogen content (Nc). Values indicate mean ± standard error. Values followed by an asterisk (*) indicate significant difference in aggregate size at each slope position given by Tukey's Multiple Comparison test. Level of significance at $P < 0.05$

The proportion of soil aggregate size classes at depth intervals 0-5, 5-15 and 15-30 cm, as indicated by the weight percentage, highlights soil aggregate stability at each sampling position. At the reference site, the weight percentage of macro-aggregates (> 2000 µm aggregate size class) is the greatest at all depth intervals, at all sampling positions, indicating stable soil aggregates (Figure 4.7). The weight percentage of aggregate size classes 250-2000 µm, 53-250 µm and <53 µm at all depth intervals at the top-, mid- and lower-slope, are greater than that of the reference site, suggesting unstable soil aggregates at these slope positions (Figure 4.7).

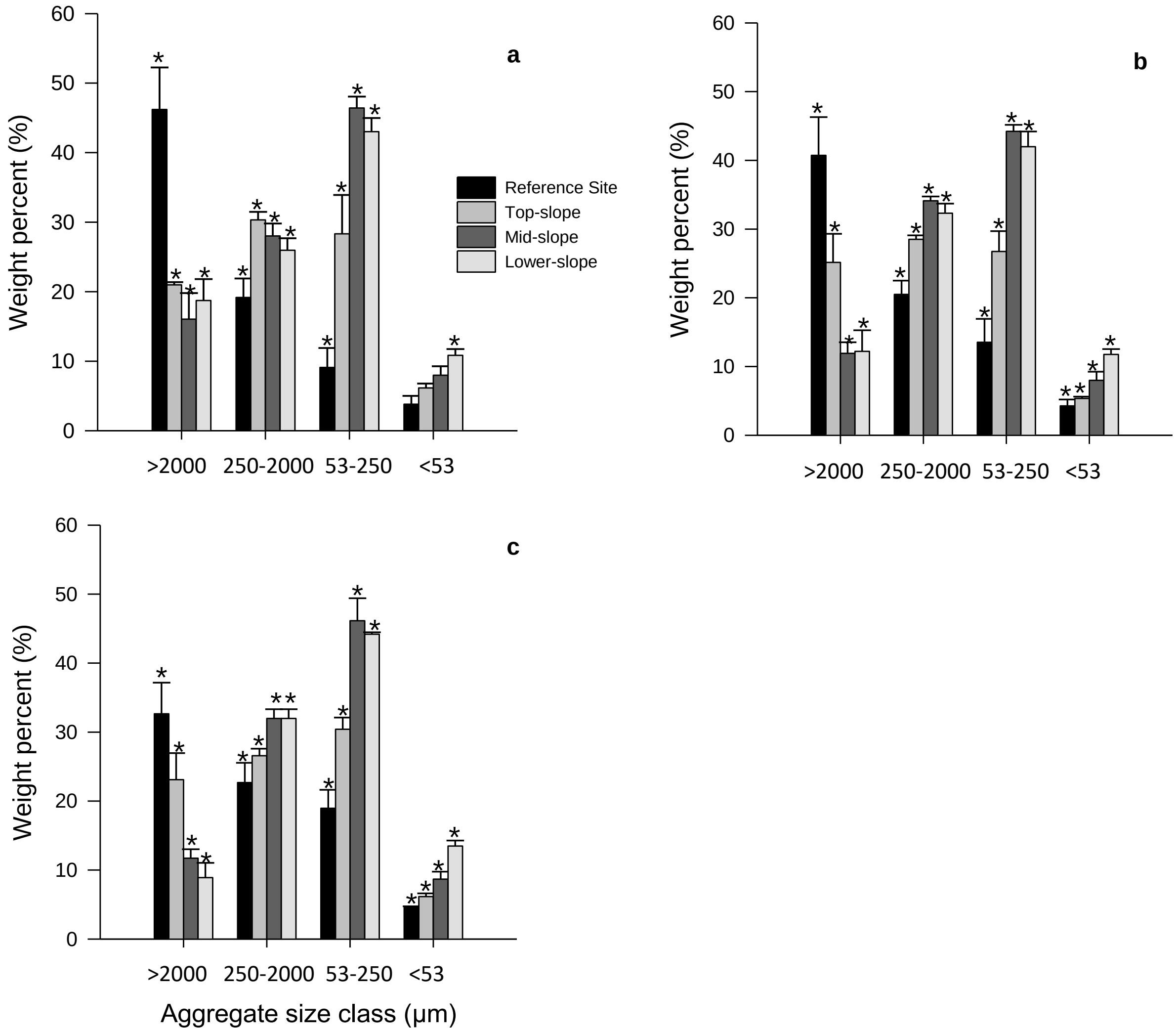

Figure 4.7. Weight percentage of slaking resistant aggregates at depths (a) 0-5 cm; (b) 5-15 cm and (c) 15-30 cm at each sampling position. Bars with an asterisk (*) indicate significant differences between aggregate size classes at each slope position. Level of significance at $P < 0.05$. Mean (n=3).

Soil organic carbon content at depths 0-5 cm (Figure 4.8a), 5-15 cm (Figure 4.8b) and 15-30 cm (Figure 4.8c) is greatest at the reference site across all aggregate size classes. The < 53 µm aggregate size class contained the greatest SOCc at each depth interval within each slope position. Soil organic carbon content within the < 53 µm aggregate size class decreases from the reference site to the lower-slope within each depth interval. At 15-30 cm (Figure 4.8c), SOCc within the > 2000 μm aggregate size class decreased from 25.81 ± 2.25 g kg^{-1} in the reference site to 3.02 ± 0.71 g kg^{-1} in the top-slope, significant at P < 0.05. A significant difference at P < 0.05 exists between the mid-slope and lower-slope, where SOCc increased by 53%.

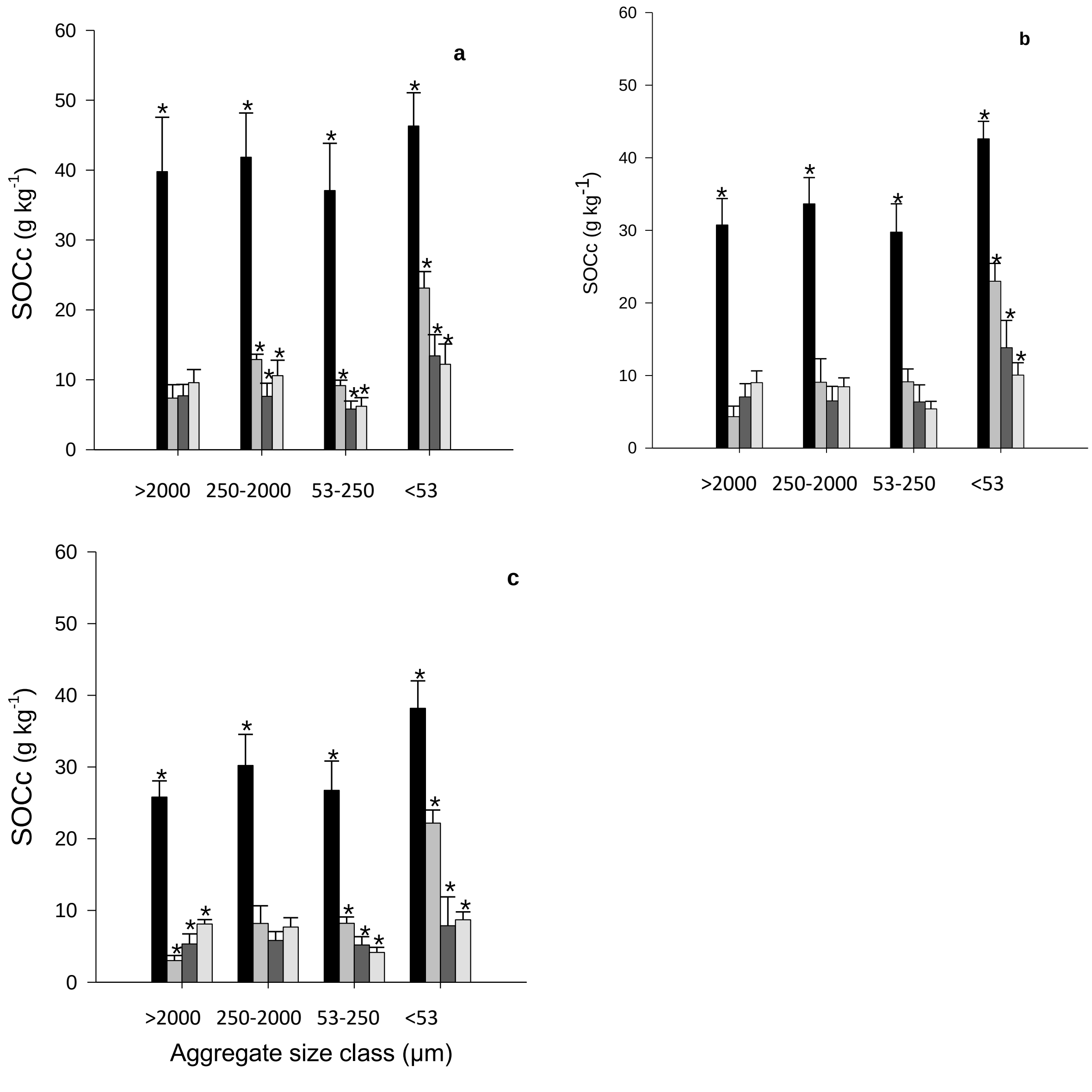

Figure 4.8. Soil organic carbon content (SOCc) at depths (a) 0-5 cm; (b) 5-15 cm and (c) 15-30 cm at each slope position. Bars with an asterisk (*) indicate significant differences between aggregate size classes at each slope position. Level of significance at P < 0.05. Mean (n=3).

Soil nitrogen content displayed a similar pattern to that of SOCc, as concentrations are greatest at the reference site at all depth intervals across all the aggregate size classes (Figure 4.9). At 5-15 cm, Nc within the < 53 μm aggregate size class, decreased in the following order: 3.19 ± 0.06 g kg^{-1} in the reference site, to 2.35 ± 0.21 g kg^{-1} in the top-slope, 1.48 ± 0.23 g kg^{-1} in the mid-slope and 0.82 ± 0.10 g kg^{-1} in the lower-slope (Figure 4.9b). This corresponded to a 74 %

decrease down the slope profile from the reference site to the lower-slope, significant at $P < 0.05$. Likewise, at 15-30 cm, Nc within the 250-53 µm aggregate size class decreases by 6 % from the reference site to the top-slope, 35% from the top-slope to mid-slope, and by 50% from the mid-slope to lower-slope, significant at $P < 0.05$ (Figure 4.9c).

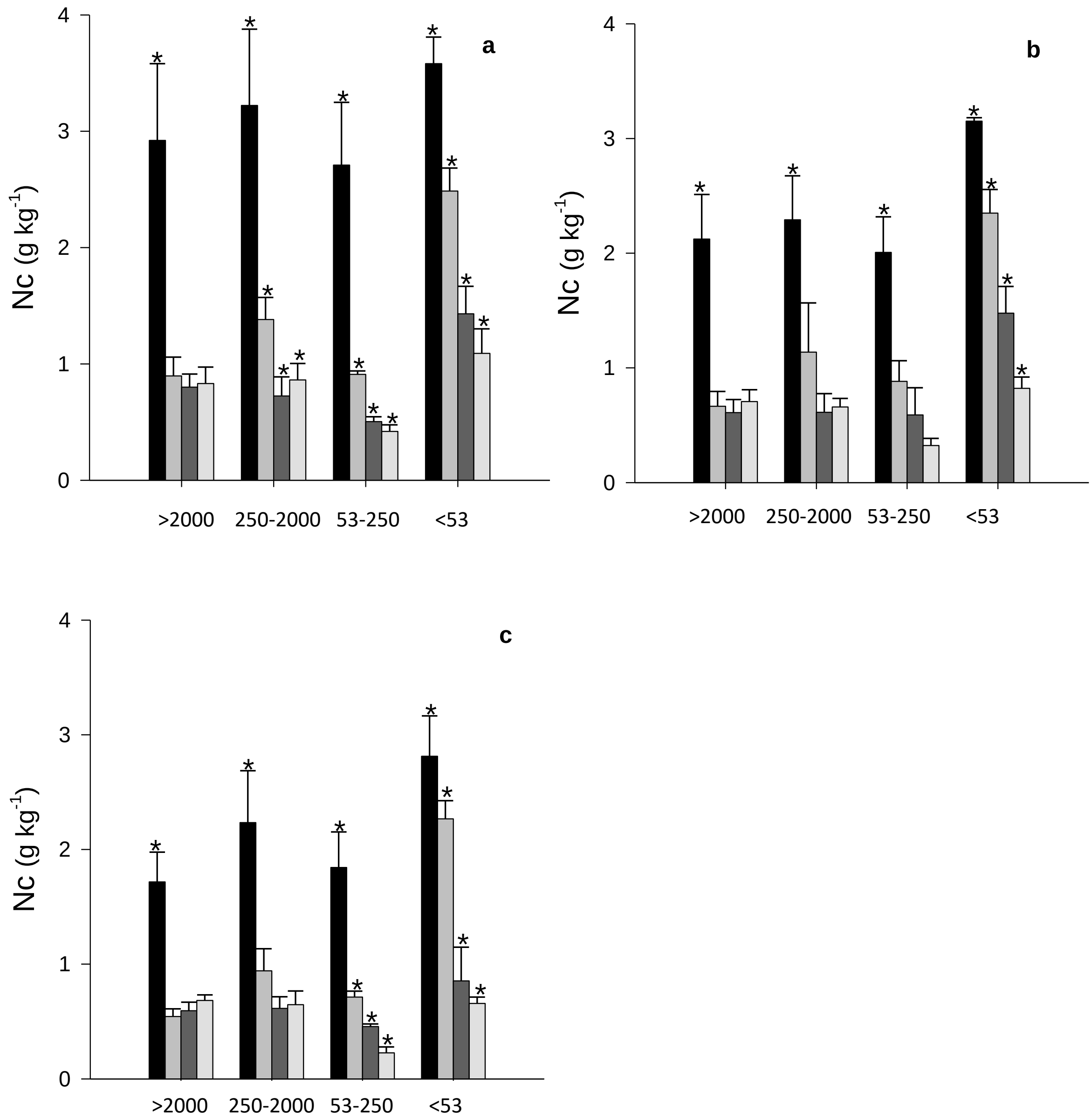

Figure 4.9. Nitrogen content (Nc) at depths (a) 0-5 cm; (b) 5-15 cm and (c) 15-30 cm at each slope position. Bars with an asterisk (*) indicate significant differences between aggregate size classes at each slope position. Level of significance at $P < 0.05$. Mean (n=3).

Soil organic carbon stocks at depths 0-5 cm (Figure 4.10a), 5-15 cm (Figure 4.10b) and 15-30 cm (Figure 4.10c) is greatest at the reference site across all aggregate size classes. The < 53 µm aggregate size class contained the greatest SOCs at each depth interval within each slope position. At 0-5 cm (Figure 4.10a) a significant difference at $P < 0.05$ exists between the top-slope and mid-slope, in the < 53 µm aggregate size class, where SOCs decreased by 35%. Similarly at 5-15 cm (Figure 4.10b) in the < 53 µm aggregate size class, SOCs decreased from 3.37 ± 0.27 g m^{-2} in the top-slope to 1.29 ± 0.17 g m^{-2} in the lower-slope, significant at $P < 0.05$. At 15-30 cm (Figure 4.10c), SOCs within the < 53 µm aggregate size class increased from 1.58 ± 0.08 g m^{-2} in the mid-slope to 1.73 ± 0.25g m^{-2} in the lower-slope, significant at $P < 0.05$.

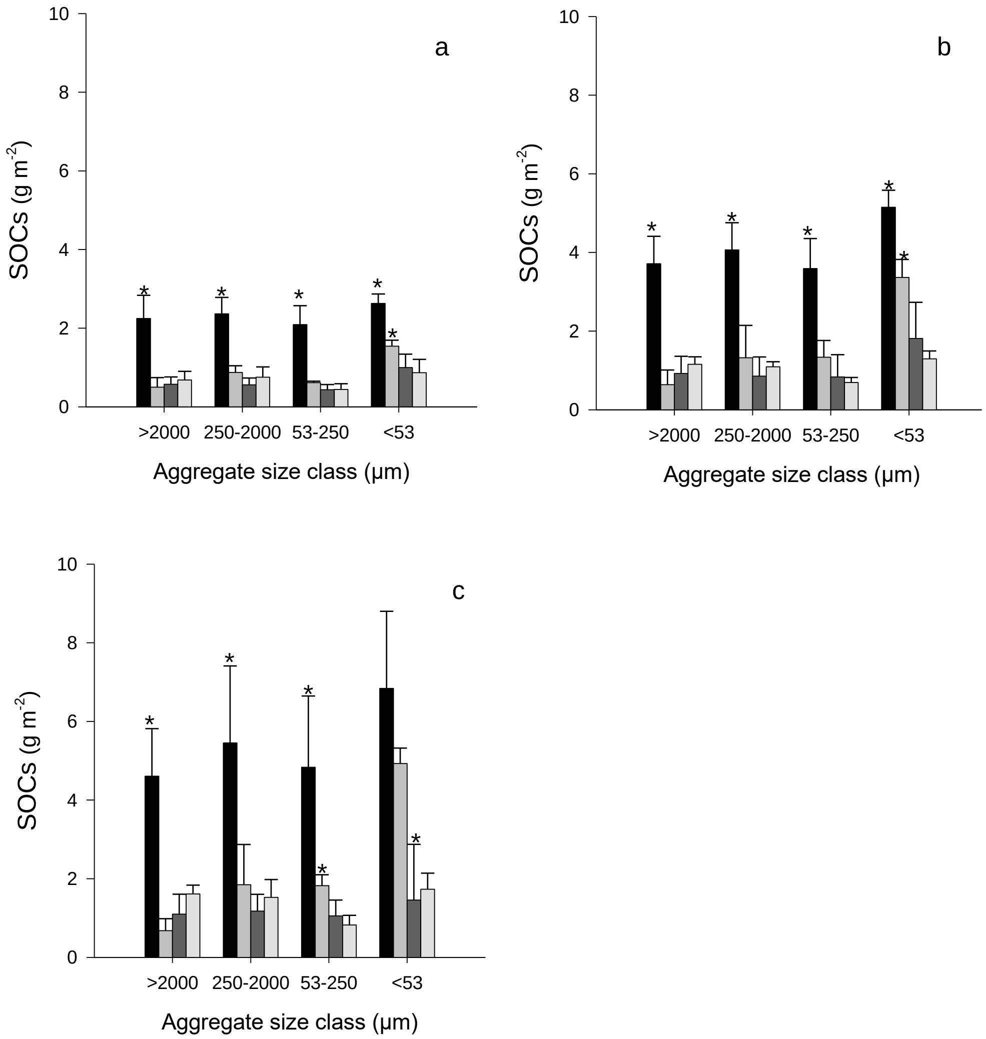

Figure 4.10. Soil organic carbon stocks (SOCs) at depths (a) 0-5 cm; (b) 5-15 cm and (c) 15-30 cm at each slope position. Bars with an asterisk (*) indicate significant differences between aggregate size classes at each slope position. Level of significance at $P < 0.05$. Mean (n=3).

Soil nitrogen stocks displayed a similar pattern to that of SOCs, as concentrations are greatest at the reference site at all depth intervals across all the aggregate size classes (Figure 4.11). The < 53 µm aggregate size class contained the greatest Ns at each depth interval within each slope position. At 5-15 cm (Figure 4.1b), Ns within the < 53 µm aggregate size class decreased from 0.19 ± 0,11 g m^{-2} in the mid-slope to 0.11 ± 1.15 g m^{-2} in the lower-slope, significant at $P < 0.05$. The same pattern exists at 15-30 cm (Figure 4.11c) in the < 53 µm aggregate size class, where Ns decreased by 24 % from the mid-slope to the lower-slope.

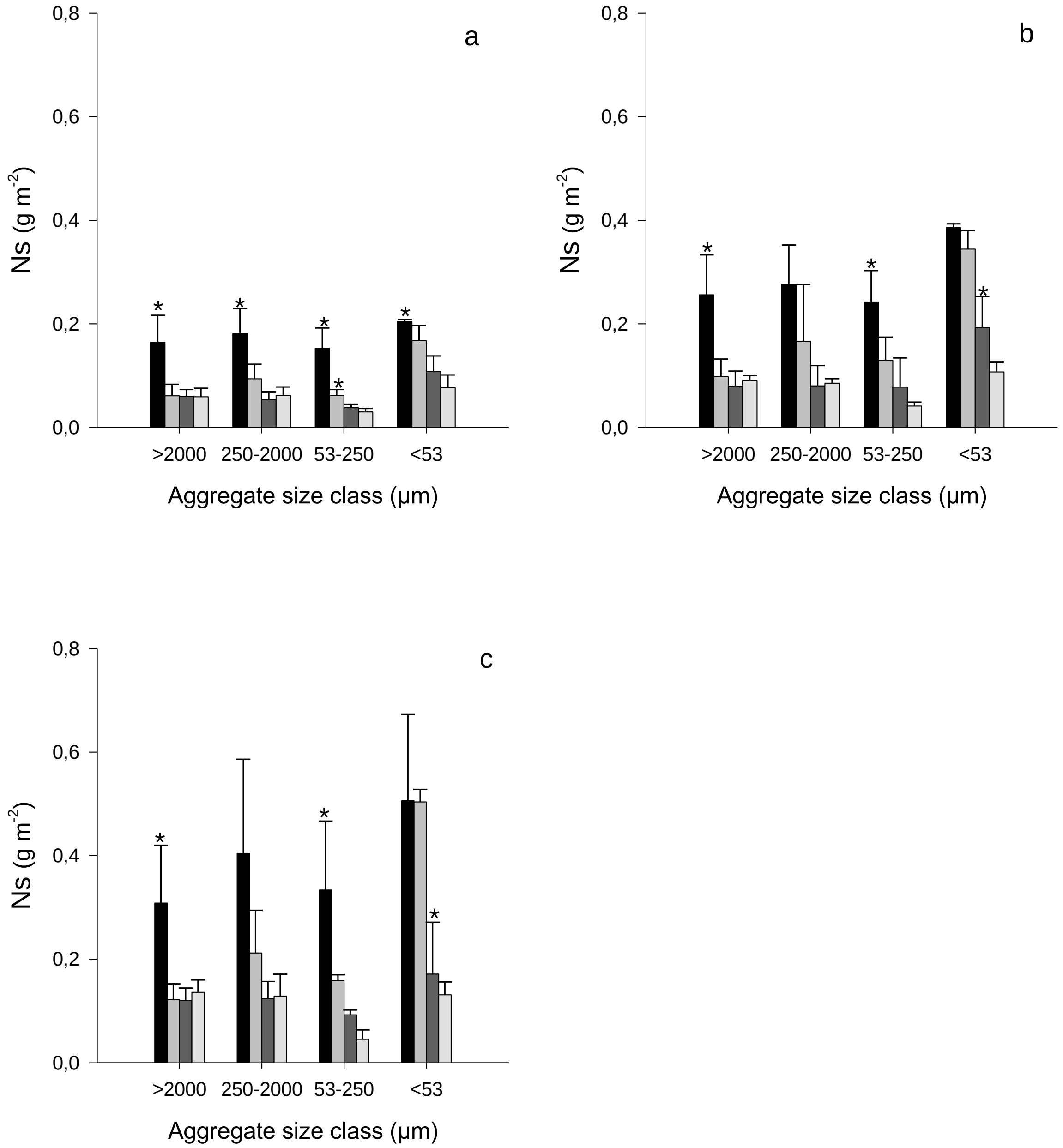

Figure 4.11. Nitrogen stocks (Ns) at depths (a) 0-5 cm; (b) 5-15 cm and (c) 15-30 cm at each slope position. Bars with an asterisk (*) indicate significant differences between aggregate size classes at each slope position. Level of significance at $P < 0.05$. Mean (n=3).

4.5 ^{137}Cs and $^{210}Pb_{ex}$ distributions

The soil samples were characterized by extremely low ^{137}Cs activities, with 75% of the samples (n=36) having activities below the detection limit of 0.05 dpm g^{-1}. The use of ^{137}Cs as an indicator for soil erosion within the Okhombe region would therefore not work due to the low concentrations. Lead-210 analyses indicated that there was considerable post-depositional movement within the study area and that it is spatially heterogeneous and temporally variable (Appendix D). As such, determining sedimentation rates outside of the reference site was not possible as $^{210}Pb_{ex}$ did not decline with depth at a consistent rate. The relationship between $^{210}Pb_{ex}$ and depth was not significant and the data could not be modelled with a significant sedimentation rate (Figure 4.12).

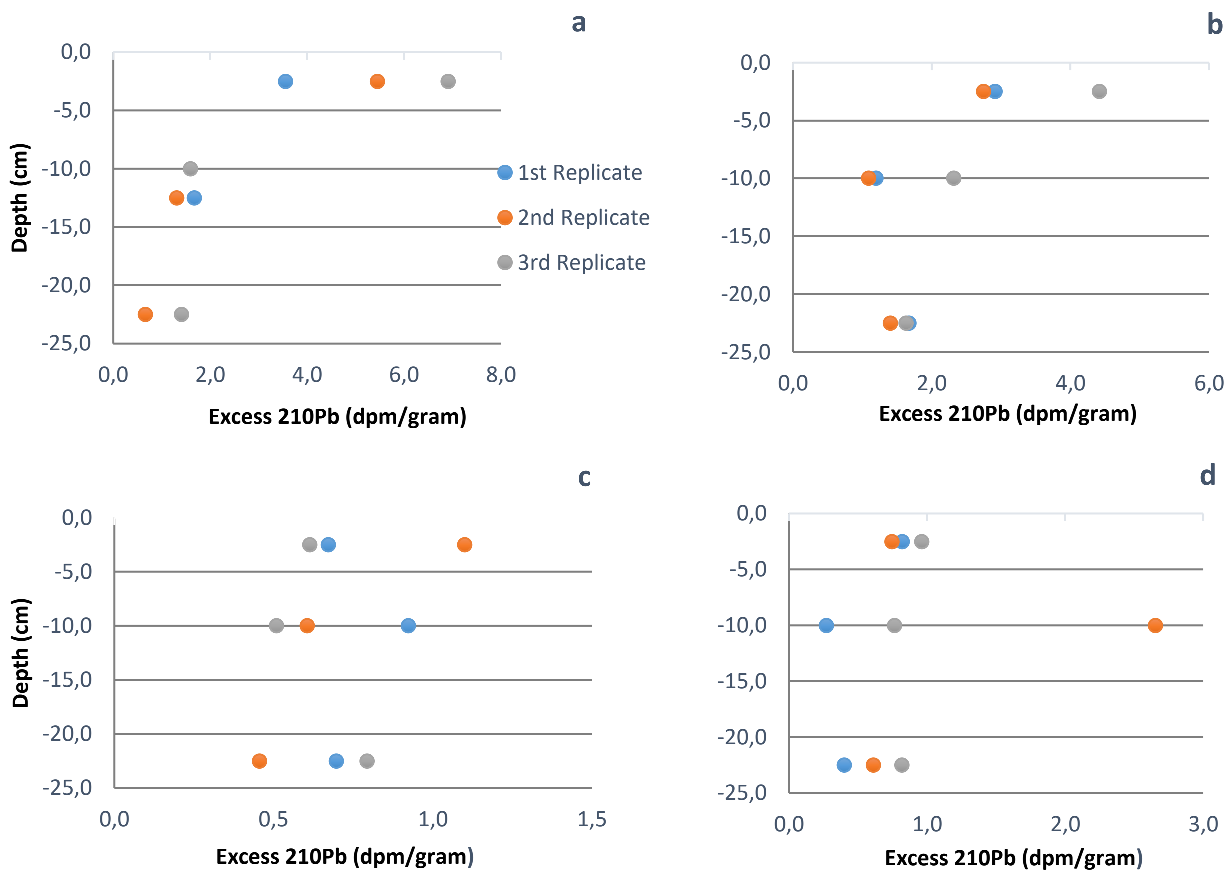

Figure 4.12. Variability of $^{210}Pb_{ex}$ within each sampling plot at the (a) reference site; (b) top-slope; (c) mid-slope and (d) lower-slope; at soil depth 0-30 cm.

At the top-slope $^{210}Pb_{ex}$ inventories are highest at 2,149 dpm cm^{-2} (accumulating) with little movement down slope. This is 66% greater than the reference site. The lowest inventories are found at the mid-slope at 791 dpm cm^{-2}, 39% less than the reference site (Table 4.5).

Table 4.5. $^{210}Pb_{ex}$ inventories at each slope position. Data are means ± SE; n = 36.

Slope Position	**$^{210}Pb_{ex}$ inventory (dpm cm^{-2})**
Reference Site	1335.67 ± 167.58
Top-slope	2668.39 ± 81.16
Mid-slope	1000.69 ± 55.3
Lower-slope	1124.10 ± 128.76

Overall, $^{210}Pb_{ex}$ inventories should decline with increasing depth in undisturbed sites (Fang *et al*., 2013). Here, inventories increased with increasing depth due to a combination of variable sedimentation rates, decay, and sampling depths that increased from 5 to 15 cm (Figure 4.13). Given the variability in $^{210}Pb_{ex}$ activities, examining $^{210}Pb_{ex}$ inventories with depth was considered of little value as inventories did not decline with increasing depth nor were they consistent between slope positions.

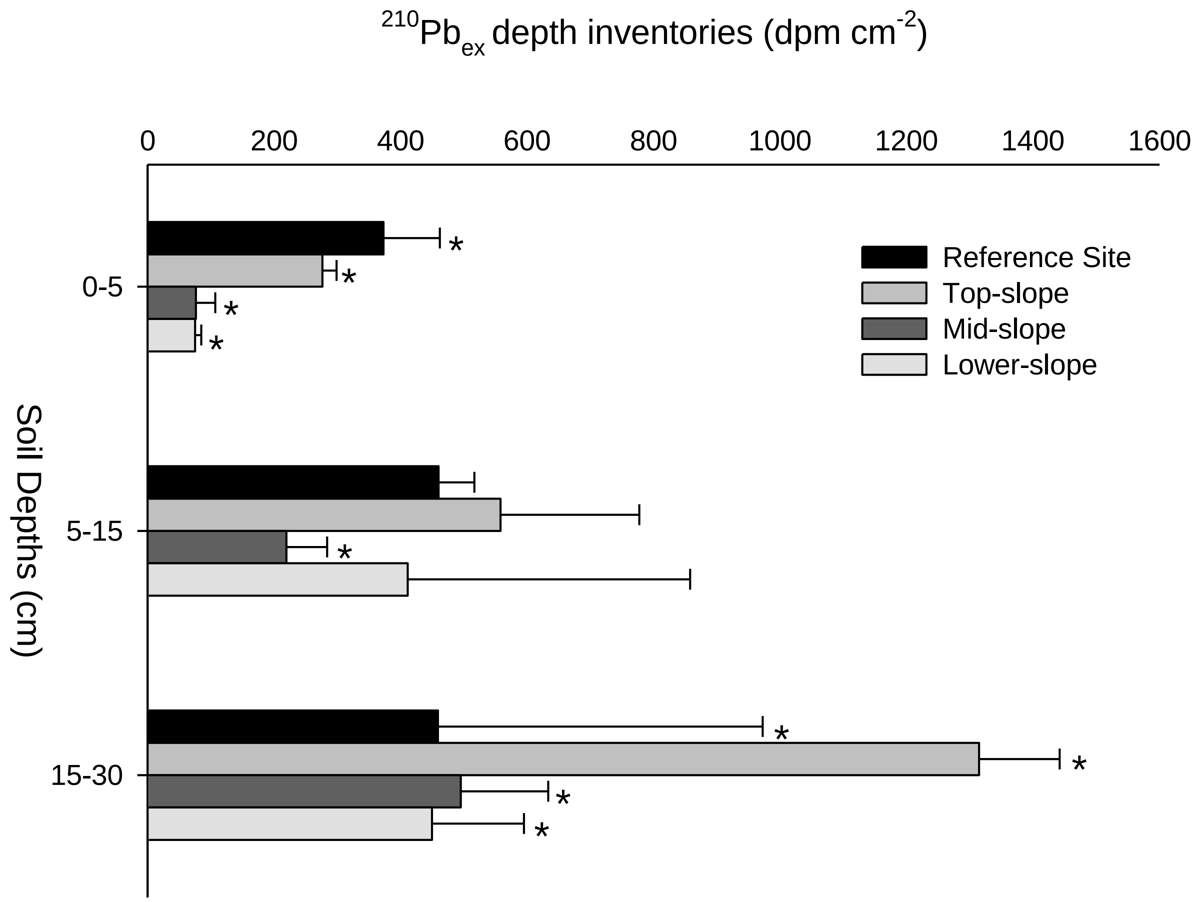

Figure 4.13. Integrated excess lead-210 ($^{210}Pb_{ex}$) activity over depth intervals 0-5, 5-15 and 15-30 cm at each slope position. Bars with an asterisk (*) indicate significant differences between depth intervals at each slope positions. Level of significance at $P < 0.05$. Mean (n=3).

4.6 Conclusion

Slope gradient for the study site was calculated to be 25% and the slope length 445 m, while grass cover in the study site was classified according to the Braun-Blanquent classification method (Zietsman, 2003). Soil organic carbon and N was greatest within the reference site compared to the degraded slope; which is expected as the reference site is level and undisturbed. Likewise, a significant difference existed between the SOCs and Ns within the reference site, compared to that of the degraded slope positions; highlighting the impact cattle path erosion has on C and N storage within the soil.

Soils within the degraded slope profile had greater bulk densities and lower concentrations of soil nutrients than that of the reference site. Within all the soil aggregate classes, SOCc, Nc, SOCs and Ns was highest in the reference site. Soil organic carbon content, in the <53 μm soil aggregate class, shows significant difference between the reference site and the top-slope, mid-slope and lower-slope; highlighting greater protection of SOC within soil aggregates of the reference site than the degraded slope positions. Soil organic nitrogen shows a similar pattern, where the overall nitrogen content is highest at the reference site. Soil organic carbon stocks show significant difference in the <53 μm soil aggregate class between the top-slope and mid-slope, at 0-5 cm and 5-15 cm. Similarly, a significant difference exists in the <53 μm soil aggregate class between the top-slope and lower-slope at 5-15 cm and 15-30 cm. Highlighting the increased protection of SOCs and Ns within the <53 μm soil aggregate class.

Excess lead-210 analyses suggested that there was significant post-depositional movement within the study area and that it is spatially heterogeneous and temporally variable. As such, determining sedimentation rates was not possible as $^{210}Pb_{ex}$ did not decline with depth at a consistent rate. Despite these results being of little value in determining sedimentation rates and distribution with depth; $^{210}Pb_{ex}$ inventories provided an indication of points of erosion and deposition along the degraded slope profile. Inventories greater than that of the reference site indicate deposition and inventories less than that of the reference site indicate erosion. According to the $^{210}Pb_{ex}$ inventories soil erosion occurs in the mid and lower-slope while sedimentation occurs in the top-slope. This occurrence however does not make sense and will be discussed further in chapter five.

Chapter Five
Discussion

5.1 Introduction

Grasslands cover approximately 40% of the Earth's surface and store 10% of the total global soil carbon stock of 1500 Gt (Egoh *et al*., 2011). They are thought to have a high potential to sequestrate carbon, depending on management practices, making them a significant part of the global carbon cycle (Dlamini *et al*., 2014). Subsequently, there is a need to improve land use management practices to ensure global sustainability and to reduce soil erosion risk (Ochoa *et al*., 2016).

In Okhombe, grasslands play a pivotal role in providing the community with feed for livestock used for milk, meat production, bride-wealth, ceremonial slaughter and transport. In addition, the grasslands provide thatch for building, firewood, medicinal plants and wild foods to the community (Peden, 2005; Sandhage-Hofmann *et al*., 2015). Due to its importance, the impact of cattle path erosion on soil organic carbon and nitrogen (SOC and N) concentrations are considered in this research. These soil properties are important for efficient plant growth, soil structure and water-holding capacity (Guoxiao *et al*., 2008), which are vital in the maintenance of a healthy functioning ecosystem. Cattle path erosion, and its associated impact on SOC and N along a degraded slope profile, were selected for this study, as cattle path erosion is known to have significant on- and off-site impacts. Much research has been undertaken on the impact of soil erosion within Okhombe but less on the impact of cattle path erosion on SOC and N. Furthermore, the use of fallout radionuclides in erosion based studies within South Africa is less common, thus making this study unique as it adds to the limited research available and is one of the first attempts of using the technique in this country.

5.2 Impact of cattle path erosion within the study site

Soil compaction, measured as bulk density (mean of 1.34 g cm^{-3}), suggests that the soils within the study area are relatively compacted, which is common of light textured (sandy) soils as total pore space is less than silt or clay soils (Castel and Cantero-Martinez, 2003; Chaudhari *et al*., 2013). Chaudhari *et al*., (2013) reported a strong positive correlation between bulk density and sandy soils while a significant negative correlation was observed between bulk density, clay and silt content. Chaudhari *et al*., (2013) also determined a strong negative correlation between porosity and bulk density of the soil samples under monsoon climate, indicating the inverse relationship that exists between bulk density and porosity. The compaction of soils within the study area is associated with a decrease in pore space resulting in less space for root growth, soil aeration and infiltration. This leads to increased surface runoff and causes the soils to be highly susceptible to erosion (de Lima *et al*., 2018; Torres-Sallan *et al*., 2018).

A further explanation for the high soil compaction at the study site could be the hoof action and trampling by cattle as they move along the slopes (Logsdon and Karlen, 2004; Hossain *et al*., 2015; de Lima *et al*., 2018). Hoof action and trampling breaks-up naturally occurring soil aggregates and causes the soil to become compressed, leading to surface crusting and increased bulk density which reduces surface infiltration, soil porosity and the availability of soil nutrients (Wilson and Seney, 1994; Evans, 1998; Castel and Cantero-Martinez, 2003; Grab and Kalibbala, 2008). As a result, vegetation on cattle paths is removed, where soils become bare and vulnerable to increased surface runoff. This is evident as sparse vegetation cover is present within the degraded slope positions as determined by the Braun-Blanquent classification method (Table 4.1). The removal of vegetation, through cattle trampling and hoof action, leave the soils exposed and prone to increased soil erosion, as above - and below - ground biomass is absent to protect the soil from detachment (Wilson and Seney, 1994; Evans, 1998; Laker, 2004; Gyssels *et al*., 2005; Pimentel, 2006).

The soils within the area are naturally of a poor quality and are acidic (pH range between 3.82 to 3.94), which restricts root growth and limits access to water and nutrients (Logsdon and Karlen, 2004). The high acidity causes major plant nutrients (nitrogen, phosphorus, potassium, calcium, manganese and magnesium) to become unavailable for uptake or only available in unsatisfactory amounts (Logsdon and Karlen, 2004; Chaudhari *et al*., 2013; Hossain *et al*., 2015). Vegetation growth is therefore reduced due to insufficient water and nutrient uptake, where exposed soils are prone to rainsplash and overland flow, which is responsible for soil erosion and gully formation within this area (Ollobarren *et al*., 2016).

Likewise, soil organic carbon and nitrogen stocks not only depend on carbon and nitrogen content but have a significant dependence on bulk density (Hossain *et al*., 2015). The low soil organic carbon and nitrogen stocks (average 1.66 g m^{-2} and 0.11 g m^{-2} respectively) are partially a result of the high bulk density of the soil. This occurs because soil organic carbon has a lower particle density than mineral particles and because soil organic matter tends to decrease with increasing bulk density (Logsdon and Karlen, 2004; Périé and Ouimet, 2008). In addition, the mean weight diameter (MWD) used to indicate aggregate stability (Blair, 2010), show that soils within the study area are unstable. This suggests that less organic carbon protection occurs within the soil aggregates as they are easily broken-down by rainsplash or through changes in land use management. Consequently, lower quantities of soil organic matter are found within unstable aggregates, implying low soil organic carbon and nitrogen content and therefore low soil organic carbon and nitrogen stocks (Chaplot and Cooper, 2015; Rawlins *et al*., 2015).

The steep slope gradient (25 %) and slope length (454 m), increases the kinetic energy of, and the duration for, runoff water as it moves downslope (Laker, 2004). This promotes the removal and transportation of sediment, which is responsible for the removal of soil organic carbon and nitrogen from the soils. Long steep slopes are common in the Drakensberg region, thus as the gradient and length of the slope increase, so too does the impact of runoff and erosion (Le Roux, 2011). The high losses in soil organic carbon and nitrogen can be explained by increased runoff rates due to a combination of factors including: the slope characteristics (a steep long slope), soil compaction, and unstable soil structures, which have low infiltration abilities and promote soil erosion (Chaplot and Cooper, 2015). These factors are evident at the study site.

5.3 Impact of cattle path erosion at slope positions

Overall, the undisturbed reference site comprising of sandy clay soils, had a lower bulk density (1.18 g cm^{-3}), higher MWD (2.86 mm), and a larger content of macronutrients (Ca = 385.44 mg l and Mg = 143.89 mg l), and trace elements, compared to the degraded slope positions (top-, mid- and lower-slope) (Table 4.2). Vegetation cover at the reference site scored five according to the Braun-Blanquet classification (Zietsman, 2003) as there was 100 % grass cover. The greatest SOCc, Nc, SOCs and Ns were found in the reference site which was expected as soil aggregates are stable as "calcium (Ca^{2+}) and magnesium (Mg^{2+}) cations improve soil structure through cationic bridging with clay particles and SOC" (Bronick and Lal, 2005:12). Larger pore spaces are available for root growth, indicating larger quantities of SOM present (Périé and Ouimet, 2008; Chaplot and Cooper, 2015; Rawlins *et al*., 2015). This indicated that the soils found in the reference site are stable in comparison to the degraded slope positions, and are able to hold greater amounts of plant nutrients and water for vegetation growth, which promotes infiltrating, thus decreasing surface runoff and erosion (Torres-Sallan *et al*., 2018).

Aggregate stability, as indicated by the mean weight diameter, was low at all of the degraded slope positions (Table 4.2). Likewise, a small difference in bulk densities existed between the degraded slope positions (top-slope = 1.44 g cm^{-3}, mid-slope = 1.39 g cm^{-3} and lower-slope = 1.36 g cm^{-3}) under sandy soil conditions. Suggesting that soils along the degraded slope profile are dense and unstable (Hossain *et al*., 2015), as hoof action and trampling by cattle contribute to soil compaction and surface crusting, which increases bulk density (Wilson and Seney, 1994; Evans, 1998; Laker, 2004; de Lima *et al*., 2018). Soils within the degraded slope profile are therefore prone to erosion as soil aggregates are sensitive to dispersion brought about through raindrop impact and sheet flow, which causes aggregates to break-down (Beare *et al.*, 1994; Guoxiao *et al*., 2008; Ma *et al*., 2014; Maïga-Yaleu *et al*., 2015; Doetterl *et al*., 2016), resulting in the detachment and transport of sediment (Wilson and Seney, 1994; Gyssels *et al*., 2005; Borrelli *et al*., 2016). This process results in the loss of soil organic carbon and nitrogen as these soil properties are carried away with the physical removal of sediment (Laker, 2004; Borrelli *et al*., 2016).

Soil porosity declines and vegetation within the top- and mid-slope is sparse (score of 3 and 2 respectively according to the Braun-Blanquet classification (Zietsman, 2003), contributing to the increased susceptibility of the soils to erosion. Despite the decrease in grass cover with slope position, 50 % grass cover occurred in the lower-slope. This was not expected, as the $^{210}Pb_{ex}$ inventory results suggest that the lower-slope is an erosional site and not a depositional site, thus one would expect less vegetation cover. An explanation for the increase in vegetation cover could be that cattle graze on the hillslopes during summer months (Sonneveld *et al.*, 2005; Birkett *et al*., 2016) and therefore grasses in the lower-slope are able to grow. However, distinct cattle paths are present in the lower-slope as cattle follow these paths to access grass on the slopes and plateau.

5.4 SOC and N distribution within the soil profile

At each sampling site higher soil organic carbon and nitrogen concentrations were measured in the 0-5 cm layer and decreased with depth, as supported by Mishra *et al*., (2007). A study conducted by Batjes (2012), in the Upper Tana River catchment in Kenya, showed that "an average of 44-50% of the SOC content in soil is stored in the upper 30 cm, the layer most vulnerable to changes in land use or management" (Gelaw *et al*., 2015:696). Furthermore, Trujillo *et al*., (1997) observed that soil organic carbon content generally decreased with depth regardless of vegetation, soil texture, and clay size fractions (Gelaw *et al*., 2015), as highlighted by this research. In comparison to the other sampling areas, greatest soil organic carbon and nitrogen content were found in the reference site as soil aggregates are more stable with greater pore space available for root growth (Castel and Cantero-Martinez, 2003). This indicates greater soil stability and high soil organic matter content present at the reference site (Périé and Ouimet, 2008).

On the contrary, soil organic carbon and nitrogen stocks increased with depth (Figure 4.6c and d). According to Hobley and Wilson (2016:1), soil organic matter content decreases with increasing depth thus "the C stabilization capacity of the sub-soil is less likely to be exhausted and subsurface soils will have a greater capacity for SOC storage". In additional, they suggest that soil organic carbon age increases with increasing depth and is more stable than soil organic carbon near the surface, allowing subsurface (0-30cm) soil organic carbon stocks to have a longer resident time. This results in the increase of subsurface soil organic carbon and nitrogen stocks with depth (0-30 cm), which promotes sub-soil organic carbon sequestration (Hobley and Wilson 2016).

Soil bulk density did not increase with depth as indicated by some research (Brady, 1984), nor did it decrease with depth as shown by Gelaw *et al.*, (2015). Rather ρb varied among the 0-5, 5-15 and 15-30 cm layers (ranging between 1.15 g cm^{-3} and 1.52 g cm^{-3}), indicating varying degrees of compaction and pore space availability within the soil profile (0-30 cm). These high ρb values, along with an aggregate stability which decreases with depth, suggests that constant surface compaction caused by hoof action results in the lack of vegetation, restricted root growth, decreased pore spaces and unstable soil aggregates. Consequently, reduced infiltration and increased runoff occur (Maïga-Yaleu *et al.*, 2015; Doetterl *et al.*, 2016).

5.5 Aggregate size distribution and SOC and N content

Higher soil organic carbon and nitrogen concentrations and stock where found in the <53 µm aggregate size class (Tables 4.3 and 4.4 and Figure 4.10 and 4.11). This indicates greater protection of soil organic matter and thus protection of soil organic carbon and nitrogen within this aggregates size class (Erktan *et al.*, 2015; Torres-Sallan *et al.*, 2018). Likewise, <53 µm aggregate size class within the reference site had the largest soil organic carbon and nitrogen content and stocks indicating the protection of soil organic matter within this aggregate size class. Aggregate associated carbon provides strength and stability to the soil to counter the impact of destructive forces such as rainsplash and is therefore important in maintaining soil structure (Gelaw *et al.*, 2015; Yigini and Panagos, 2016).

The proportion (weight %) of macro-aggregates (>2000 µm) at depths intervals 0-5, 5-15 and 15-30 cm within the reference site is greater than at the other sampling sites (Figure 4.7), implying greater aggregate stability compared to the degraded slope positions. As indicated by ρb and MWD, soils within the reference site are stable and macro-aggregates dominant as soil aggregates are not impacted by land use management or broken-down by rainsplash as they are protected by vegetation cover which increases soil organic matter (Blair, 2010; Liu *et al*., 2014). Within all aggregate size classes at depth intervals 0-5, 5-15 and 15-30 cm, soil organic carbon content and nitrogen content are significantly higher at the reference site compared to the degraded downslope positions.

Less macro-aggregates are found at depth intervals 0-5, 5-15 and 15-30 cm within the top-, mid-and lower-slope, compared to the reference site. This is due to the break-down of macro-aggregates within these sites, as the soil structures are weaker. Unsuitable land use management practices, through overstocking and overgrazing, affects soil aggregate stability (Maïga-Yaleu *et al*., 2015; Doetterl *et al*., 2016). The hoof action and trampling by cattle, as they move up and down along the slopes, lead to vegetation removal and promote soil compaction along cattle paths (Logsdon and Karlen, 2004; Hossain *et al*., 2015; de Lima *et al*., 2018). These bare soils become exposed to direct raindrop impact which breaks soil surface aggregates and results in soil surface crusting and compaction (Beare *et al.*, 1994; Guoxiao *et al*., 2008; Ma *et al*., 2014; Chaplot and Cooper 2015; Maïga-Yaleu *et al*., 2015; Doetterl *et al*., 2016).

At the top-, mid- and lower-slope, the low quantities of soil organic carbon content and nitrogen content found within all aggregate size classes and at depth intervals 0-5, 5-15 and 15-30 cm, indicate the low protection of SOM within these aggregates. The soil organic carbon and nitrogen content are lower within the macro-aggregate size class and greatest within the silt plus clay fraction. This occurs because macro-aggregates are less stable than micro-aggregates and because macro-aggregates have a lower protective effect against microbial attack and dispersion brought about through raindrop impact. This lower protective effect causes the SOC associated with these macro-aggregates to be lost more rapidly as they are more sensitive to changes in land use than micro-aggregates (Liu *et al*., 2014; Gelaw *et al*., 2015; Torres-Sallan *et al*., 2018). Macro-aggregates are more easily broken-down, resulting in lower protection of soil organic carbon and nitrogen content within this aggregate size class.

The break-down of soil aggregates is prominent at the degraded slope positions (top-, mid- and lower-slope) as the susceptibility to erosion increases due to soil compaction and slope gradient

(25%). Raindrop impact and overland flow causes aggregates to break-down and reduces infiltration, thus increasing surface runoff and erosion (Guoxiao *et al*., 2008; Ma *et al*., 2014; Maïga-Yaleu *et al*., 2015; Doetterl *et al*., 2016). Water erosion therefore has the most significant impact on soil organic carbon and nitrogen storage as soil organic matter is not only detached and transported, causing soil organic carbon and nitrogen to be physically removed, but the break-down of aggregates increase the exposure of organic matter to oxidizing conditions resulting in increased CO_2 emissions (Wilson and Seney, 1994; Laker, 2004; Gyssels *et al*., 2005; Chaplot and Cooper, 2015; Borrelli *et al*., 2016). Soil erodibility therefore increases as aggregate stability decreases, creating a land use management issue, as the effects of degradation are experienced throughout the ecosystem.

5.6 Fallout radionuclides and soil erosion

5.6.1 Cattle path erosion

The use of fallout radionuclides presented an alternative method to traditional techniques used in soil erosion studies (Li and Lindstrom, 2001; Mabit *et al*., 2013). They present a unique opportunity to document sediment transportation and deposition rates and to trace the movement of sediment through landscapes (Walling, 2012). Bomb testing of the late 1950s to early 1960s, injected ^{137}Cs into the stratosphere distributing it globally. Despite maximum fallout of ^{137}Cs being received in the mid-latitudes of the northern hemisphere, of that fallout 30% was received in the southern hemisphere (Walling, 2012). Considering the lower inventories received, measurement constraints are said to be presented in the southern hemisphere (Walling, 2012). However, Humphries *et al*., (2010:89) conducted a study which represented “the first attempt known to the authors to derive sediment accumulation rates using ^{137}Cs and ^{210}Pb in a southern African wetland.” The study was conducted on the Mkuze River floodplain in South Africa and concluded that radionuclides could be used in wetland studies within the region. Furthermore, ^{137}Cs and ^{210}Pb$_{ex}$ were successfully used in a study conducted for sediment tracing and for the determining environmental history within two small catchments of the Karoo Uplands in South Africa (Foster *et al*., 2007). Unfortunately, the use of ^{137}Cs as an indicator for soil erosion within Okhombe could not be determined as the soil samples were characterized by low ^{137}Cs activities below detection levels.

Lead-210 in soils is derived from atmospheric aerosol deposition and from *in situ* decay from radium containing soils. Once deposited, atmospherically derived ^{210}Pb, is buried and decays. As a result, ^{210}Pb$_{ex}$ activities should decrease with increasing depth (Fang *et al*., 2013; Gaspar *et al*., 2014; Szmytkiewicz and Zalewska, 2014). Soil results for this research, however, show an increase in $^{210}Pb_{ex}$ activities with depth. This increase of inventories with depth occur due to a combination of factors including sedimentation rates and decay. This indicates that net soil accumulation rates are highly variable and inconsistent between slope positions. In other words, erosive processes within the study area are not constant over time and have varied significantly during the past 100-150 years (Lubis, 2006). The large variability in $^{210}Pb_{ex}$ inventories indicates significant lateral redistribution of $^{210}Pb_{ex}$ after deposition as atmospheric deposition rates are unlikely to have varied to such a large extent, causing these results to be of little value in determining sedimentation rates (Meusburger *et al*., 2018).

Using $^{210}Pb_{ex}$ inventories (Table 4.5), points of erosion and deposition are identified by comparing the measured inventory with those of a reference inventory - areas of erosion will have inventories less than that of the reference site, and areas of deposition will have inventories greater than that of the reference site (Walling, 2012; Poręba, 2006; Mabit *et al*., 2014). According to the results, cattle path erosion occurs at the mid-slope and lower-slope, as inventories are less than that of the reference site. Alternately, material accumulation occurs at the top-slope relative to the reference site, which was not expected due to factors including: bulk density measurements (1.44 ± 0.05 g cm^{-3}) which indicate soil compaction, unstable soil aggregates and soil structure according to MWD (1.76 ± 0.07 mm) and low weight percentage of macro-aggregates, low soil organic carbon and nitrogen content, and acidic soils which restrict root growth and limit access to water and nutrients (Logsdon and Karlen, 2004). These factors suggest soil erosion and not deposition.

The occurrence of $^{210}Pb_{ex}$ inventories at the top-slope being greater than that found at the reference site, is therefore not understood. It was initially assumed that the difference in $^{210}Pb_{ex}$ was a result of a dilution effect, whereby soil organic matter within the mid and lower-slopes could have 'diluted' the mineral associated ^{210}Pb, leading to lower inventories within these slope positions (Binford and Brenner, 1986; Stille *et al*., 2011). Therefore, rather than sediment 'accumulation' occurring in the top-slope, minimal dilution of $^{210}Pb_{ex}$ could have occurred, resulting in higher $^{210}Pb_{ex}$ inventories. This assumption however does not hold, as the concentration of soil properties (such as SOC, N, P, Ca, Mg, Zn, Mg and Cu) found at the top-slope are greater than the concentrations found at the mid- and lower-slope, therefore a diluted effect could not have occurred. In other words, if a dilution affect did occur, maximum dilution should have occurred in the top-slope due to the higher concentration of soil properties present and $^{210}Pb_{ex}$ inventories would be low. However this is not the case. Another explanation for this occurrence could be the extreme variability and inconsistency of the net soil accumulation rates that exits within the study area. This could have resulted in sediment accumulation at the top-slope and soil erosion at the mid- and lower-slope. However, research supporting and explaining the reason for this occurrence was not found.

5.6.2 SOC and N distribution

The relationship between $^{210}Pb_{ex}$ and soil organic carbon is poorly understood. Teramage *et al*., (2013) conducted a study to investigate the relationship of soil organic carbon with $^{210}Pb_{ex}$ and ^{137}Cs where it was hypothesised that "$^{210}Pb_{ex}$ can be associated with and directly quantify SOC in forested areas" (Teramage *et al*., 2013:60). The results of the study indicated that higher values of SOCc are associated with higher concentrations of $^{210}Pb_{ex}$, suggesting that $^{210}Pb_{ex}$ and soil organic carbon are likely to move together in the course of soil erosion processes. This is due to $^{210}Pb_{ex}$ being constantly deposited into the soil from the atmosphere, which is similar to the replenishment of soil organic carbon from sources of soil organic matter. On the contrary, the relationship between $^{210}Pb_{ex}$ and soil organic carbon in sloping landscapes are poorly studied. Results for this study do not show high values of soil organic carbon content associated with high $^{210}Pb_{ex}$ concentrations, as suggested by Teramage *et al*., (2013). This is due to the significant variability in $^{210}Pb_{ex}$ activities within the study area. As such, determining the relationship between soil organic carbon, nitrogen and $^{210}Pb_{ex}$ distribution within Okhombe was not possible.

However, according to the $^{210}Pb_{ex}$ inventories, erosion occurs in the mid- and lower-slope (Table 4.5), where soil organic carbon and nitrogen concentrations are low (Table 4.2). This shows that the detachment and transportation of soil particles by sheet erosion results in the physical removal of soil organic carbon and nitrogen, as these soil properties are carried away through erosion (Borrelli *et al*., 2016).

5.6.3 Limitations

One of the limitations of the use of radionuclides as a proxy for soil erosion is the cost of analysis. The number of soil samples and the depth to which samples were collected for analyses was restricted to 36 samples to depth 30 cm due to the limited budget. Having a few soil samples collected to 30 cm and analysed for ^{137}Cs and $^{210}Pb_{ex}$ inventories and distributions, carries the risk of the results not being representative of the study area. This may lead to discrepancies in data and results reported.

The use of ^{137}Cs as a proxy for soil erosion within the southern hemisphere presented another limitation, as ^{137}Cs fell between the 1950s and 1960s within the northern hemisphere. This is evident within the results where the analysis of ^{137}Cs showed extremely low activity, with 75% of the samples (n=36) having activities below the detection limit of 0.05 dpm g^{-1}. Due to the extensive variability of $^{210}Pb_{ex}$ activities within the study area, sedimentation rates were not determined, nor was the relationship between $^{210}Pb_{ex}$ inventories and soil organic carbon and nitrogen determined, presenting another limitation to the study as this was one of the study's objectives.

5.7 Conclusion

Soils at Okhombe are naturally acidic and low in nutrients, where cattle path formation exacerbates the occurrence of erosion impacting on the soil structure and properties in this region. The undisturbed reference site is completely covered by vegetation and has a stable soil structure with stable soil aggregates, and therefore high soil organic carbon and nitrogen content and stock. Hoof action and trampling by cattle have however resulted in the formation of cattle paths which have led to increased soil compaction, decreased vegetation cover, and poor soil structure and aggregate stability within the degraded slope profile. In addition, $^{210}Pb_{ex}$ inventories demonstrate that in areas of soil erosion, soil organic carbon and nitrogen concentrations are low. This occurs as soil aggregates along the degraded slope are unstable and vulnerable to dispersion through rainsplash. This results in high losses of soil organic carbon and nitrogen as these properties are not protected within soil aggregates and are therefore lost with the removal of soil particles through sheet erosion.

The loss in soil nutrients highlight the negative impact of cattle path erosion, as the combination of unstable soil aggregates and structure, sparse vegetation, soil compaction and a steep slope gradient, increases the susceptibility of the degraded slope to sheet erosion. The development of cattle paths therefore promotes increased runoff and resultant soil erosion, which can be detrimental to the Ohkombe community.

Chapter Six

Conclusion

6.1 Conclusion

This thesis investigated the impact of cattle path erosion on soil properties along a steep slope in a communal grassland area in Okhombe Valley, Drakensberg, KwaZulu-Natal, South Africa. The objectives were set to highlight soil organic carbon and nitrogen dynamics as a result of cattle path formation, as the loss of grazing land through excessive erosion, and the depth and extent of ever expanding gullies, are of utmost concern to the community. The specific objectives of this study were to:

1. Identify an applicable reference site to be used as a control and applicable sampling sites along the degraded slope (top-, mid- and lower-slope) that are intercepted by cattle paths.
2. Determine the soil properties and trace elements of the degraded slope.
3. Evaluate soil organic carbon and nitrogen within the soil profile and soil aggregates.
4. Evaluate fallout radionuclides caesium-137 (^{137}Cs) and excess lead-210 ($^{210}Pb_{ex}$) to estimate soil deposition rates, and to link the findings to soil organic carbon and nitrogen distribution.

The main conclusions drawn were as follows:

In response to the first objective, the context of the study relates to a degraded slope within a rural area, with specific focus on the impact of cattle path erosion on soil organic carbon and nitrogen. Selecting an applicable reference site is vital for the successful use of ^{137}Cs and $^{210}Pb_{ex}$ in erosion based studies (Walling, 2012). The reference site refers to a stable undisturbed site, where no erosion or deposition occurs. This site was used to establish an inventory for ^{137}Cs and $^{210}Pb_{ex}$ in the study area. Caesium-137 and $^{210}Pb_{ex}$ inventories obtained from sampling points are compared with those of the reference inventory, where from this, areas of erosion and deposition within the study area can be identified (Ritchie *et al*., 2007; Walling, 2012). The selected reference site was located on the plateau of a hill at 1460 m above sea level (Plate 4), were no soil erosion or deposition occurred. Applicable sampling sites along the degraded slope were located at the top-slope 1439 m above sea level, the mid-slope 1403 m above sea level, and the lower-slope 1362 m above sea level. All positions were intercepted by cattle paths.

Determining the soil properties, trace elements and soil organic carbon and nitrogen within the study area in response to objectives two and three indicated:

i. greater soil organic carbon and nitrogen concentrations and stocks,
ii. higher nutrient content, and
iii. greater carbon and nitrogen protection within soil aggregates; were found at the reference site.

These results occurred at the undisturbed reference site as no soil erosion or deposition took place, compared to the other slope positions which where degraded due to cattle path erosion. In addition, significant soil compaction and soil instability occurred along the degraded slope profile compared to the undisturbed reference site. Cattle path formation results in loss of vegetation and increased soil compaction due to hoof action and trampling by cattle as they move up and down the slopes (Wilson and Seney, 1994; de Lima *et al*., 2018). This shows that greater nutrient loss occurs within the study area as a result of cattle path erosion.

Measuring fallout radionuclides ^{137}Cs and ^{210}Pb$_{ex}$ to estimate soil erosion and deposition rates, and to link the findings to soil organic carbon and nitrogen distribution- according to objective four indicated that:

i. extremely low levels of ^{137}Cs exist in the study area,
ii. erosive processes are not constant over time and have varied significantly during the past 100-150 years,
iii. soil redistribution is dominant in the slope sediments, with accumulation in the top-slope and removal from the mid- and lower-slopes, and
iv. soil organic carbon and nitrogen are physically removed with soil particles as they are detached and transported by sheet erosion.

It can be concluded that cattle path erosion in Okhombe plays a significant role in the loss of soil organic carbon and nitrogen within the degraded slope profile. This is evident through the impact that hoof action and trampling by cattle has had on the soil structure and soil properties within the degraded slope profile. The existing slope characteristics and topography of the region present an initial risk to soil erosion, however it is the cumulative impact of slope gradient and length, reduced vegetation cover, increased soil compaction, and reduced soil water infiltration, due to cattle path formation, that leads to increased surface runoff and the loss of soil organic carbon and nitrogen through erosion. Findings suggest that erosion at Okhombe is highly variable and has not been constant over the past 100-150 years.

The results from this study imply that poor soil nutrition and reduced vegetation cover, as a result of cattle path erosion, will significantly impact on the functioning of the ecosystem as the loss of land through excessive erosion, and the depth and extent of ever expanding gullies, are of utmost concern to the surrounding community who are reliant on these grasslands. This is significant as deep expanding gullies increase the risk of flooding and present a safety hazard to livestock and community members.

Soil erosion is a major issue threatening land resources throughout SA (Sonneveld *et al*., 2005; Wessels *et al*., 2007). This threat has both on- and off-site impacts that negatively influence the natural ecosystems. This study provided insight into cattle path erosion and soil organic carbon and nitrogen loss and transportation within a rural community, which relies on the grasslands for the provision of their livelihoods. This information will contribute to the ongoing efforts made through the LandCare Project to minimise land degradation and to assistant in the recovery and rehabilitation of grasslands within rural landscapes. This knowledge will aid in the development of models used to predict soil organic carbon and nitrogen distribution within landscapes, allowing for the design and implementation of effective soil erosion and sediment control strategies.

6.2 Recommendations and future research

Understanding the factors affecting sedimentation rates within the study area will allow for better understanding of the erosion processes and dynamics present. Such a study requires further field observations and additional data collected to a greater soil depths. This will provide insight into the movement of soil properties within the soil profile. The presence of vegetation cover within the undisturbed reference site, compared to the degraded slope profile, resulted in a stable soil structure and soils rich in nutrients. This highlights the significant influence of vegetation cover in protecting soil aggregates from breaking-down, and preventing the loss in soil nutrients through erosion. The rehabilitation of the degraded areas is therefore recommended, as improved soil structures and soil nutrients will be beneficial to the community through more efficient provision of ecosystem services. In addition, alternating the use of cattle paths will allow cattle paths to ‘recover’ as vegetation will be able to grow and soil structure improve. This will lower the impact of cattle path erosion on the livelihood of the community.

The use of fallout radionuclide ^{137}Cs as an indicator for soil erosion within Okhombe was unsuccessful due to very low activities within the study area. Using ^{210}Pb$_{ex}$ inventories allowed for the determining of points of erosion and deposition within the study site, however soil deposition rates and the relationship between ^{210}Pb$_{ex}$ and soil organic carbon and nitrogen was not determined. It is recommended that soil erosion plots would be a better method to evaluate soil erosion within this region, compared to ^{137}Cs and ^{210}Pb$_{ex}$.

The short duration of the study and the distance to the study area did not allow for *in situ* soil erosion measurements, using plot scale, and for long-term assessment, which incorporated greater plant, soil and environmental variables, to be made. Future research should therefore include measuring soil erosion *in situ* and over a longer period of time to obtain a more detailed understanding of the dynamics that exist within Okhombe. This can be achieved through the use of citizen science, which will allow community members to be involved in the continuous measuring and monitoring of erosion within the region.

This study is unique, as it adds to the limited research available on the impacts of cattle path erosion on soil properties within Ohkombe, and it is one of the first attempts to use the radionuclide technique in this country. This research will provide useful knowledge on the impacts of cattle path erosion on soil properties, and will aid in creating awareness of soil erosion impacts on, and the rehabilitation of grasslands within Ohkombe Valley, KwaZulu-Natal Drakensberg, South Africa.

References

Abdalla, K., Chivenge, P., Everson, C., Mathieu, O., Thevenot, M., Chaplot, V., 2016. Long-term annual burning of grassland increases CO_2 emissions from soils. *Geoderma*, 282, 80-86.

Arthur, E., Schjønning, Moldrup, P., Razzaghi, F., Tuller, M., and De Jonge, L.., 2014. Soil structure and microbial activity dynamics in 20-month field-incubated organic-amended soils. *European Journal of Soil Science*, 65, 218-230.

Batjes, N., 2012. Projected changes in soil organic carbon stocks upon adoption of recommended soil and water conservation practices in the upper Tana river catchment, Kenya. *Land Degradation and Development*, 25 (3), 278-287.

Beare, M., Cabrera, M., Hendrix, P., and Coleman, D., 1994. Aggregate-Protected and Unprotected Organic Matter Pools in Conventional- and No-Tillage Soils. *Soil Science of America Journal*, 58, 787-795.

Bilskie, J., 2001. Soil water status: content and potential. Campbell Scientific, Inc. App. Note: http://s.campbellsci.com/documents/cn/technical-papers/soilh20c.pdf. (Accessed March 2017).

Binford, M., and Brenner, M., 1986. Dilution of ^{210}Pb by organic sedimentation in lakes of different trophic states, and application to studies of sediment-water interactions. *The American Society of Limnology and Oceanography*, 31, 584-595.

Birkett, C., Hill, T., Zuma, K., and Everson, T., 2016. Bringing Rain to the Land: Rainfall Simulation as a Participatory Teaching Aid to Understanding Erosion. *Journal of Environmental Protection*, 7, 1305-1316.

Blair, N., 2010. *The impact of soil water content and water temperature on wet aggregate stability*. What answer do you want? 19th World Congress of Soil Science, Soil Solutions for a Changing World, Brisbane, Australia.

Borrelli, Paustian, K., Panagos, P., Jones, A., Schütt, B., and Lugato, E., 2016. Effect of Good Agricultural and Environmental Conditions on erosion and soil organic carbon balance: A national case study. *Land Use Policy*, 50, 408-421.

Brady, N., 1984. *The Nature and Properties of Soils*. Ninth Edition. Macmillian Publishing Company, New York.

Bronick, C.J. and Lal, R., 2005. Soil structure and management: a review. *Geoderma* 124, 3 – 22.

Castel, J., and Cantero-Martinez, C., 2003. Soil Bulk Density and Penetration Resistance Under Different Tillage and Crop Management Systems and Their Relationship with Barley Root Growth. *Agronomy Journal*, 95, 526-536.

Chaplot, V., 2013. Impact of terrain attributes, parent material and soil types on gully erosion. *Geomorphology*, 186, 1-11.

Chaplot, V., and Cooper, M., 2015. Soil aggregate to predict organic carbon from soils. *Geoderma*, 243/244, 205-213.

Chaudhari, P., Ahire, D., Ahire, V., Chkravarty, M., and Maity, S., 2013. Soil Bulk Density as related to Soil Texture, Organic Matter Content and available total Nutrients of Coimbatore Soil. *International Journal of Scientific and Research Publications,* 3 (2), 1-8.

Chicas, S., Omine, K., and Ford, J., 2016. Identifying erosion hotspots and assessing communities' perspectives on the drivers, underlying causes and impacts of soil erosion in Toledo's Rio Grande Watershed: Belize. *Applied Geography*, 68, 57-67.

Christensen, B., 2001. Physical fractionation of soil and structural and functional complexity in organic matter turnover. *European Journal of Soil Science*, 52, 345-353.

Collins, A., Walling, D., Sichingabula, H., and Leeks, G., 2001. Using ^{137}Cs measurements to quantify soil erosion and redistribution rates for areas under different land use in the Upper Kaleya River basin, southern Zambia. *Geoderma*, 104, 299-323.

Correa, S., Mello, C., Chou, S., Curi, N., and Norton, L., 2016. Soil erosion risk associated with climate change at Mantaro River basin, Peruvian Andes. *Catena*, 147, 110-124.

Courtier, J., Sdraulig, S., Hirth, G., 2017. ^{7}Be and ^{210}Pb wet/dry deposition in Melbourne, Australia and the development of deployable units for radiological emergency monitoring. *Journal of Environmental Radioactivity*, 178/179, 419-425.

Cuomo, S., Sala, M., and Novità, A., 2015. Physically based modelling of erosion induced by rainfall in small mountain basins. *Geomorphology*, 243, 106-115.

Dabney, S., Liu, Z., Lane, M., Douglas, J., Zhu, J., and Flanagan, D., 1999. Landscape benching from tillage erosion between grass hedges. *Soil and Tillage Research*, 51, 219-231.

De Gryze, S., Six, J., Paustian, K., Morris, S., Paul, E., and Merck, R., 2004. Soil organic carbon pool changes following land-use conversions. *Global Change Biology*, 10, 1120-1132.

De Beer, J., Dreyer, J., Hattingh, J., Irwin, P., Le Grange, L., Le Roux, C., Lotz-sisitka, H., and Schulze, S., 2005. *Environmental Education – some South African perspectives*. Ed CP Loubser, Van Schaik Publishers, Pretoria.

de Neergaard, A., Magid, J., and Mertz, O., 2008. Soil erosion from shifting cultivation and other smallholder land use in Sarawak, Malaysia. *Agriculture, Ecosystems and Environment*, 125, 182-190.

de Lima, R., da Silva, A., Giarola, N., da Silva, A., Rolim, M., and Keller, T., 2018. Impact of initial bulk density and matric suction on compressive properties of two Oxisols under no-till. *Soil and Tillage Research,* 175, 168-177.

Dlamini, P., Orchard, C., Jewitt, G., Lorentz, S., Titshall, L., Chaplot, V., 2011. Controlling factors of sheet erosion under degraded grasslands in the sloping lands of KwaZulu-Natal, South Africa. *Agricultural Water Management*, 98, 1711-1718.

Dlamini, P., Chienge, P., Manson, A., and Chaplot, V., 2014. Land degradation impact on soil organic carbon and nitrogen stocks of sub-tropical humid grasslands in South Africa. *Geoderma*, 235/236, 372-381.

DEA. Department of Environmental Affairs., 2012. 2nd South Africa Environment Outlook. *A report on the state of the environment.* Department of Environmental Affairs, Pretoria. 328 pp.

Di Stefano, C., Ferro, V., Pampalone, V., and Sanzone, F., 2013. Field investigation of rill and ephemeral gully erosion in the Sparacia experimental area, South Italy. *Catena*, 101, 226-234.

Doetterl, S., Berhe, A., Nadeu, E., Wang, Z., Sommer, M., Fiener, P., 2016. Erosion, deposition and soil carbon: A review of process-level controls, experimental tools and models to address C cycling in dynamic landscapes. *Earth-Science Review*, 154, 102-122.

Egoh, B., Reyers, B., Rouget, M. and Richardson, D., 2011. Identifying priority areas for ecosystem service management in South African grasslands. *Journal of Environmental Management*, 92, 1642-1650.

Ellerbrock, R., Gerke, H., and Deumlich, D., 2016. Soil organic matter composition along a slope in an erosion-affected arable landscape in North East Germany. *Soil and Tillage Research*, 156, 209-218.

Elliott, E., 1986. Aggregate structure and carbon, nitrogen and phosphorus in native and cultivated soils. *Soil Science Society of America Journal*, 50, 627–633.

Erktan, A., Cécillon, L., Graf, F., Roumet, C., Legout, C., and Rey, F., 2015. Increase in soil aggregate stability along a Mediterranean successional gradient in severely eroded gully bed ecosystems: combined effects of soil, root traits and plant community characteristics. *Plant and Soil*, 398 (1), 121-137.

Evans, R., 1998. The erosional impacts of grazing animals. *Progress on Physical Geography*, 22(2), 251-268.

Everson, T., Everson, C., and Zuma, K., 2007. Community based research on the influence of rehabilitation techniques on the management of degraded catchments. Water Research Commission, Report No 1316/1/07.

Fang, H., Sheng, M., Tang, Z., and Cai, Q., 2013. Assessment of soil redistribution and spatial pattern for a small catchment in the black soil region, Northeastern China: Using fallout $^{210}Pb_{ex}$. *Soil and Tillage Research*, 133, 85-92.

Field, J., 2001. Channel avulsion on alluvial fans in southern Arizona. *Geomorphology*, 37, 93-104.

Forrester, D., Pares, A., Hara, C., Khanna, P., and Bauhus, J., 2013. Soil Organic Carbon is increased in Mixed-Species Plantations of Eucalyptus and Nitrogen-Fixing Acacia. *Ecosystems*, 16, 132-132.

Foster, I., Boardman, J., and Keay-Bright, J., 2007. Sediment tracing and environmental history for two small catchments, Karoo Uplands, South Africa. *Geomorphology*, 90, 126-143.

Fu B., Wang, J., Chen, L., Qiu, Y., 2003. The effects of land use on soil moisture variation in the Danangou catchment of the Loess Plateau, China, *Catena*, 54, 197–213.

Gamoun, M., Tarhouni, M., Belgacem, A., Hanchi, B., and Neffati, M., 2010. Effects of grazing and Trampling on Primary Production and Soil Surface in North African Ranglands. *Ekológia*, 29, 219-226.

Gao, Y., Dang, X., Yu, Y., Li, Y., Liu, Y., and Wang, J., 2016. Effects of Tillage Methods on Soil Carbon and Wind Erosion. *Land Degradation and Development*, 27, 583-591.

Gaspar, L., Navas, A., Walling, D., Machín, J., and Gómez Arozamena, J., 2013. Using ^{137}Cs $^{210}Pb_{ex}$ to assess soil redistribution on slopes at different temporal scales. *Catena*, 102, 46-54.

Gelaw, A., Singh, B., and Lal, R., 2015. Organic carbon and nitrogen associated with soil aggregates and particle sizes under different land uses in Tigray, Northern Ethiopia. *Land Degradation and Development*, 26, 690-700.

Grab, S., and Kalibbala, F., 2008. 'Anti-erosion' logs across paths in the southern uKhahlamba-

Drakensberg Transfrontier Park, South Africa: Cure or curse? *Catena*, 73, 134-145.

Guo, L., and Gifford, R., 2002. Soil carbon stocks and land use change: a meta-analysis. *Global Change Biology*, 8, 345-360.

Guoxiao, W., Yibo, W., and Yan lin, W., 2008. Using ^{137}Cs to quantify the redistribution of soil organic carbon and total N affected by intensive soil erosion in the headwaters of the Yangtze River, China. *Applied Radiation and Isotopes*, 66, 2007-2012.

Gyssels, G., Poesen, J., Bochet, E., and Li, Y., 2005. Impact of plant roots on the resistance of soils to erosion by water: a review. *Progress in Physical Geography*, 29 (2), 189-217.

Hagos, D., 2004. A Distributed sediment delivery ratio concept for sediment yield modelling. (Master's Thesis). School of Bioresources Engineering and Environmental Hydrology, University of KwaZulu-Natal, Pietermaritzburg, South Africa.

Han, X., Gao, G., Chang, R., Li, Z., Ma, Y., Wang, S., Wang, C., Lü, Y., and Fu, B., 2018. Changes in soil organic and inorganic carbon stocks in deep profiles following cropland abandonment along a precipitation gradient across the Loess Plateau of China. *Agriculture, Ecosystems and Environment*, 258, 1-13.

Harrison, Y., and Shackleton, C., 1999. Resilience of South African Communal Grazing Lands after the Removal of High Grazing Pressure. *Land Degradation and Development*, 10, 225-239.

Hobley, E., and Wilson, B., 2016. The depth distribution of organic carbon in the soils of eastern Australia. *Ecosphere*, 7, 1-21.

Hossain, M., Chen, W., and Zhang, Y., 2015. Bulk density of mineral and organic soils in the Canada's arctic and sub-arctic. *Information Processing in Agriculture*, 2, 183-190.

Hunter, A., 1974. *Tentative ISFEI soil extraction procedure*. International Soil Fertility and Improvement Project. N.C. State University, Raleigh, NC.

Humphries, M., Kindness, A., Ellery, W., Hughes, J., and Benitez-Nelson C., 2010. ^{137}Cs and ^{210}Pb derived sediment accumulation rates and their role in the long-term development of the Mkuze River floodplain, South Africa. *Geomorphology*, 19, 88-96.

Janueau, J., Gillard, L., Grellier, S., Jouquet, P., Thi Phuong Quynh, L., Thi Nguyet Minh, L., Quoc Anh, N., Orange, D., Dinh Rinh, P., Duc Toan, T., Sy Hai, T., Anh Duc, A., Valentin, C., Rochelle-Newall, E., 2014. Soil erosion, dissolved organic carbon and nutrient losses under different land use systems in a small catchment in northern Vietnam. *Agricultural Water Management*, 146, 314-323.

Jha, A., Schkade, U., and Kirchner, G., 2015. Estimating short-term soil erosion rates after single and multiple rainfall events by modelling the vertical distribution of cosmogenic ^{7}Be in soils. *Geoderma*, 243/244, 149-156.

Jobbágy, E., and Jackson, R., 2000. The vertical distribution of soil organic carbon and its relation to climate and vegetation. *Ecological Applications*, 423-436.

Keesstra, S., Pereira, P., Novara, A., Brevik, E., Azorin-Molina, C., Parras-Alcántara, L., Jordán, A., and Cerdà, A., 2016. Effects of soil management techniques on soil water erosion in apricot orchards. *Science of the Total Environment*, 551/552, 357-366.

Laker, M.C., 2004. Advances in soil erosion, soil conservation, land suitability evaluation and land use planning research in South Africa, 1978–2003, *South African Journal of Plant and Soil*, 21(5), 345-368.

Lal, R., 2003. Soil erosion and the global carbon budget. *Environment International*, 29, 437-450.

Lal, R., 2008. Carbon Sequestration. *Philosophical Transactions of the Royal Society of London B: Biological Sciences*, 363, 815-830.

Le Roux, J.J., Newby, T.S., and Sumner, P.D., 2007. Monitoring soil erosion in South Africa at a regional scale: review and recommendations. *South African Journal of Science*, 103, 329-335.

Le Roux, J.J., Morgenthal, T.L., Malherbe, J., Pretorius, D.J., Sumner, P.D., 2008. Water erosion prediction at a national scale for South Africa. *Water SA*, 34, 305-314.

Le Roux, J.J., 2011. Monitoring soil erosion in South Africa at a regional scale. Report for the Council of Geoscience Geohazards Project. Agricultural Research Council Institute for Soil, Climate and Water. ARC-ISCW report no GW/A/2011/23.

Li, Y., and Lindstrom, M., 2001. Evaluating Soil Quality-Soil Redistribution Relationship on Terraces and Steep Hillslope. *Soil Science Society of America Journal*, 65, 1500-1508.

Li, Z., Zhang, G., Geng, R., and Wang, H., 2015. Rill erodibility as influenced by soil and land use in a small watershed of the Loess Plateau, China. *Biosystems Engineering*, 129, 248-257.

Li, Z., Zhang, Y., Zhu, Q., Yang, S., Li, H., and Ma, H., 2017. A Gully erosion assessment model for the Chinese Loess Plateau based on changes in gully length and area. *Catena*, 148, 195-203.

Liu, Z., Yao, Z., Huang, H, Wu, S., and Liu, G., 2012. Land use and Climate changes and their impacts on runoff in the Yarlung Zangbo River Basin, China. *Land Degradation and Development*, 25, 203-215.

Liu, M., Chang, Q., Qi, Y., Liu, J., and Chen, T., 2014. Aggregation and soil organic carbon fractions under different land uses on the tableland of the Loess Plateau of China. *Catena*, 115, 19-28.

Logsdon, S., and Karlen, D., 2004. Bulk density as a soil quality indicator during conversion to no-tillage. *Soil and Tillage Research*, 78, 143-149.

Lubis, A., 2006. Constant rate of supply (CRS) model for determining the sediment accumulation rates in the coastal area using ^{210}Pb. *Journal of Coastal Development*, 10, 9-18.

Luffman, I., Nandi, A., and Spiegel, T., 2015. Gully morphology, hillslope erosion, and precipitation characteristics in the Appalachian Valley and Ridge province, south eastern USA. *Catena*, 133, 221-232.

Lu, J., Zheng, F., Li, G., Bian, F., and An, J., 2016. The effects of raindrop impact and runoff detachment on hillslope soil erosion and soil aggregate loss in the Mollisol region of Northeast China. *Soil and Tillage Research*, 161, 79-85.

Ma, W., Li, Z., Ding, K., Huang, J., Nie, X., Zeng, G., Wang, S., and Liu, G., 2014. Effect of soil erosion on dissolved organic carbon redistribution in subtropical red soil under rainfall simulation. *Geomorphology*, 226, 217-225.

Maalim, F., Melesse, A., Belmont, P., and Gran, K., 2013. Modeling the impact of land use changes on runoff and sediment yield in the Le Sueur watershed, Minnesota using GeoWEPP. *Catena*, 107, 35-45.

Mabit, L., Meusburger, K., Fulajtar, E., and Alewell, C., 2013. The usefulness of ^{137}Cs as a tracer for soil erosion assessment: A critical reply to Parsons and Foster (2011). *Earth-Science Review*, 127, 300-307.

Mabit, L., Benmansour, M., Abril, J., Walling, D., Meusburger, K., Iurian, A., Bernard, C., Tarján, S., Owens, P., Blake, W., and Alewell, C., 2014. Fallout ^{210}Pb as a soil and sediment tracer in catchment sediment budget investigations: A review. *Earth-Science Review*, 138, 335-351.

Mucina, L., and M.C. Rutherford. 2006. The vegetation of South Africa, Lesotho and Swaziland. South African National Biodiversity Institute (SANBI). Cape Town, South Africa.

Mugade, U., and Sapkale, J., 2015. Influence of Aggradation and Degradation on River

Channels: A Review. *International Journal of Engineering and Technical Research*, 3, 209-212.

Maïga-Yaleu, S., Chivenge, P., Yacouba, H., Guiguemde, I., Karambiri, H., Ribolzi, O., Bary, A., and Chaplot, V., 2015. Impact of sheet erosion mechanisms on organic carbon losses from crusted soils in the Sahel. *Catena*, 126, 60-67.

Moni, C., Derrien, D., Hatton, P., Zeller, B., and Kleber, M., 2012. Density fractions versus size separates: does physical fractionation isolate functional soil compartments. *Biogeosciences*, 9, 5181-5197.

Mansour, K., Mutanga, O., Everson, T., and Adam, E., 2012. Discriminating indicator grass species for rangeland degradation assessment using hyperspectral data resampled to AISA Eagle resolution. *ISPRS Journal of Photogrammetry and Remote Sensing,* 70, 56-65.

Márquez, C., Garcia, V., Cambardella, C., Schultz, R., and Isenhart, T., 2004. Aggregate-Size Stability Distribution and Soil Stability. *Soil Science Society of America Journal*, 68, 725-735.

Marx, D., 2011. An assessment of ecological impacts of community-based restoration on communal grasslands in Drakensberg foothills. Percy FitzPatrick Institute, University of Cape Town, Rondebosch, Cape Town.

Meusburger, K., Porto, P., Mabit, L., La Spada, C., Arata, L., and Alewell, C., 2018. Excess Lead-210 and Plutonium-239 + 240: Two suitable radiogenic soil erosion tracers for mountain grassland sites. *Environmental Research*, 160, 195-202.

Mishra, U., Lal, R., Slater, B., Calhoun, F., Liu, D., and Van Meirvenne, M., 2007. Predicting Soil Organic Carbon Stock Using Profile Depth Distribution Functions and Ordinary Kriging. *Soil Science Society American Journal*, 73, 614-621.

Mousazadech, F., and Salleh, K., 2014. Factors controlling gully erosion development in Toroud basin-Iran. *Procedia-Social and Behavioural Sciences*, 120, 506-512.

Murphy, J., and Riley, J., 1962. A modified single solution method for the determination of phosphate in natural waters. *Analytica Chimica Acta*, 27, 31-36.

Nel, W., Sumner, P., 2007. Intensity, energy and erosivity attributes of rainstorms in the KwaZulu-Natal Drakensberg, South Africa, *South African Journal of Science* 103, 398-402.

Nosrati, K., Haddadchi, A., Zare, M., Shirzadi, L., 2015. An evaluation of the role of hillslope components and land use in soil erosion using ^{137}Cs inventory and soil organic carbon stock. *Geoderma*, 243/244, 29-40.

Oakes, E.M., Hughes, J.C., Jewitt, G.P., Lorentz, S.A., and Chaplot, V., 2012. Controls on a scale explicit analysis of sheet erosion. *Earth Surface Processes and Landforms*, 37, 847-854.

Ochoa, P., Fries, A., Mejía, D., Burneo, J., Ruíz-Sinoga, J., and Cerdà, A., 2016. Effects of climate, land cover and topography on soil erosion risk in a semiarid basin of the Andes. *Catena*, 140, 31-42.

Ollobarren, P., Capra, A., Gelsomino, A., La Spada, C., 2016. Effects of ephemeral gully erosion on soil degradation in a cultivated area in Sicily (Italy). *Catena*, 145, 334-345.

Parsons, A., and Dumont, B., 2003. Spatial heterogeneity and grazing processes. *Animal Research*, 52, 161-179.

Parsons, A., and Foster, I., 2011. What can we learn about soil erosion from the use of ^{137}Cs? *Earth-Science Reviews*, 108, 101-113.

Parsakhoo, A., Lotfalian, M., Kavian, A., and Hosseini, S., 2014. Prediction of the soil erosion in a forest and sediment yield from road network through GIS and SEDMODL. *International Journal of Sediment Research*, 29, 118-125.

Parwada, C., and Van Tol, J., 2017. Soil properties influencing erodibility of soils in the Ntabelanga area, Eastern Cape Province, South Africa. *Soil and Plant Science*, 67, 67-76.

Paul, S., Veldkamp, E., and Flessa, H., 2008. Soil organic carbon in density fractions of tropical soils under forest – pasture – secondary forest land use changes. *European Journal of Soil Science*, 2008, 359-371.

Peden, M., 2005. Tackling 'the most avoided issue': communal rangeland management in KwaZulu-Natal, South Africa. *African Journal of Range and Forage Science*, 22 (3), 167-175.

Pennock, D., and Appleby, P., 2002. 'Site Selection and Sampling Design', 15-40. In Zapata, F., 2002 (Eds) *Handbook for the Assessment of Soil Erosion and Sedimentation Using Environmental Radionuclides*. Secaucus, NJ, USA: Kluwer Academic Publishers.

Périé, C., and Ouimet, R., 2008. Organic carbon, organic matter and bulk density relationships in boreal forest soils. *Canadian Journal Soil Science*, 88, 315-325.

Pile, K., 1996. Soil Erosion, policy and people's perceptions in a rural community in KwaZulu-

Natal, South Africa. *GeoJournal*, 39, 59-64.

Pimental, D., 2006. Soil Erosion: A Food and Environmental Threat. *Environment, Development and Sustainability*, 8, 119-137.

Porto, P., Walling, D., Tamburino, V., and Callegari, G., 2003. Relating caesium-137 and soil loss from cultivated land. *Catena*, 53, 303-326.

Poesen, J., Nachtergaele, G., Verstraeten, G., and Valentin, C., 2003. Gully erosion and environmental change: importance and research needs. *Catena*, 50, 91-133.

Poręba, G., 2006. Caesium-137 as a soil erosion tracer: a review. *Geochronometria*, 25, 37-46.

Rawlins, B., Turner, G., Wragg, J., McLachlan, P., and Lark, R., 2015. An improved method for measurement of soil aggregate stability using laser granulometry applied at regional scale. *European Journal of Soil Science*, 66, 604-614.

Resh, S., Binkley, D., and Parrotta, J., 2002. Greater Soil Carbon Sequestration under Nitrogen-fixing Tress Compared with *Eucalyptus* Species. *Ecosystems*, 5, 217-231.

Ritchie, J., McCarty, G., Venteris, E., and Kaspar, T., 2007. Soil and soil organic redistribution on the landscape. *Geomorphology*, 89, 163-171.

Rowntree, K., Duma, M., Kakembo, V., and Thornes, J., 2004. Debunking the myth of overgrazing and soil erosion. *Land Degradation and Development*, 15, 203-214.

Saiz, G., Wandera, F., Pelster, D., Ngetich, W., Okalebo, J., Rufino, M., and Betterbach-Bahl, K., 2016. Long-term assessment of soil and water conservation measures (Fanya-juu terraces) on soil organic matter in South Eastern Kenya. *Geoderma*, 274, 1-9.

Sarno, J., Afandi, T., Yoko, O., Masaharu, S., and Akira, W., 2004. Effect of weed management in coffee plantation on soil chemical properties. *Nutrient Cycling in Agroecosystems*, 69, 1-4.

Saedi, T., Shorafa, M., Gorji, M., Khalili Moghadam, B., 2016. Indirect and direct effects of soil properties on soil splash erosion rate in calcareous soils of the central Zagross, Iran: A laboratory study. *Geoderma*, 271, 1-9.

Sandhage-Hofmann, A., Kotzé, E., van Delden, L., Dominiak, M., Fouché, H., van der Westhuizen, H., Oomen, R., du Preez, C., and Amelung, W., 2015. Rangeland management effects on soil properties in the savanna biome, South Africa: A case study along grazing gradients in communal and commercial farms. *Journal of Arid Environments*, 120, 14-25.

Schmiedel, U., Kruspe, M., Kayser, L., Oettlé, N., 2017. The ecological and financial impact of soil erosion and its control-A case study from the Semiarid Northern Cape Province, South Africa. *Land Degradation and Development,* 28, 74-82.

Shellberg,J., Spencer, J., Brooks, A., and Pietsch, T., 2016. Degradation of the Mitchell River fluvial megafan by alluvial gully erosion increased by post-European land use change, Queensland, Australia. *Geomorphology*, 266, 105-120.

Shen, H., Zheng, F., Wen, L., Han, Y., Hu, W., 2016. Impacts of rainfall intensity and slope gradient on rill erosion processes at loessial hillslope. *Soil and Tillage Research*, 155, 429-436.

Six, J., Elliot, E., and Paustian, K., 2000. Soil macroaggregate turnover and microaggregate formation: a mechanism for C sequestration under no-tillage agriculture. *Soil Biology and Biochemistry,* 32, 2099-2103.

Six, J., Callewaert, P., Lenders, S., De Gryze, S., Morris, S., Gregorich, E., Paul, E., and Paustian, K., 2002. Measuring and Understanding Carbon Storage in Afforested Soils by Physical Fractionation. *Soil Science American Journal*, 66, 1981-1987.

Smith, H., van Zyl, A., Claassens, A., Schoeman, J., and Laker, M., 2000. Soil loss modelling in the Lesotho Highlands Water Project catchment areas. *South African Geographical Journal*, 82, 64-69.

Sonneveld, M., Everson, T., and Veldkamp, A., 2005. Multi-scale analysis of soil erosion dynamics in KwaZulu-Natal, South Africa. *Land Degradation and Development*, 16, 287-301.

South Africa. Department Strategic Planning and Economic Development. 2010. *Draft IDP Review 2009/2010*. Ladysmith: Uthukela District Municipality.

Soil Classification Working Group., 1991. *Soil Classification: A Taxonomic System for South Africa*. Memoirs on the Agricultural Natural Resources of South Africa No. 15. Department of Agricultural Development, Pretoria, South Africa.

Stille, P., Pourcelot, L., Granet, M., Pierret, M., Guéguen, F., Perrone, T., Morvan, G., and Chabaux, F., 2011. Deposition and migration of atmospheric Pb in soils from a forested silicate catchment today and in the past (Stengbach case): Evidence from ^{210}Pb activities and Pb isotope ratios. *Chemical Geology*, 289, 140-153.

Status of the World’s Soil Resources (SWSR) – Main Report., 2015. Food and Agriculture Organization of the United Nations and Intergovernmental Technical Panel on Soils, Rome, Italy.

Szmytkiewicz, A., and Zalewska, T., 2014. Sediment deposition and accumulation rates determined by sediment trap and ^{210}Pb isotope methods in the Outer Puck Bay (Baltic Sea). *Oceanologia*, 56, 85-106.

Takenaka, C., Onda, Y., and Hamajima, Y., 1998. Distribution of cesium-137 in Japanese forest soils: Correlation with the contents of organic carbon. *The Science of Total Environment*, 222, 193-199.

Tau, M., 2005. Grazing management in the Communal Rangelands of the Upper Thukela, KwaZulu-Natal. (Master's Thesis). School of Biological and Conservation Sciences, University of KwaZulu-Natal, Pietermaritzburg, South Africa.

Temme, A., Baartman, J., Botha, G., Veldkamp, A., Jongmans, A., and Walling, J., 2008. Climate controls on late Pleistocene landscape evolution of the Okhombe valley, KwaZulu-Natal, South Africa. *Geomorphology*, 99, 280-295.

Temme, A., Baartman, J., and Schoorl, J., 2009. Can uncertain landscape evolution models discriminate between landscape responses to stable and changing future climate? A millennial-scale test. *Global and Planetary Change*, 9, 48-58.

Teramage, M., Onda, Y., Kato, H., Wakiyama, Y., Mizugaki, S., and Hiramatsu, S., 2013. The relationship of soil organic carbon to $^{210}Pb_{ex}$ and ^{137}Cs during surface soil erosion in a hillslope forested environment. *Geoderma*, 192, 59-67.

Totsche, K., Amelung, W., Gerzabek, M., Guggenberger, G., Klumpp, E., Knief, C., Lehndorff, E., Mikutta, R., Peth, S., Prechtel, A., Ray, N., and Kögel-Knabner, I., 2017. Review Article, Micro-aggregates in soils. *Journal of Plant Nutrition Soil Science*, 1-33.

Torres-Sallan, G., Creamer, R., Lanigan, G., Reidy, B., and Byrne, K., 2018. Effects of soil type and depth on carbon distribution within soil macro-aggregates from temperate grassland systems. *Geoderma*, 313, 52-56.

Trujillo, W., Amezquita, E., Fisher, M., and Lal, R., 1997. 'Soil organic carbon dynamics and land use in the Colombian Savannas'. In Lal, R., Kimble, J., Follet, R., and Stewart, B., (Eds), *Soil Processes and the Carbon Cycle*. CRC/Lewis Press, Boca Raton, FL, 267–280.

Valentin, C., Poesen, J., and Yong, Li., 2005. Gully erosion: Impacts, factors and control. *Catena*, 63, 132-153.

Van Oost, K., Cerdan, O., and Quine, T., 2009. Accelerated sediment fluxes by water and tillage erosion on European agricultural land. *Earth Surface Processes and Landforms*, 1-10.

van Oudtshoorn, F., 2012. *Guide to Grasses of southern Africa*. Third revised edition, Briza

Publications, Pretoria, South Africa.

Wakiyama, Y., Onda, Y., Mizugaki, S., Asai, H., and Hiramatsu, S., 2010. Soil erosion rates on forested mountain slopes estimates using ^{137}Cs and $^{210}Pb_{ex}$. *Geoderma*, 159, 39-52.

Walling, D., 2012. 'Fallout Radionuclides and the Study of Erosion and Sedimentation'. In Meyers, R., 2012 (Eds) *Encyclopaedia of Sustainability Science and Technology*. Springer Science and Business Media, LLC.

Walling, D., He, Q., and Appleby, P., 2002. 'Conversion Models for use in soil-erosion, soil-redistribution and sedimentation investigations', 111-164. In Zapata, F., 2002 (Eds) *Handbook for the Assessment of Soil Erosion and Sedimentation Using Environmental Radionuclides*. Secaucus, NJ, USA: Kluwer Academic Publishers.

Wang, C., Zhang, Y., Yang, Y., Yang, Q., Kush, J., Xu, Y., and Xu, L., 2016. Assessment of sustainable livelihoods of different farmers in hilly red soil erosion areas of southern China. *Ecological Indicators*, 64, 123-131.

Weil, R., and Brady, N., 2016. *The Nature and Properties of Soils.* Fifteenth Edition. Pearson Education, Columbus.

Wessels, K., Prince, S., Malherbe, J., Small, J., Frost, P., and VanZyl, D., 2007. Can human-induced land degradation be distinguished from the effects of rainfall variability? A case study in South Africa. *Journal of Arid Environments*, 68, 271-297.

Wessels, K., Pretorius, D., and Prince, S., 2008. The Reality of Rangeland Degradation Mapping with Remote Sensing: The South African Experience. Remote Sensing Research Unit, Meraka Institute, Council for Scientific and Industrial Research (CSIR), Pretoria, South Africa.

Wilson, J., and Seney, J., 1994. Erosional Impact of Hikers, Horses, Motorcycles, and off-road Bicycles on Mountain Trails in Montana. *Mountain Research and Development*, 14, 77-88.

Wirtz, S., Seeger, M., and Ries, J., 2012. Field experiments for understanding and quantification of rill erosion processes. *Catena*, 91, 21-34.

Yigini, Y., and Panagos, P., 2016. Assessment of soil organic carbon stocks under future climate and land changes in Europe. *Science of the Total Environment*, 557-558, 838-850.

Yüksel, A., Akay, A., Gundogan, R., Rets, M., and Cetiner, M., 2008. Application of GeoWEPP for Determining Sediment Yield and Runoff in the Orcan Creek Watershed in Kahramanmaras, Turkey. *Sensors*, 8, 1222-1236.

Zapata, F., Garcia-Agudo, E., Ritchie, J., and Appleby, P., 2002. 'Introduction', 1-13. In Zapata, F., 2002 (ed) *Handbook for the Assessáent of Soil Erosion and Sedimentation Using Environmental Radionuclides*. Secaucus, NJ, USA: Kluwer Academic Publishers.

Zietsman, M., 2003. Phytosociological study of Andrews field and Tsaba-Tsaba nature reserve, Bredasdorp district, Western Cape. (Master's Thesis). Department of Botany, University of Pretoria, Gauteng, South Africa.

Appendices

Appendix A – Calculation of slope profile

Plot 1 measurements and slope profile.

Angle downslope	Angle	Distance (m)	Sin angle	HD	HD CUM	vd
					0	
1,5	-1,5	40	0,0261	-1,047	-1,047	39,986
12,5	-12,5	40	0,2164	-8,657	-9,704	39,051
10	-10	34	0,1736	-5,904	-15,608	33,483
12	-12	10	0,2079	-2,079	-17,687	9,781
30	-30	50	0,5	-25	-42,687	43,301
25	-25	50	0,4226	-21,130	-63,818	45,315
23	-23	50	0,3907	-19,536	-83,355	46,025
12	-12	50	0,2079	-10,395	-93,750	48,907
14	-14	50	0,2419	-12,096	-105,847	48,514
10,5	-10,5	50	0,1822	-9,111	-114,959	49,162
7	-7	50	0,1218	-6,093	-121,052	49,627
				-121,052		453,157
	Slope Length	474	Slope %	-27%		

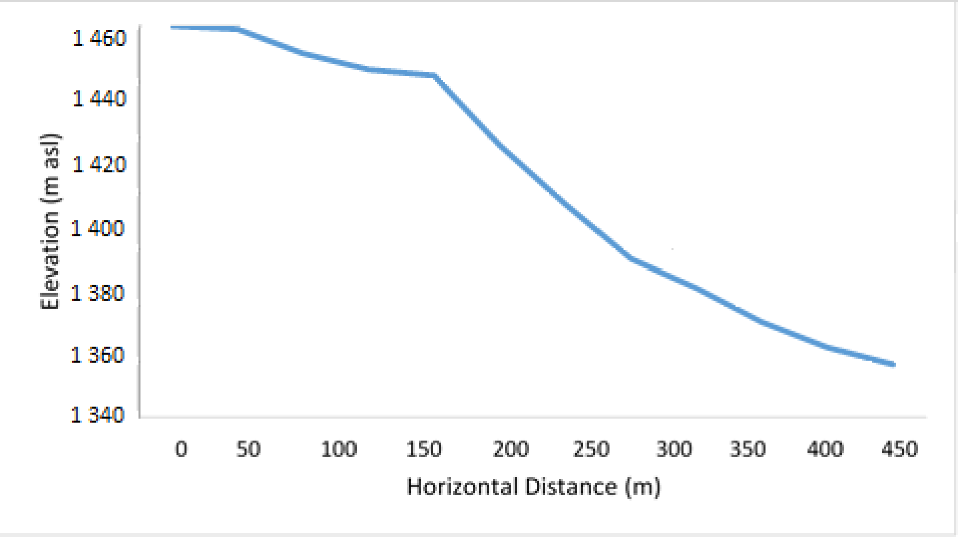

HD= Horizontal Distance of the slope
HD CUM= Cumulative horizontal distance

Plot 2 measurements and slope profile

Angle downslope	Angle	Distance (m)	Sin angle	HD	HD CUM	vd
					0	
4	-4	40	0,069	-2,790	-2,790	39,902
13,5	-13,5	40	0,233	-9,337	-12,128	38,894
13,5	-13,5	34	0,233	-7,937	-20,065	33,060
14	-14	10	0,241	-2,419	-22,484	9,702
23	-23	21	0,390	-8,205	-30,689	19,330
26	-26	50	0,438	-21,918	-52,608	44,939
21	-21	50	0,358	-17,918	-70,526	46,679
11,5	-11,5	50	0,199	-9,968	-80,495	48,996
14,5	-14,5	50	0,250	-12,519	-93,014	48,407
9,5	-9,5	50	0,165	-8,252	-101,266	49,314
6	-6	50	0,104	-5,226	-106,493	49,726
				-106,493		428,954
	Slope Length	445	Slope %	-25%		

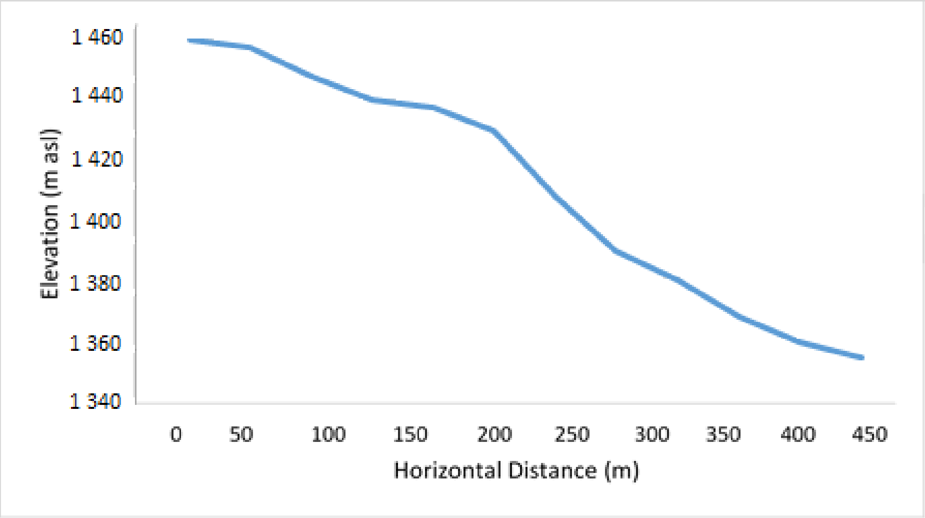

Plot 3 measurements and slope profile

Angle downslope	Angle	Distance (m)	Sin angle	HD	HD CUM	vd
					0	
4	-4	40	0,069	-2,790	-2,790	39,902
10	-10	40	0,173	-6,945	-9,736	39,392
14	-14	34	0,241	-8,225	-17,961	32,990
13	-13	10	0,224	-2,249	-20,211	9,743
22,5	-22,5	21	0,382	-8,036	-28,247	19,401
23	-23	50	0,390	-19,536	-47,783	46,025
19,5	-19,5	50	0,333	-16,690	-64,474	47,132
15,5	-15,5	50	0,267	-13,361	-77,836	48,181
13	-13	50	0,224	-11,247	-89,083	48,718
12	-12	50	0,207	-10,395	-99,479	48,907
8	-8	50	0,139	-6,958	-106,438	49,513
				-106,438		429,908
	Slope Length	445	Slope %	-25%		

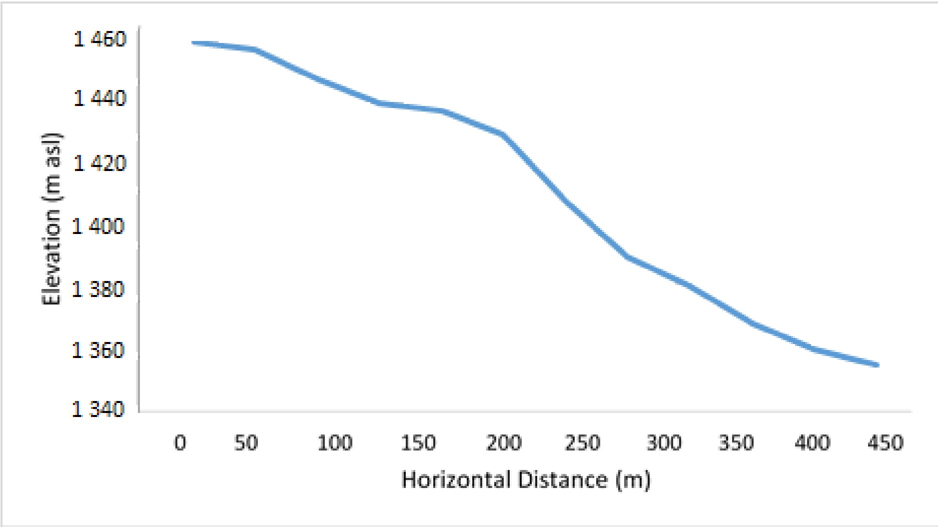

Average measurements used and slope profile

Angle downslope	Distance (m)	Sin angle	HD	HD CUM	vd
				0	
3,2	40	0,055	-2,232	-2,232	39,937
12,0	40	0,207	-8,316	-10,549	39,125
12,5	34	0,216	-7,358	-17,908	33,194
13,0	10	0,224	-2,249	-20,157	9,743
22,8	21	0,387	-8,137	-28,295	19,359
24,5	50	0,414	-20,734	-49,030	45,498
20,3	50	0,346	-17,346	-66,377	46,894
13,5	50	0,233	-11,672	-78,049	48,618
13,8	50	0,238	-11,926	-89,975	48,556
10,8	50	0,187	-9,369	-99,345	49,114
7,0	50	0,121	-6,093	-105,438	49,627
			-105,438		429,669
Slope Length	445	Slope %	-25%		

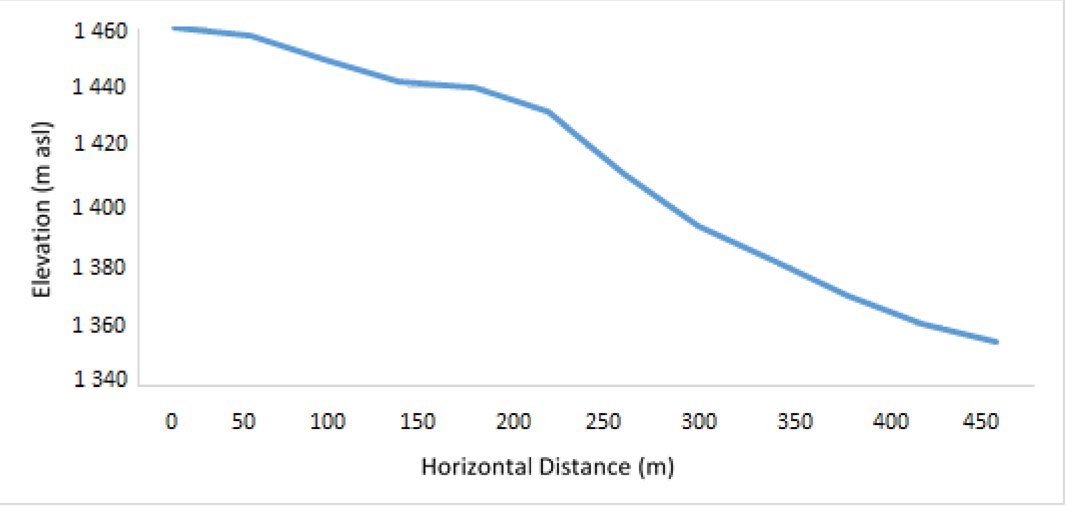

Appendix B – Soil properties at depth intervals 0-5, 5-15 and 15-30 cm at each slope position. Constant = 0,001

Slope Position	Replicate	Depth Distribution (cm)	Depth (m)	Total C (%)	Total N (%)	SOC (g/kg)	N (g/kg)	C/N (g/kg)	BD (g/cm^3)	SOCs (g C m^2)	Soil Moisture Content (%)	Ns (kg C m^2)	MWD (mm)
Reference	1	0-5	0,05	2,89	0,23	28,9	2,32	12,4	1,25	1,81	9,70	0,15	2,61
Reference	2	0-5	0,05	3,28	0,23	32,8	2,28	13,9	1,14	1,87	9,30	0,13	3,26
Reference	3	0-5	0,05	4,76	0,37	47,6	3,67	14,0	1,05	2,50	15,40	0,19	3,88
Reference	1	5-15	0,1	2,87	0,21	28,7	2,06	14,4	1,22	3,50	13,50	0,25	2,52
Reference	2	5-15	0,1	2,69	0,17	26,9	1,73	15,5	1,22	3,28	14,30	0,21	2,6
Reference	3	5-15	0,1	3,66	0,26	36,6	2,58	17,8	1,19	4,36	21,10	0,31	3,58
Reference	1	15-30	0,15	2,57	0,18	25,7	1,83	13,0	1,28	4,93	15,00	0,35	2,88
Reference	2	15-30	0,15	2,14	0,12	21,4	1,20	14,2	0,98	3,15	15,40	0,18	2,07
Reference	3	15-30	0,15	3,25	0,22	32,5	2,17	15,0	1,28	6,24	21.2	0,42	2,34
Top-slope	1	0-5	0,05	1,07	0,08	10,7	0,82	13,0	1,41	0,75	5,40	0,06	1,84
Top-slope	2	0-5	0,05	0,74	0,04	7,48	0,46	16,4	1,58	0,59	5,00	0,04	1,75
Top-slope	3	0-5	0,05	1,02	0,07	10,2	0,74	14,4	1,09	0,56	3,60	0,04	1,48
Top-slope	1	5-15	0,1	0,95	0,05	9,59	0,58	16,0	1,48	1,42	7,20	0,09	2,00
Top-slope	2	5-15	0,1	0,43	0,02	4,37	0,29	14,7	1,54	0,67	4,70	0,05	1,61
Top-slope	3	5-15	0,1	1,06	0,09	10,6	0,96	16,4	1,4	1,48	5,80	0,13	2,03
Top-slope	1	15-30	0,15	0,79	0,05	7,93	0,55	13,7	1,55	1,84	8,40	0,13	1,65
Top-slope	2	15-30	0,15	0,53	0,03	5,37	0,32	11,0	1,55	1,25	4,80	0,08	1,58
Top-slope	3	15-30	0,15	0,86	0,06	8,62	0,68	12,6	1,37	1,77	5,30	0,14	1,94
Mid-Slope	1	0-5	0,05	0,61	0,03	6,18	0,38	16,0	1,61	0,50	4,50	0,03	0,97
Mid-Slope	2	0-5	0,05	0,45	0,04	4,57	0,40	15,3	1,61	0,37	6,00	0,03	1,11
Mid-Slope	3	0-5	0,05	0,76	0,03	7,69	0,35	17,0	1,33	0,51	4,00	0,02	1,54
Mid-Slope	1	5-15	0,1	0,50	0,03	5,03	0,32	11,4	1,27	0,64	8,40	0,04	1,03
Mid-Slope	2	5-15	0,1	0,2	0,02	2	0,21	9,3	1,28	0,26	9,40	0,03	0,97
Mid-Slope	3	5-15	0,1	0,83	0,03	8,34	0,31	11,0	1,35	1,13	8,20	0,04	1,21
Mid-Slope	1	15-30	0,15	0,45	0,02	4,55	0,26	21,8	1,4	0,96	8,60	0,06	0,95
Mid-Slope	2	15-30	0,15	0,25	0,02	2,53	0,23	26,3	1,32	0,50	11,40	0,05	1,17
Mid-Slope	3	15-30	0,15	0,68	0,02	6,84	0,24	28,0	1,34	1,37	9,30	0,05	0,98

Lower slope	1	0-5	0,05	0,56	0,01	5,61	0,15	36,9	1,5	0,42	5,70	0,01	1,44
Lower-slope	2	0-5	0,05	0,49	0,04	4,9	0,43	46,0	1,39	0,34	5,30	0,03	1,05
Lower-slope	3	0-5	0,05	0,98	0,06	9,85	0,69	20,8	1,4	0,69	4,50	0,05	1,45
Lower-slope	1	5-15	0,1	0,41	0,00	4,19	0,09	11,3	1,45	0,61	9,60	0,01	0,85
Lower-slope	2	5-15	0,1	0,52	0,02	5,22	0,26	19,7	1,39	0,73	6,80	0,04	0,99
Lower-slope	3	5-15	0,1	0,84	0,04	8,43	0,43	31,4	1,12	0,94	6,90	0,05	1,34
Lower-slope	1	15-30	0,15	0,52	0,02	5,22	0,25	14,2	1,42	1,11	10,50	0,05	0,79
Lower-slope	2	15-30	0,15	0,40	0,01	4,05	0,12	19,2	1,23	0,75	8,00	0,02	0,80
Lower-slope	3	15-30	0,15	0,69	0,03	6,92	0,33	20,5	1,32	1,37	8,20	0,07	1,07

Appendix C – Soil properties within aggregate size classes > 2000, 250-2000, 53-250 and < 53 µm at depth intervals 0-5, 5-15 and 15-30 cm, at each slope position.

				>2000 µm						
				Dry						
Sample	Depth (cm)	Initial SM (g)	Container (g)	Sample+ Cont. (g)	Dry soil (g)	N (%)	N (g/kg)	N (mg)	C (%)	C (g/kg)
R 1	0-5	80,06	8,46	36,88	28,42	0,242	2,429	0,494	3,315	33,154
R 1	5-15	80,36	8,12	35,55	27,43	0,174	1,745	0,351	2,728	27,280
R 1	15-30	80,13	8,1	41,35	33,25	0,149	1,491	0,301	2,401	24,012
R 2	0-5	80,03	8,27	45,63	37,36	0,210	2,106	0,438	3,088	30,883
R 2	5-15	80,2	8,12	37,22	29,1	0,172	1,720	0,357	2,695	26,951
R 2	15-30	80,31	8,2	29,62	21,42	0,142	1,424	0,285	2,312	23,122
R 3	0-5	80,74	8,27	53,85	45,58	0,422	4,228	0,865	5,530	55,303
R 3	5-15	80,21	8,07	49,6	41,53	0,290	2,901	0,580	3,798	37,983
R 3	15-30	80,63	8,22	32,23	24,01	0,223	2,236	0,449	3,028	30,284
T1	0-5	80,06	8,17	25,61	17,44	0,121	1,215	0,249	1,106	11,065
T1	5-15	80,39	8,14	28,23	20,09	0,092	0,924	0,196	0,7227	7,227
T1	15-30	80,61	8,25	24,3	16,05	0,067	0,674	0,137	0,443	4,438
T2	0-5	80,06	8,2	24,65	16,45	0,069	0,691	0,138	0,470	4,700
T2	5-15	80,21	8,1	22,58	14,48	0,054	0,547	0,113	0,265	2,651
T2	15-30	80,44	8,05	23,04	14,99	0,046	0,466	0,095	0,218	2,184
T3	0-5	80,9	8,17	24,83	16,66	0,078	0,783	0,162	0,636	6,364
T3	5-15	80,17	8,17	34,16	25,99	0,052	0,524	0,107	0,309	3,098
T3	15-30	80,76	8,08	32,93	24,85	0,049	0,490	0,100	0,242	2,428

M1	0-5	80,26	8,11	16,47	8,36	0,090	0,901	0,182	0,885	8,857
M1	5-15	80,08	8,08	16,97	8,89	0,048	0,489	0,098	0,709	7,09
M1	15-30	80,7	8,03	15,89	7,86	0,047	0,475	0,096	0,410	4,101
M2	0-5	80,88	8,09	19,8	11,71	0,057	0,575	0,117	0,451	4,512
M2	5-15	80,8	8,08	15,87	7,79	0,050	0,502	0,100	0,389	3,890
M2	15-30	80,36	8,13	19,53	11,4	0,057	0,576	0,116	0,378	3,783
M3	0-5	80,08	8,1	26,68	18,58	0,092	0,924	0,186	0,975	9,754
M3	5-15	80,61	8,03	20,15	12,12	0,083	0,838	0,173	1,016	10,162
M3	15-30	80,6	8,05	17,1	9,05	0,073	0,730	0,149	0,811	8,115
L1	0-5	80,48	8,04	25,36	17,32	0,071	0,713	0,146	0,777	7,772
L1	5-15	80,3	8,05	14,54	6,49	0,057	0,579	0,116	0,733	7,338
L1	15-30	80,61	8,03	13,55	5,52	0,070	0,707	0,141	0,750	7,500
L2	0-5	80,62	8,11	18,28	10,17	0,066	0,667	0,136	0,766	7,666
L2	5-15	80,73	8,09	16,43	8,34	0,063	0,63	0,134	0,739	7,399
L2	15-30	80,56	8,09	13,52	5,43	0,059	0,590	0,119	0,756	7,568
L3	0-5	80,14	8,04	25,73	17,69	0,111	1,113	0,229	1,334	13,341
L3	5-15	80,04	8,15	22,73	14,58	0,090	0,908	0,185	1,227	12,278
L3	15-30	80,41	8,13	18,7	10,57	0,075	0,753	0,157	0,930	9,307

Note: Reference replicate 1 (R1), Reference replicate 2 (R2), Reference replicate 3 (R3) etc.

				250-2000 µm						
				Dry						
Sample	**Depth (cm)**	**Initial SM (g)**	**Container (g)**	**Sample+ Cont. (g)**	**Dry soil (g)**	**N (%)**	**N (g/kg)**	**N (mg)**	**C (%)**	**C (g/kg)**
R 1	0-5	80,06	8,4	27,29	18,89	0,245	2,456	0,494	3,276	32,766
R 1	5-15	80,36	8,15	27,26	19,11	0,198	1,985	0,406	3,120	31,201
R 1	15-30	80,13	8,32	22,48	14,16	0,195	1,952	0,402	2,916	29,164
R 2	0-5	80,03	8,22	23,98	15,76	0,268	2,682	0,545	3,880	38,801
R 2	5-15	80,2	8,08	24,82	16,74	0,183	1,835	0,368	2,898	28,988
R 2	15-30	80,31	8,24	26,57	18,33	0,162	1,628	0,333	2,329	23,297
R 3	0-5	80,74	8,28	19,76	11,48	0,452	4,527	0,905	5,400	54,001
R 3	5-15	80,21	8,09	21,6	13,51	0,305	3,052	0,615	4,074	40,747
R 3	15-30	80,63	8,13	30,36	22,23	0,312	3,121	0,644	3,820	38,203
T1	0-5	80,06	8,37	31,86	23,49	0,175	1,754	0,354	1,432	14,321
T1	5-15	80,39	8,16	30,2	22,04	0,194	1,940	0,396	1,467	14,674
T1	15-30	80,61	8,26	28,46	20,2	0,132	1,320	0,265	1,301	13,01
T2	0-5	80,06	8,19	31,41	23,22	0,114	1,144	0,240	1,182	11,828
T2	5-15	80,21	8,22	31,38	23,16	0,047	0,472	0,096	0,344	3,445
T2	15-30	80,44	8,08	29,16	21,08	0,069	0,699	0,145	0,503	5,034
T3	0-5	80,9	8,08	34,47	26,39	0,124	1,247	0,261	1,256	12,56
T3	5-15	80,17	8,18	31,63	23,45	0,099	0,998	0,209	0,906	9,066
T3	15-30	80,76	8,28	31,29	23,01	0,080	0,807	0,166	0,656	6,566
M1	0-5	80,26	8,08	33,45	25,37	0,046	0,466	0,094	0,610	6,104

M1	5-15	80,08	8,06	35,85	27,79	0,062	0,621	0,123	0,530	5,302
M1	15-30	80,7	8,15	35,39	27,24	0,041	0,410	0,082	0,432	4,326
M2	0-5	80,88	8,11	29,44	21,33	0,067	0,676	0,138	0,537	5,371
M2	5-15	80,8	8,07	36,18	28,11	0,032	0,324	0,067	0,377	3,777
M2	15-30	80,36	8,04	34,39	26,35	0,069	0,698	0,144	0,483	4,834
M3	0-5	80,08	8,29	29,14	20,85	0,102	1,029	0,216	1,137	11,37
M3	5-15	80,61	8,04	34,52	26,48	0,089	0,891	0,184	1,042	10,42
M3	15-30	80,6	8,09	31,74	23,65	0,073	0,733	0,150	0,829	8,293
L1	0-5	80,48	8,06	28,11	20,05	0,075	0,756	0,153	0,891	8,916
L1	5-15	80,3	8,24	33,63	25,39	0,063	0,631	0,132	0,760	7,601
L1	15-30	80,61	8,09	34,13	26,04	0,057	0,574	0,120	0,641	6,412
L2	0-5	80,62	8,12	31,77	23,65	0,068	0,685	0,141	0,790	7,901
L2	5-15	80,73	8,14	36,38	28,24	0,054	0,544	0,111	0,691	6,915
L2	15-30	80,56	8,07	35,54	27,47	0,048	0,487	0,101	0,637	6,376
L3	0-5	80,14	8,07	27,03	18,96	0,114	1,142	0,232	1,495	14,955
L3	5-15	80,04	8,14	32,42	24,28	0,079	0,799	0,165	1,084	10,84
L3	15-30	80,41	8,28	31,99	23,71	0,087	0,879	0,183	1,029	10,292

Note: Reference replicate 1 (R1), Reference replicate 2 (R2), Reference replicate 3 (R3) etc.

				53-250 µm						
				Dry						
Sample	**Depth (cm)**	**Initial SM (g)**	**Container (g)**	**Sample+ Cont. (g)**	**Dry soil (g)**	**N (%)**	**N (g/kg)**	**N (mg)**	**C (%)**	**C (g/kg)**
R 1	0-5	80,06	8,47	19,44	10,97	0,205	2,056	0,422	2,846	28,466
R 1	5-15	80,36	8,1	20,7	12,6	0,178	1,782	0,366	2,731	27,313
R 1	15-30	80,13	8,3	21,4	13,1	0,177	1,777	0,361	2,604	26,048
R 2	0-5	80,03	8,12	15,76	7,64	0,229	2,293	0,461	3,234	32,343
R 2	5-15	80,2	8,11	22,6	14,49	0,162	1,620	0,335	2,452	24,523
R 2	15-30	80,31	8,37	27,88	19,51	0,133	1,339	0,270	2,004	20,046
R 3	0-5	80,74	8,26	11,51	3,25	0,377	3,778	0,770	5,04	50,4
R 3	5-15	80,21	8,2	13,7	5,5	0,261	2,618	0,542	3,738	37,383
R 3	15-30	80,63	8,23	21,32	13,09	0,240	2,409	0,497	3,416	34,161
T1	0-5	80,06	8,4	24,96	16,56	0,085	0,853	0,174	0,919	9,198
T1	5-15	80,39	8,25	25,53	17,28	0,120	1,203	0,250	1,179	11,794
T1	15-30	80,61	8,16	30,68	22,52	0,070	0,709	0,143	0,873	8,734
T2	0-5	80,06	8,19	28,25	20,06	0,093	0,936	0,194	0,785	7,851
T2	5-15	80,21	8,01	29,62	21,61	0,058	0,583	0,119	0,581	5,818
T2	15-30	80,44	8,04	31,88	23,84	0,062	0,624	0,128	0,649	6,495
T3	0-5	80,9	8,07	39,78	31,71	0,094	0,942	0,193	1,046	10,468
T3	5-15	80,17	8,15	33,63	25,48	0,086	0,861	0,174	0,979	9,794
T3	15-30	80,76	8,1	35,28	27,18	0,080	0,804	0,161	0,940	9,400
M1	0-5	80,26	8,13	47,43	39,3	0,056	0,568	0,116	0,673	6,731
M1	5-15	80,08	8,15	44,68	36,53	0,050	0,505	0,101	0,566	5,661

M1	15-30	80,7	8,18	46,46	38,28	0,046	0,464	0,091	0,478	4,789
M2	0-5	80,88	8,06	46,05	37,99	0,042	0,425	0,086	0,356	3,569
M2	5-15	80,8	8,33	42,57	34,24	0,022	0,229	0,046	0,265	2,654
M2	15-30	80,36	8,39	40,5	32,11	0,041	0,413	0,084	0,342	3,429
M3	0-5	80,08	8,08	42,78	34,7	0,051	0,517	0,104	0,715	7,150
M3	5-15	80,61	8,12	44,09	35,97	0,103	1,036	0,217	1,073	10,732
M3	15-30	80,6	8,18	49,31	41,13	0,048	0,489	0,099	0,736	7,361
L1	0-5	80,48	8,11	41,48	33,37	0,038	0,380	0,079	0,518	5,185
L1	5-15	80,3	8,25	44,66	36,41	0,026	0,262	0,054	0,447	4,475
L1	15-30	80,61	8,14	44,22	36,08	0,020	0,203	0,041	0,344	3,445
L2	0-5	80,62	8,11	45,94	37,83	0,034	0,347	0,071	0,475	4,753
L2	5-15	80,73	8,18	42,71	34,53	0,025	0,259	0,054	0,421	4,218
L2	15-30	80,56	8,26	43,68	35,42	0,015	0,152	0,032	0,346	3,465
L3	0-5	80,14	8,15	40,75	32,6	0,053	0,530	0,106	0,864	8,643
L3	5-15	80,04	8,21	38,51	30,3	0,044	0,447	0,090	0,747	7,475
L3	15-30	80,41	8,28	43,55	35,27	0,032	0,325	0,067	0,555	5,558

Note: Reference replicate 1 (R1), Reference replicate 2 (R2), Reference replicate 3 (R3) etc.

				< 53 µm						
				Dry						
Sample	**Depth (cm)**	**Initial SM (g)**	**Container (g)**	**Sample+ Cont. (g)**	**Dry soil (g)**	**N (%)**	**N (g/kg)**	**N (mg)**	**C (%)**	**C (g/kg)**
R 1	0-5	80,06	32,66	37,62	4,96	0,320	3,200	0,644	3,907	39,073
R 1	5-15	80,36	32,69	37,22	4,53	0,309	3,094	0,629	3,939	39,398
R 1	15-30	80,13	32,65	36,18	3,53	0,267	2,677	0,546	3,604	36,049
R 2	0-5	80,03	32,58	34,95	2,37	0,36	3,554	0,73	4,46	44,586
R 2	5-15	80,2	32,65	36,4	3,75	0,318	3,180	0,663	4,105	41,051
R 2	15-30	80,31	32,79	36,73	3,94	0,228	2,280	0,465	3,290	32,905
R 3	0-5	80,74	32,41	34,27	1,86	0,398	3,989	0,809	5,526	55,266
R 3	5-15	80,21	32,85	34,85	2	0,329	3,293	0,679	4,734	47,345
R 3	15-30	80,63	32,84	36,36	3,52	0,347	3,479	0,702	4,561	45,618
T1	0-5	80,06	32,6	38,45	5,85	0,211	2,118	0,431	2,003	20,037
T1	5-15	80,39	32,76	37,47	4,71	0,231	2,313	0,472	2,244	22,442
T1	15-30	80,61	32,88	38,53	5,65	0,214	2,144	0,447	2,167	21,671
T2	0-5	80,06	32,85	36,9	4,05	0,254	2,549	0,528	2,162	21,626
T2	5-15	80,21	32,51	36,52	4,01	0,200	2,009	0,411	1,903	19,037
T2	15-30	80,44	32,37	37,18	4,81	0,207	2,076	0,430	1,930	19,303
T3	0-5	80,9	32,63	37,53	4,9	0,279	2,792	0,561	2,771	27,715
T3	5-15	80,17	32,65	36,84	4,19	0,272	2,723	0,543	2,745	27,455
T3	15-30	80,76	32,79	37,23	4,44	0,258	2,580	0,527	2,557	25,575
M1	0-5	80,26	32,73	38,9	6,17	0,171	1,713	0,351	1,514	15,149
M1	5-15	80,08	32,74	38,78	6,04	0,130	1,301	0,259	1,212	12,126

M1	15-30	80,7	32,71	38,82	6,11	0,027	0,271	0,053	0,104	1,046
M2	0-5	80,88	32,69	41,06	8,37	0,096	0,962	0,193	0,753	7,539
M2	5-15	80,8	32,47	40,83	8,36	0,118	1,189	0,247	0,833	8,332
M2	15-30	80,36	32,58	41,3	8,72	0,108	1,085	0,219	0,765	7,651
M3	0-5	80,08	32,72	37,43	4,71	0,161	1,619	0,334	1,757	17,577
M3	5-15	80,61	32,74	37,61	4,87	0,193	1,938	0,396	2,100	21,002
M3	15-30	80,6	32,64	38,81	6,17	0,120	1,204	0,242	1,493	14,935
L1	0-5	80,48	32,55	41,45	8,9	0,076	0,766	0,155	0,891	8,912
L1	5-15	80,3	32,56	43,2	10,64	0,087	0,872	0,178	0,888	8,880
L1	15-30	80,61	32,83	44,73	11,9	0,068	0,681	0,140	0,820	8,207
L2	0-5	80,62	32,74	40,15	7,41	0,102	1,021	0,204	0,970	9,705
L2	5-15	80,73	32,78	41,36	8,58	0,063	0,631	0,131	0,789	7,891
L2	15-30	80,56	32,65	43,65	11	0,055	0,554	0,114	0,713	7,137
L3	0-5	80,14	32,61	42,46	9,85	0,148	1,484	0,307	1,801	18,011
L3	5-15	80,04	32,7	41,82	9,12	0,096	0,961	0,194	1,339	13,392
L3	15-30	80,41	32,66	42,34	9,68	0,073	0,739	0,152	1,078	10,788

Note: Reference replicate 1 (R1), Reference replicate 2 (R2), Reference replicate 3 (R3) etc.

Appendix D - $^{210}Pb_{ex}$ Inventory and sedimentation calculations

Sample	Core Depth cm	Core Depth cm	Core Depth cm	BD g/cm³	TOTAL 210Pb dpm/gm	±	137Cs dpm/gm	±	EXCESS 210Pb dpm/gm	±	LN (EXCESS) 210Pb dpm/gm
R 1	0-5	5	-2,5	1,3	5,1	0,3	0,30	0,03	3,5	0,8	1,267
R 1	5-15	10	-12,5	1,2	3,3	0,3	0,18	0,03	1,7	0,6	0,513
R 1	15-30	15	-22,5	1,28	1,4	0,2	BD		-0,2	0,5	0,000
R 2	0-5	5	-2,5	1,1	7,1	0,4	0,30	0,03	5,5	0,7	1,696
R 2	5-15	10	-12,5	1,2	3,0	0,2	BD		1,3	0,3	0,268
R 2	15-30	15	-22,5	0,98	2,4	0,3	BD		0,7	0,3	-0,413
R 3	0-5	5	-2,5	1,1	8,5	0,3	0,34	0,03	6,9	0,4	1,933
R 3	5-15	10	-10,0	1,2	3,2	0,2	BD		1,6	0,5	0,464
R 3	15-30	15	-22,5	1,28	3,0	0,3	BD		1,4	0,3	0,342
T1	0-5	5	-2,5	1,4	4,7	0,2	0,13	0,02	2,9	0,6	1,069
T1	5-15	10	-10,0	1,5	2,9	0,3	BD		1,2	1,0	0,180
T1	15-30	15	-22,5	1,55	3,2	0,3	BD		1,7	0,7	0,516
T2	0-5	5	-2,5	1,6	4,0	0,2	0,11	0,03	2,7	0,6	1,011
T2	5-15	10	-10,0	1,5	2,5	0,2	BD		1,1	0,4	0,088
T2	15-30	15	-22,5	1,55	2,8	0,2	0,10	0,02	1,4	0,2	0,341
T3	0-5	5	-2,5	1,1	5,8	0,3	0,34	0,04	4,4	0,4	1,486
T3	5-15	10	-10,0	1,4	3,7	0,2	0,23	0,03	2,3	0,2	0,840
T3	15-30	15	-22,5	1,37	3,1	0,3	BD		1,6	0,6	0,490
M1	0-5	5	-2,5	1,61	2,2	0,3	BD		0,7	0,6	-0,398
M1	5-15	10	-10	1,27	2,5	0,2	BD		0,9	0,6	-0,080
M1	15-30	15	-22,5	1,4	2,3	0,3	BD		0,7	0,6	-0,360
M2	0-5	5	-2,5	1,6	3,0	0,4	BD		1,1	1,1	0,095

M2	5-15	10	-10,0	1,3	2,3	0,2	BD		0,6	0,8	-0,502
M2	15-30	15	-22,5	1,32	2,2	0,3	BD		0,5	0,6	-0,786
M3	0-5	5	-2,5	1,3	2,1	0,2	BD		0,6	0,5	-0,488
M3	5-15	10	-10,0	1,4	2,1	0,2	BD		0,5	1,1	-0,676
M3	15-30	15	-22,5	1,34	2,4	0,2	BD		0,8	0,9	-0,231
L1	0-5	5	-2,5	1,5	2,4	0,2	BD		0,8	0,3	-0,198
L1	5-15	10	-10,0	1,5	1,8	0,3	BD		0,3	1,1	-1,305
L1	15-30	15	-22,5	1,42	1,8	0,2	BD		0,4	0,5	-0,914
L2	0-5	5	-2,5	1,4	2,3	0,3	BD		0,7	0,7	-0,294
L2	5-15	10	-10,0	1,4	4,1	0,5	BD		2,7	1,0	0,976
L2	15-30	15	-22,5	1,23	2,0	0,3	BD		0,6	0,3	-0,493
L3	0-5	5	-2,5	1,4	2,5	0,2	BD		1,0	0,9	-0,040
L3	5-15	10	-10,0	1,1	2,2	0,2	BD		0,8	0,3	-0,269
L3	15-30	15	-22,5	1,32	2,4	0,3	BD		0,8	0,4	-0,202

Note: Reference replicate 1 (R1), Reference replicate 2 (R2), Reference replicate 3 (R3) etc.

Sample	Core Depth cm	210Pb Inventory Calculation	210Pb Inventory dpm/cm^2	210Pb Inventory dpm/cm^2	Assume density	2,5	g/cm^3
				Reference site			
R 1	0-5	22,185	277,314	786,62			
R 1	5-15	20,372	509,306				
R 1	15-30	-4,752	0,000				
R 2	0-5	31,070	388,371	1151,93			
R 2	5-15	15,951	398,783				
R 2	15-30	9,727	364,777		**So at reference Site Average:**	**1293**	dpm/cm^2
R 3	0-5	36,276	453,450	1939,84	**stdev:**	**589**	dpm/cm^2
R 3	5-15	18,921	473,030		**SE**	**340,275**	
R 3	15-30	27,023	1013,360				
T1	0-5	20,538	256,726	**Top-slope**			
T1	5-15	17,725	443,133	2160,51			
T1	15-30	38,951	1460,653				
T2	0-5	21,712	271,399	1917,475	**Top-slope**		
T2	5-15	16,810	420,248		**average:**	**2149**	dpm/cm^2
T2	15-30	32,689	1225,828		**stdev:**	**226**	dpm/cm^2
T3	0-5	24,084	301,047	2369,710	**SE**	**130,671**	
T3	5-15	32,443	811,068				
T3	15-30	33,536	1257,595				
M1	0-5	5,408	67,603	**Mid-slope**			
M1	5-15	11,722	293,058	909,91			
M1	15-30	14,647	549,249				

M2	0-5	8,854	110,672	642,700	**Mid-slope**		
M2	5-15	7,749	193,718		**average:**	**791**	dpm/cm^2
M2	15-30	9,022	338,310		**stdev:**	**136**	dpm/cm^2
M3	0-5	4,081	51,015	821,107	**SE**	**78,569**	
M3	5-15	6,866	171,662				
M3	15-30	15,958	598,429				
L1	0-5	6,150	76,874	**Lower-slope**			
L1	5-15	3,932	98,292	495,37			
L1	15-30	8,539	320,209				
L2	0-5	5,178	64,723	1409,773	**Bottom Slope**		
L2	5-15	36,900	922,488		**average:**	**937**	dpm/cm^2
L2	15-30	11,268	422,562		**stdev:**	**458**	dpm/cm^2
L3	0-5	6,725	84,065	905,040	**SE**	**264,439**	
L3	5-15	8,562	214,043				
L3	15-30	16,185	606,931				

Inventory Calculation

Excess 210Pb * density * sample depth interval
Results should be in dpm/cm^2
Add each core interval until $^{210}Pb_{ex}$ is zero

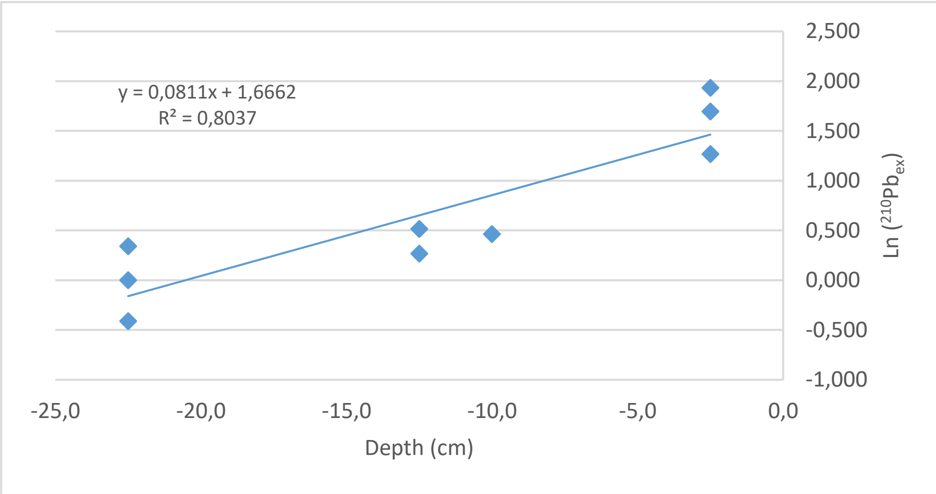

Reference site 0.38 cm/yr

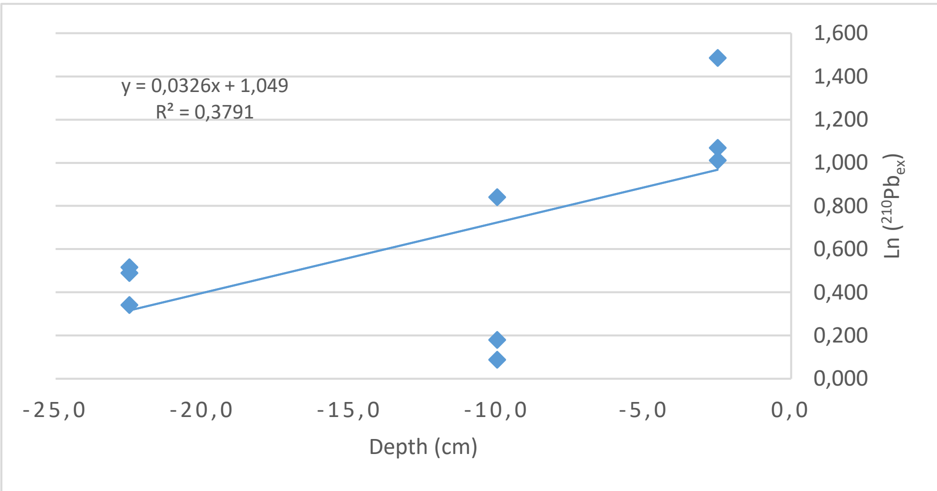

Top-slope 0.95 cm/yr

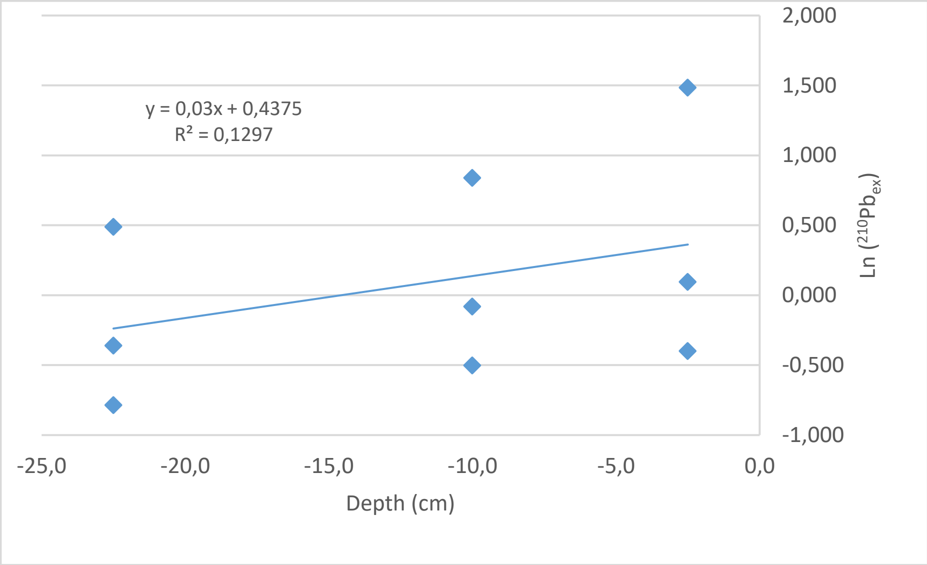

Mid-slope 1.04 cm/yr

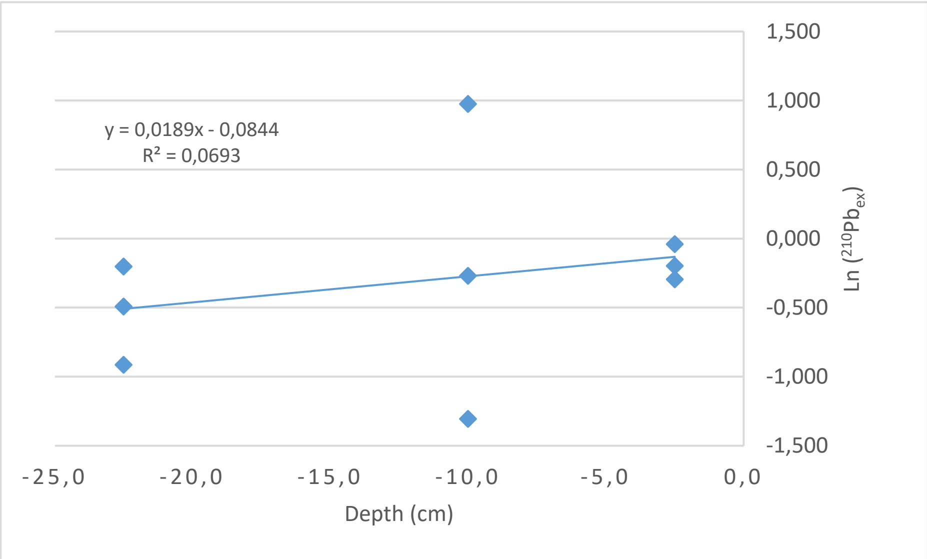

Lower-slope 0.37 cm/yr